Simulation and Statistical Methods in Proactive and Strategic Obsolescence Management

James K. Starling

A dissertation
submitted in partial fulfillment of the
requirements for the degree of

Doctor of Philosophy

University of Washington

2020

Reading Committee:

Christina M. Mastrangelo, Chair

Youngjun Choe, Chair

Zelda B. Zabinsky

Program Authorized to Offer Degree:
Industrial and Systems Engineering

University of Washington

Abstract

Simulation and Statistical Methods in
Proactive and Strategic Obsolescence Management

James K. Starling

Co-Chairs of the Supervisory Committee:
Prof. Christina M. Mastrangelo
Department of Industrial and Systems Engineering

Prof. Youngjun Choe
Department of Industrial and Systems Engineering

In fields with sustainment-dominated systems, where the sustainment costs are larger than the original system costs, managing the life-cycle costs is a non-trivial task. These fields include aviation, power plants, medical, military, telecommunications, and civilian safety. In recent years, many of these fields have begun to rely on commercial off-the-shelf (COTS) parts whose lifetimes are driven by market forces outside of the control of the system managers, serving to exacerbate obsolescence issues. While the procurement lifetimes of commercial electronics typically span 12-18 months, many of these fields have systems in excess of 30 years. Efficient management of supply chains and obsolescence issues is crucial to keep key systems operational.

This dissertation provides proactive and strategic diminishing manufacturing sources and material shortages (DMSMS) (or obsolescence) management frameworks to forecast availability risk and identify optimal technology refresh strategies. First, a proactive technique evaluates reducing the bias associated with maximum likelihood estimation (MLE) for part-level forecasting. Second, a model is presented to measure the availability risk across a system of parts, taking into account DMSMS issue mitigation. Third, optimal technology

refresh strategies are explored, focusing on the trade-off between lifetime buy and technology refreshes mitigation decisions for a system.

The first contribution of this research identifies the amount of oversampling required to reduce the bias in Weibull parameter estimates for generalized Type I censoring. A common method to estimate Weibull parameters with censored data is to use MLE, but bias in parameter estimates tends to increase as the percent of censored observations increases and/or the sample size decreases. The bias can affect the accuracy of forecasting or simulating procurement lifetimes in a DMSMS context. This dissertation combines previous work to reduce the bias in the Weibull shape parameter and oversampling, with a technique akin to synthetic minority oversampling technique (SMOTE), to reduce the bias in the scale parameter. Using the Kullback-Liebler divergence, the amounts of oversampling that results in a decrease in the estimated distribution's deviation from the true distribution are identified according to the sample size and the percent of censoring for a data set. A case study is presented using microelectronic parts to highlight application of the proposed methodology.

The second contribution of this research quantifies the risk associated with parts as they move through the procurement life-cycle curve. Often a single part becoming obsolete, or being non-procurable, does not lead to a serious DMSMS issue as these are quickly mitigated with like-part substitutions. In addition, having more than one manufacturer for a part is a recommended strategy to minimize the risk associated with DMSMS issues. A discrete event simulation (DES) model is created using a finite-source capacitated queuing model and two risk metrics are developed. The DES results are verified with analytic results. Additionally, model extensions are presented to improve the realism of the model.

The third contribution of this research presents a strategic DMSMS management study which compares the trade-off between lifetime buys (LTBs) and technology refreshes over a system's lifetime. This research provides a way to quantify and compare proactive and reactive DMSMS management strategies. Two models are compared: the first uses a ranking and selection (R&S) method while the second uses a rolling horizon (RH) framework. Optimal strategies from both models are compared with sensitivity to the relative costs between LTBs and technology refreshes. The solutions provide DMSMS managers a set of (near-)optimal scheduling strategies at minimal cost.

TABLE OF CONTENTS

LIST OF FIGURES

LIST OF TABLES

GLOSSARY

Abbreviations

BC-2/3	Bias Correction stochastic estimation method 2nd/3rd order
BOM	Bill Of Materials
COTS	Commercial Off-the-Shelf
CP	Configuration Part
CTMC	Continuous-Time Markov Chain
DES	Discrete Event Simulation
DMSMS	Diminishing Manufacturing Sources and Material Shortages
DoD	Department of Defense
EOL	End-Of-Life
FFF / F3	Form/Fit/Function
FH	Finite Horizon
HSD	(Tukey's) Honestly Significant Difference test
IHO	Infinite Horizon Optimization
IZ	Indifference Zone
KN	Kim and Nelson (ranking and selection method)
LSE	Least-Squares Estimation / Estimator
LTB	Life-Time Buy
MAE	Mean Absolute Error
MGF	Moment Generating Function
MLE	Maximum Likelihood Estimation
MLM	Method of Logarithmic Moment
MM	Method of Moments
MMLE	Modified profile Maximum Likelihood Estimate
MRI	Material Risk Index
NPV	Net-Present Value
NSGS	Nelson, Swann, Goldsman, Song (ranking and selection method)
OEM	Original Equipment Manufacturer

PDF	Probability Density Function
R&S	Ranking and Selection
RDT	Reliability Demonstration Test
RH	Rolling Horizon
RMSE	Root Mean-Squared Error
SCRM	Supply Chain Risk Management
SME	Subject Matter Expert
SMOTE	Synthetic Minority Oversampling Technique
VP	Vendor Part
WPP	Weibull Probability Plot
YTEOL	Years To End Of Life

ACKNOWLEDGMENTS

I would like to express my deepest thanks to my advisors, Professors Christina Mastrangelo and Youngjun Choe. Thank you all for the many hours of guidance, discussion, and assistance. I would also like to thank my committee members, Professors Zelda Zabinsky and Bob Odom, for their great feedback and assistance to improve my final product. Finally, I would like to thank all of the numerous professors who have challenged me along the way during my time at the University of Washington.

DEDICATION

To my best friend, Joni.

Chapter 1

INTRODUCTION

In fields with sustainment-dominated systems, where the sustainment costs are larger than the original system costs [7, 104], managing the life-cycle costs is a non-trivial task. These fields include aviation, power plants, medical, military, telecommunications, and civilian safety [128]. In recent years, many of these fields have begun to rely on commercial off-the-shelf (COTS) parts whose lifetimes are driven by market forces outside the control of system managers [23], serving to exacerbate obsolescence issues. Many of these fields have systems that have lifetimes in excess of 30 years [114] whereas the commercial electronics have lifetimes of 12-18 months [52]. Efficient management of supply chains and obsolescence issues is crucial to keep key systems operational.

A *diminishing manufacturing sources and material shortages* (DMSMS) issue is defined as the "loss, or impending loss, of manufacturers or suppliers of items, raw materials, or software" [23]. Causes of DMSMS issues include technology, function, regulation (or legal), supportability, and market demand [23, 47]. Although there are nuances between the terms *obsolescence* and *DMSMS*, the two have often been regarded as synonymous [98, 114]. In particular, the term *technology obsolescence* refers to systems that are heavily reliant on technology which will experience this type of obsolescence most frequently [104]. This dissertation will refer to *obsolescence* and *DMSMS* synonymously unless specified.

DMSMS issues break down into three generally accepted DMSMS management strategies: reactive, proactive, and strategic [7, 94]. A similar breakdown of the three management strategies is provided by [114] but uses levels 1–3. It is important to note that the U.S. Department of Defense (DoD) handbook for DMSMS management only explicitly mentions reactive and proactive management styles [23].

Reactive DMSMS management deals with the decisions after a part has become obsolete or threatens to become obsolete [94]. Often, the goal is to find the lowest cost option to mitigate the obsolescence issue [104]. Examples of reactive tactics are using existing stock, lifetime buy (LTB), repair, refurbishment, reclamation, extension of product support, substitution, developing a new source, or redesigns [7, 23].

Proactive DMSMS management involves using tools to predict part obsolescence before it happens and proactively scheduling mitigation methods. Typically, this involves forecasting obsolescence risk [69] and prioritizing important parts to be proactively monitored while others are managed reactively [7]. Examples of proactive DMSMS management include using procurement lifetime forecasting [84, 99, 101] and modeling life-cycle curves [9, 106].

Finally, strategic DMSMS management uses a mix of reactive and proactive methods with the goal of minimizing the overall life-cycle costs and takes into account demand, inventory, and spares [69, 94]. Some examples of strategic management include creating *material risk indexes* (MRI) and *technology refresh planning* or *design refresh planning* [104,107,128]. Examples of strategic management frameworks include design refresh planning tools that use discrete event simulation with Monte-Carlo analysis [32, 104], mixed-integer linear programming models [69], and ranking and selection [107].

The main research objective in this dissertation is to provide a collection of proactive and strategic DMSMS management models. The first contribution provides a method to reduce the bias in estimating parameters when assuming an underlying Weibull distribution for procurement lifetimes. The second contribution presents a risk-based framework to model part availability, taking into account the market size. Finally, a third contribution applies and compares two methods to identify optimal technology refresh strategies.

1.1 Procurement Lifetime Forecasting Bias with Censored Data

At the heart of proactive DMSMS management is the ability to forecast procurement lifetimes for individual parts. One of the earliest studies involving product lifetimes evaluated whether the lifetimes were getting shorter over time and used maximum likelihood estimation (MLE) [9]. Other studies have also used MLE [84, 97, 99], machine learning [47], and data mining [101]. Sandborn [97] describes two methods that can be used to describe the procurement lifetimes using data; those with and without *evolutionary parametric drivers*. These evolutionary parametric drivers are defined as "a combination of parameters describing the part that evolves over time" [97]. An example of an evolutionary parametric driver is memory size for flash memory. For other parts that do not have a evolutionary parametric driver, he provides a method using regression to predict procurement lifetimes, or the difference between introduction date and end-of-life (EOL) date.

One aspect of using DMSMS part lifetime data is that it typically contains censored data. Right (left) censored data has a missing or unknown EOL (introduction) date. Interval censored have unknown or missing introduction and EOL dates, but can use estimated dates. Fields other than DMSMS also include censored data, such as reliability [55, 63, 79], medical [46, 65], environmental/ecological [39, 85], and manufacturing [49, 61]. In reliability demonstration tests (RDT) Type I or Type II censoring mechanisms are typically used; however, in many real-life applications a *generalized* Type I censoring mechanism, where each observation may have their own censoring times, may be more applicable. These examples occur in medical studies, structural risk analyses, and obsolescence predictions where the items in the study may have different introduction dates but have lifetimes from the same probability distribution. Ignoring the censored data is possible but ill-advised as one may potentially be throwing away informative data; however, including the data can introduce increased biases when estimating parameters especially when the number of observations is smaller or the percent of censored observations increases [40, 65, 125]. A summary of recommended methods for censored data are presented by [39] and are broken down by the percent censored and the number of observations. These methods include some non-parametric methods (Kaplan-Meier and Turnbull), imputation, reporting percentage threshold values, and MLE. This dissertation will focus only on the use of MLE for various sample sizes and percent censored values to provide insights on the impact of using right censored data for the procurement lifetime estimates.

Due to its flexibility, the Weibull distribution, consisting of a shape (β) and scale (α) parameter, is often used in the aforementioned studies and is highlighted in many other studies [81]. The shape describes the rate of change for the hazard function. If the shape is less than 1 ($\beta < 1$), there will be a greater number of deaths at the beginning and a decreasing hazard function. If the shape is greater than 1 ($\beta > 1$), there will be a increasing number of deaths at the end of the life-cycle. If the shape is equal to 1, the distribution is the same as the exponential distribution. The scale parameter also has a direct interpretation in that is represents the the characteristic life and that 36.8% parts will survive up until the value of the scale, regardless of the shape parameter value [51].

One drawback to using censored data is that parameter estimates tend to be biased as the true procurement lifetimes are unknown. Previous methods reduce the bias in the shape parameter, but typically do not seek to decrease an estimated probability density function's (PDF) deviation from the true PDF. Chapter 2 extends these previous methods to the generalized Type I censoring case and proposes a method to reduce the overall bias in the PDF, as measured using the Kullback-Liebler divergence. The proposed method combines a method by [123], which improves the Weibull shape parameter estimate using a profile likelihood, and a modified *synthetic minority oversampling technique* (SMOTE) to reduce the overall bias for the Weibull PDF. The proposed method can be applied to applications outside of DMSMS models.

1.2 Availability Risk

The majority of DMSMS-centric studies have focused on component-level or individual part-level forecasts [90], but do not take into account the product life-cycle curve of a technology [78] and the size of the marketplace [89, 121]. Most of the literature describes between four to six stages of the product life-cycle curve to describe changing markets [87]. The life-cycle curves are usually presented as a bell-shaped curve although the actual curves may take on different shapes in reality. One study in particular tied the life-cycle curve to the number of competitors in the market [106].

In many instances, a part reaching the end of its procurement lifetime or the loss of an original equipment manufacturer (OEM) does not necessarily equate to a DMSMS issue. One study conducted by the United States Department of Defense (DoD) found a large majority (roughly two-thirds) of these cases initially flagged as DMSMS issues are mitigated with using an “approved item” (a part already approved by the system drawings) or a “simple substitute” (an alternate part that may require minimal effort to certify use) [22]. Although there is a cost associated with these actions, it is typically much smaller than other mitigation options such as refurbishment, developing new sources or parts, or redesigning a system [23].

Proactive DMSMS approaches must consider system-level availability risk, not just the risk for an individual part’s obsolescence. Additionally, the part forecasts must consider substitutions in their models as well as taking into account the market size. Chapter 3 develops two models to quantify the risk of part unavailability in probabilistic and temporal terms. The models are built upon a finite-source queuing model and uses discrete event simulation (DES) to calculate the associated risk for parts with varying market sizes and individual part procurement lifetimes. The first model can be used to inform MRI studies, while the second model can be used to improve estimates for individual part availability when conducting technology refresh planning.

1.3 Optimal Technology Refresh Planning Strategies

With a multitude of DMSMS mitigation options available and at varying costs and impacts, the choice of an optimal sequence is non-trivial. In some cases, a lower cost DMSMS mitigation option may be best for a near-term solution but may not be optimal over a longer time period. This refers to the proverbial “kicking the can down the road”, which increases the potential for catastrophic issues at a later time. Technology refresh planning is the strategic DMSMS tool that tackles this issue by minimizing life-cycle costs but ensures continued operational capability.

A related model in other management literature is the equipment replacement model, where the goal is to find the “optimal procedure for replacing old equipment with new” [11].

The replacement decisions can be expanded to include many other decisions that are related to capital budgeting [54]. Some of the first studies in equipment replacement focused on modeling using discounted costs and an infinite horizon to ensure no end of study effects have an impact on the strategies [35]. In some cases, there is justification for using a finite horizon model such as when equipment is acquired for a very specific use [38]. In DoD applications a finite horizon model can be an acceptable assumption due to the definitive life-cycles of aircraft, naval vessels, trucks, etc. The DMSMS decision to conduct a technology refresh is essentially the same problem as the equipment replacement model. Many previous studies related to redesigns and equipment replacement, typically do not consider replacements due to obsolescence issues [104].

DMSMS specific studies have modeled this problem, most use a combination of refreshes with LTB as a mitigation option. One of the first technology refresh studies tackled this problem by examining the trade-off between LTBs and redesigns but assumed obsolescence at the start of the study and did not allow for successive redesigns in the model [83]. A study by [69] used mixed integer programming to model a multi-part system with deterministic procurement lifetimes and costs but only considered a single refresh. While other studies have allowed for multiple technology refreshes and take the horizon length into account for their solutions [104, 105].

Chapter 4 will compare two models to identify optimal technology refresh strategies for a fixed system lifetime, or a finite horizon. The first model yields a set of optimal solutions within an indifference zone and uses a ranking and selection (R&S) method with stochastic procurement lifetimes. The second model uses a rolling horizon framework where the optimal current decision is identified before moving on to the next decision period and repeating the process. Each decision is determined by approximating an infinite horizon, conditioned on the sequence of previous decisions. The results of the two models are compared and discussed in terms of DMSMS management.

Chapter 2

IMPROVING WEIBULL DISTRIBUTION ESTIMATION FOR GENERALIZED TYPE I CENSORED DATA USING MODIFIED SMOTE

This chapter presents a working manuscript for future journal submission.

Abstract

Using maximum-likelihood estimation (MLE) to estimate the parameters of survival functions is common in practice when dealing with parametric distributions, especially with (right) censored observations. However, using MLE with censored data introduces an inherent bias which tends to increase as the number of observations decreases and/or the percent of censored observations increases. In reliability demonstration tests (RDT) Type I or Type II censoring mechanisms are typically used; however, in many real-life applications a *generalized* Type I censoring mechanism, where each observation may have their own censoring times, may be more applicable. These examples occur in medical studies, structural risk analyses, and obsolescence predictions where the items in the study may have different introduction dates but have lifetimes from the same probability distribution. This research seeks to improve the parameter estimates of a Weibull distribution as a means to minimize the deviation from a true distribution, by reducing the bias in the shape and scale parameters. Improving both the scale and shape parameter estimates through MLE modification and oversampling can potentially improve simulation and forecasting applications. Empirical results are presented with recommendations for preferred oversampling sizes, which is dependent upon the percent censored and sample size of the data, using the Kullback-Liebler divergence as a metric to measure the difference between the known distribution and esti-

mated distributions.

2.1 Introduction

Censored data occurs naturally in survivability analysis studies. This type of data occurs often and is varied among reliability [55, 63, 79], medical [46, 65], environmental/ecological [39, 85], manufacturing [49, 61], and obsolescence prediction applications [97]. Ignoring the censored data is possible but ill-advised as informative data may be thrown away; however, including the data can increase bias when estimating distribution parameters especially when the number of observations is smaller or the percent of censored observations increases [40, 65, 125].

Due to its flexibility, the Weibull distribution is often used in the aforementioned studies and is highlighted in many other studies [81]. Various approaches exist in the literature for estimating the Weibull shape and scale parameters and is an often studied topic. [1] use a particle swarm method to estimate parameters for a three-parameter Weibull distribution. However, in their application of estimating strengths of glass fibers they only consider complete (non-censored) data. A Bayesian estimation method is used by [27] for heavily censored data, however, the study uses large (100+) sample sizes. [125] evaluates the use of least-squares estimation (LSE) which relies on the Weibull probability plot (WPP). One benefit to their study is that they evaluate censoring levels of 10, 50, and 70% and also include small samples sizes as low as 10. One drawback to their study is the use of randomly selected censoring. This type of censoring randomly selects a certain percentage of the population to be censored and then conducts MLE estimates. This allows for easy comparison with analytic results, but may be hard to justify in reality. Other methods include the method of logarithmic moment (MLM), the percentile method, and the method of moments (MM); however the maximum likelihood estimation (MLE) is most often used [112]. This paper focuses on removing bias when using MLE and small sample sizes and/or large censoring percentages.

Previous studies have focused on the Weibull shape parameter as it indicates the failure modes related to the hazard function. A shape parameter between 0 and 1 indicates early failures, while a shape parameter greater than one indicates wear-out, and a shape parameter equal to one has a constant hazard rate [51]. As such, an accurate estimate of the shape parameter is important. One approach is to use a scaling factor to modify the shape parameter estimate. Ross [91] provided a bias correction factor for the shape parameter that accounts for population size. [40] provided a bias correction method for the shape and scale parameters using a fourth-order approximation of the bias function also taking into account the population size. Whereas Ross and Hirose only consider complete (all non-censored) data, [125] reduce the bias of the Weibull shape parameter the least squares estimator (LSE) method and a bias correction function that accounts for the percent censored and sample size. One drawback to the methods by [40, 91, 125] is that they seek to correct the outputs of the estimation method *after* conducting the estimation, e.g. MLE and LSE, as opposed to correcting the bias inherent in the method used. [124] and [123] use the profile likelihood, which parameterizes the MLE function as a single variable function using a method outlined in [20]. Shen and Yang [103] also explore a bias-correcting measure for a common shape parameter using a third-order stochastic expansion of the bias term for a profile likelihood. All three studies ([103, 123, 124]) explore complete and censored data and focus on small sample sizes as well as higher levels of censoring. However, they do not explore the effects of the methods on the scale parameter nor when a *generalized* Type I censoring mechanism occurs.

While estimating the bias in one of the Weibull parameters may be sufficient for gaining insight on the failure rate trends, it may not be sufficient in forecasting applications. Furthermore, the scale parameter must also be considered. The primary contribution of this research is a method that reduces the bias (in expectation) in the Weibull scale parameter, after estimating the Weibull shape parameter using the methods by [103, 123, 124] when a *generalized* Type I censoring mechanism is present. *Generalized* Type I censoring is right-censored data that does not have a fixed testing period and items are introduced into the study at varying times (this censoring mechanism is described in greater detail in Section 2.2.1 and the

Appendix). Results from a simulation study indicate that methods from [103, 123, 124] show improvements (i.e. reduced bias) in the shape parameter estimates, but tend to increase bias in the scale parameter estimates. As a goodness-of-fit test, the Kullback-Liebler divergence metric is used to gain insights on the overall effect of simultaneously improving the shape and scale parameters on the overall probability density functions (PDFs).

The rest of the paper is organized as follows. Section 2.2 defines the notation for censored data, outlines the methods used to estimate the Weibull parameters, oversampling, and the Kullback-Liebler divergence metric. Section 2.3 shows the efficacy of applying previous bias reduction methods to generalized Type I censoring data using Monte-Carlo simulation. Section 2.4 shows how the methodology reduces the bias in the scale parameter and decreases the estimated distribution's deviation from the known distribution. Section 2.5 presents empirical results of the proposed method. Section 2.6 uses microelectronic data to demonstrate how the methodology would be utilized in practice. Section 2.7 discusses the findings and concludes the study.

2.2 Background

This section will highlight the bias correction methods using a modified profile likelihood method [123, 124] and the second- and third-order stochastic expansion of the Weibull MLE [103]. While the work in [103, 123] assumes a common shape parameter for k Weibull distributions, this paper will assume that observations are only derived from a single population ($k = 1$). The equations shown in this section modify the original equations to accommodate this assumption. Additionally, oversampling of minority and majority classes is discussed, specifically the synthetic minority over-sampling technique (SMOTE).

2.2.1 Types of Censored Data

Right censored data results from two mechanisms [56, 63]. The first, Type I, has a fixed censoring time while the second, Type II, creates censored observations when a predefined number (or percentage) of failures (non-censored values) occur. While Type I censoring can control for the time aspect it is unable to control for the number of failures; likewise, Type II can control the number of failures but cannot control the time at which these failures occur. For *standard* Type I censoring and Type II censoring, the parts are introduced at the beginning of the experimental or observational period. This is the typical setup in many studies, specifically in [39, 46, 49, 55, 61, 63, 65, 79, 85, 97] and [103, 123–125]. Another type of censoring, *generalized Type-I right censoring*, occurs when each observation has a unique censoring time as well as varying introduction dates [21, 56]. In standard reliability demonstration test (RDT) cases, as outlined in [55], the standard Type I or Type II censoring mechanisms are used. However, in many other instances generalized Type I censoring naturally occur. Examples include: medical studies (patients arrive a various times), structural risk analysis (buildings or structures are observed at different times), and obsolescence prediction (parts are introduced into the market at various times). Similar to standard Type I censoring, the generalized Type I censoring cannot control for the amount of censored parts. 2.8 presents mathematical analysis for the expected amount of censoring for a given set of Weibull parameters, assuming uniform introduction dates for the observations.

Figure 2.1 shows a visual example of the difference between the standard Type I and Type II censoring and generalized Type I censoring. The left side of Figure 2.1 shows 6 items under observation with the same introduction date. The censoring time, T_C, is a predefined time for Type I censoring that is established before the study begins. For Type II censoring, the value for T_C will vary, dependent upon reaching the predefined percent of failures. The right side of of Figure 2.1 showcases generalized Type I censoring where the items have varying introduction dates. Typically in this case the T_C is related to a “date of analysis” which can be the last observation time, or in cases where one has access to real-time data, “today”.

Right censored data for an observed lifetime i will consist of two values $\{T_i, \delta_i\}$, with $T_i \in \mathbb{R}^+$ and $\delta_i \in \{0, 1\}$. In the generalized Type I case, the current lifetime, $T_i = L_i + D_i$, consists of a lifetime, $L_i \sim f_L(\theta_L)$, and a introduction date, $D_i \sim f_D(\theta_D)$, where f_L, θ_L are the probability density function (PDF) and parameters of the lifetime and f_D, θ_D are the PDF and parameters of the introduction date. The lifetime, T_i, can be either an observed

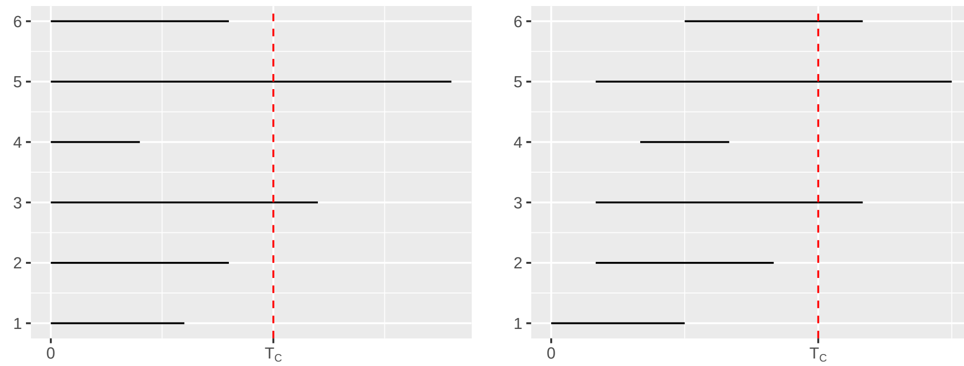

Figure 2.1: The difference between standard Type 1 and 2 censoring and generalized Type 1 censoring. Standard Type 1 and 2 censoring has all elements start at the same time (left figure), while generalized Type 1 censoring has different introduction dates (right figure). The majority of studies typically refer to the standard types of censoring, while there has been little research with generalized Type I data.

or censored value, while the censoring indicator $\delta_i = 0$ when an observation is censored (e.g. $T_i > T_C$) and $\delta_i = 1$ when an observation is non-censored (e.g. $T_i \leq T_C$).

2.2.2 Modified profile likelihood estimation

[124] present a modified profile likelihood to improve the estimate for the shape parameter in a Weibull distribution. [123] improves the estimates and extend to include multiple populations with a common shape parameter but with different scale parameters. Given the Weibull probability distribution function (pdf):

$$f(t|\alpha, \beta) = \frac{\beta}{\alpha}\left(\frac{t}{\alpha}\right)^{\beta-1} \exp\left\{-\left(\frac{t}{\alpha}\right)^{\beta}\right\}$$

where α and β are the scale and shape parameters, respectively.

The log-likelihood function for a two-parameter Weibull distribution (for one population) is given by:

$$l(\alpha, \beta) = r \log \beta + (\beta - 1) \sum_{i=1}^{n} \delta_i \log t_i - \beta\, r \log \alpha - \sum_{i=1}^{n} \left\{ \frac{t_i}{\alpha} \right\}^{\beta}, \tag{2.1}$$

where t_i are the n observed lifetimes or censored lifetimes; the failure indicator $\delta_i = 1$ if the lifetime is known or $\delta_i = 0$ if the lifetime is censored; $r = \sum_{i=1}^{n} \delta_i$ is the total number of observed and known lifetimes; for $i = \{1, 2, \dots, n\}$. Maximizing (2.1) w.r.t. α (e.g. taking the partial derivative w.r.t. α, setting equal to 0 and solving for α) gives:

$$\hat{\alpha}(\beta) = \left\{ \frac{1}{r} \sum_{i=1}^{n} t_i^{\beta} \right\}^{1/\beta}. \tag{2.2}$$

The *profile* (or *concentrated*) likelihood function is found by substituting (2.2) into (2.1), yielding:

$$l_p(\beta) = l(\hat{\alpha}(\beta), \beta) = r \log r - r + r \log \beta + (\beta - 1) \sum_{i=1}^{n} \delta_i \log t_i - r \log \sum_{i=1}^{n} t_i^{\beta}.$$

To solve for the MLE for the shape parameter, maximize $l_p(\beta)$, or equivalently solve

$$S_p(\beta) \equiv \frac{d}{d\beta}(l_p(\beta)) = 0. \tag{2.3}$$

For right censored data, the profile (MLE) and modified profile (MMLE) scores are:

$$S_p(\beta) = \frac{r}{\beta} - r \frac{\sum_{i=1}^{n} t_i^{\beta} \log t_i}{\sum_{i=1}^{n} t_i^{\beta}} + \sum_{i \in D}^{n} \log t_i \tag{2.4}$$

$$S_m(\beta) = \frac{r-1}{\beta} - r \frac{\sum_{i=1}^{n} t_i^{\beta} \log t_i}{\sum_{i=1} t_i^{\beta}} + \sum_{i \in D} \log t_i \tag{2.5}$$

where D is the set of non-censored observations and r is the number of non-censored observations. Solving (2.4) and (2.5) with (2.3) will yield estimates, $\hat{\beta}_p$ and $\hat{\beta}_m$, which are the profile and modified Weibull scale parameter estimates, respectively. Estimates for the scale estimate associated with the profile shape, $\alpha_p = \alpha(\beta_p)$, and the scale estimate associated with the modified shape, $\alpha_m = \alpha(\beta_p)$, can be calculated using (2.2).

2.2.3 Second- and Third-order Stochastic Expansion of the MLE

To improve on the bias reduction in [123, 124], the work in [103] evaluates the second- and third-order stochastic bias in the shape estimate, $\hat{\beta}$. [103] defines the third-order stochastic expansion of the bias by

$$\hat{\beta} - \beta = a_{1/2} + a_{-1} + a_{-3/2} + O_p(n^{-2}) \ ,$$

where $a_{i/2}, i = 1, 2, 3$, are defined to be the terms of order $O_p(n^{-i/2})$, and are functions consisting of the score function (2.3) and derivatives of the score function. They define the second-order bias as $b_2 = E(a_{-1/2} + a_{-1})$, and the third-order bias as $b_3 = E(a_{-3/2})$. As there is not an analytical solution to these bias terms, one can calculate the second- and third-order bias corrected MLEs using a bootstrap method described in their paper [103]. After estimating the bias terms, the shape estimates are calculated using

$$\hat{\beta}_n^{bc2} = \hat{\beta}_n - \hat{b}_2 \quad (2.6)$$

$$\hat{\beta}_n^{bc3} = \hat{\beta}_n - \hat{b}_2 - \hat{b}_3 \ . \quad (2.7)$$

The second-order stochastic estimate, (2.6), will be referred to as BC-2 while the third-order stochastic estimate, (2.7), will be referred to as BC-3 .

2.2.4 Oversampling

Over-sampling and under-sampling of minority and majority class observations has been used to improve classifier performance [3]. The Synthetic Minority Oversampling Technique (SMOTE) is "the 'de facto' standard or benchmark in learning from imbalanced data set[s]" [33]. The standard SMOTE as originally introduced by [16] involves oversampling observations from the minority class by creating new synthetic examples within a neighborhood of the minority class observations. The synthetic examples are created by randomly selecting an observation and another observation within a specified neighborhood. A random point along the interpolated line segment between the two observations is chosen as the synthetic example. The process is repeated until a specified number of synthetic examples are created. The majority of the extensions to the standard SMOTE algorithm are related to classifications problems.

Although MLE is not the same as a classification problem, dealing with censored data can present a similar problem by having a minority class with far fewer observations than the majority class. Depending upon the amount of censoring, the minority (or majority) class may be the censored or non-censored sets. A handful of studies that have expanded SMOTE to applications other than classification problems include regression, such as the SMOTER algorithm [115]. The SMOTER method was applied to time series forecasting in [70]. However, in both of these studies the data sets under consideration were not "small" (> 198 for [115] and > 500 for [70]). As this paper considers small sample sizes, it will expand the SMOTE algorithm to allow over-sampling of the minority and majority classes when estimating the Weibull scale parameter ($\hat{\alpha}$) to allow for the increase of the overall sample sizes.

2.2.5 Goodness of Fit Measure

While this paper seeks to decrease the bias in the scale parameter estimates it is necessary to evaluate the overall effect of reducing the bias for both parameters in a Weibull distribution. The Kullback-Leibler divergence is one method to measure the relative information loss, or relative entropy, when representing one distribution by another [57]. It is defined as

$$D_{KL}(P||Q) = \int_{-\infty}^{\infty} p(x) \ln \frac{p(x)}{q(x)} dx,$$

where P is a known or reference distribution and Q is an estimated distribution. A smaller K-L divergence indicates a smaller loss of information while a larger K-L divergence indicates a larger loss of information. [8] provides an analytic solution for the case where P and Q are both Weibull distributions. Given a reference distribution with density $p(x|\alpha_1, \beta_1)$ and an approximated distribution with density $q(x|\alpha_2, \beta_2)$, the K-L divergence is calculated by

$$\begin{aligned} D_{KL}(P||Q) &= \int_0^\infty p(x|\alpha_1, \beta_1) \ln \frac{p(x|\alpha_1, \beta_1)}{q(x|\alpha_2, \beta_2)} dx \\ &= \ln \frac{\beta_1}{\alpha_1^{\beta_1}} - \ln \frac{\beta_2}{\alpha_2^{\beta_2}} + (\beta_1 - \beta_2) \left[\ln \alpha_1 - \frac{\gamma}{\beta_1} \right] + \left(\frac{\alpha_1}{\alpha_2} \right)^{\beta_2} \Gamma \left(\frac{\beta_2}{\beta_1} + 1 \right) - 1 \, , \end{aligned} \tag{2.8}$$

where $\gamma = 0.5772$ is the Euler-Mascheroni constant and $\Gamma(\,)$ is the gamma function.

One criticism of the K-L divergence is that it does not satisfy the triangle inequality due to asymmetry and is not a true distance metric [66]. This should not be an issue with the current application as it seeks to measure the loss of information when modeling the distribution P with the estimated distribution Q, which can be allowed to be asymmetric. If the use of a symmetric divergence metric is desired, one can use the Jeffreys divergence [77] which is calculated

$$J(P, Q) = D_{KL}(P||Q) + D_{KL}(Q||P).$$

Another alternative is the Jensen-Shannon divergence [66] which is calculated

$$JS(P, Q) = D_{KL}(P||(P + Q)/2) + D_{KL}(Q||(P + Q)/2).$$

While the Jeffreys divergence between two distributions can rely upon the analytic solution (2.8), the Jensen-Shannon divergence may not have an easily attained analytic solution due to averaging the distributions and must rely upon numerical integration. In this paper, (2.8) will be used to measure the impact of simultaneously reducing the bias in both the shape and scale. This use of the K-L divergence is also aligned with our use of MLE, which in principle also aims to minimize the K-L divergence [17].

2.3 Extending Profile Methods to Generalized Type I Censoring

This section demonstrates how the modified profile (MMLE) method proposed by [123] and the stochastic expansion methods (BC-2 and BC-3) by [103] can reduce the bias in the shape parameter with a generalized Type I censoring mechanism. When considering the profile likelihood, the methods described in Section 2.2 only focus on removing the bias related to the shape parameter. The scale parameter is estimated using (2.2) and there is no guarantee in regards to the bias reduction for this parameter. This section will also show that the bias in the scale parameter as measured with RMSE and MAE may actually increase.

2.3.1 Generalized Type I Censoring Artificial Data

To simulate generalized Type-1 censored data requires generating lifetimes as well as introduction dates. For this study, the lifetimes will be assumed to come from a Weibull distribution ($L \sim Weib(\alpha, \beta)$) while the introduction dates will assume to uniformly distributed ($D \sim U(0, T_C)$). Random variates are generated for T_i as described in Section 2.2. A new random variable is introduced which is the sum of the lifetime and the introduction date, $T = L + D$. An item will have a censored lifetime if $T \geq T_C$, where T_C is the censoring time.

The generalized Type I data is generated using scale value of 100 ($\alpha = 100$) and varying shapes of 0.5, 1.0, and 2.0 ($\beta = \{0.5, 1.0, 2.0\}$). Three values for the expected percent censored are chosen ($pc = \{30, 50, 70\}$). For each combination of β and pc, values for T_C are chosen using (2.16) shown in 2.8. To ensure that the generated data is 'close' to the target pc value, an acceptance-rejection method is used. For each value of pc, values outside of $\pm 5\%$ are rejected. For example, a target percent censored of $pc = 30$, will only keep data with a percent censored in the range $[25, 35]$, $pc = 50, [45, 55]$, and $pc = 70, [65, 75]$. Additionally, the number of items, or sample size, n is varied from 20 to 50 ($n = \{20, 30, 50\}$). Values for T_C that will ensure the expected percent censored are shown in Table 2.1.

Using the methods described in Section 2.2 to estimate the shape parameters, the profile shape estimate, $\hat{\beta}_p$, is calculated using (2.4); the modified profile shape estimate, $\hat{\beta}_m$, is calculated using (2.5); and the second- and third-order stochastic expansion shape estimates, $\hat{\beta}_{bc2}$ and $\hat{\beta}_{bc3}$, are calculated using (2.6) and (2.7), respectively. Estimates for the scale parameter for each method are calculated using (2.2), e.g. $\hat{\alpha}_p = \hat{\alpha}(\hat{\beta}_p)$; $\hat{\alpha}_m = \hat{\alpha}(\hat{\beta}_m)$; $\hat{\alpha}_{bc2} = \hat{\alpha}(\hat{\beta}_{bc2})$; and $\hat{\alpha}_{bc3} = \hat{\alpha}(\hat{\beta}_{bc3})$.

Table 2.1: Values of T_C that give the expected values of percent censored ($pc = E[\%\text{ cens}]$) for $\alpha = 100$ and various β and T_C values. The value in parenthesis is the actual expected percent censored for the associated value of T_C.

	pc		
β	$30\,([25, 35])$	$50\,([45, 55])$	$70\,([65, 75])$
0.5	375 (30.75%)	120 (49.88%)	30 (70%)
1.0	330 (29.19%)	160 (49.88%)	75 (70.35%)
2.0	290 (30.56%)	175 (49.97%)	110 (70.91%)

2.3.2 Numerical Results for Shape and Scale Estimates

The two loss functions used to measure the bias in shape and scale parameter estimates are the root mean-squared error (RMSE)

$$RMSE = \sqrt{\frac{\sum_{i=1}^{m}(\alpha - \hat{\alpha}_i)^2}{m}}\ ,$$

and the mean absolute error (MAE)

$$MAE = \frac{1}{m}\sum_{i=1}^{m}|\alpha - \hat{\alpha}_i| \tag{2.9}$$

Where α is the known scale value used in step 1 above and $\hat{\alpha}$ is the i^{th} sample replication for each of m samples. The shape value β can be substituted in for instances of α as necessary.

The relative improvement for both the RMSE and MAE are given in Tables 2.2 and 2.3. This measures the relative improvement for the MMLE, BC-2, or BC-3 methods over the standard MLE method. For example, the relative improvement of the scale estimate when using the MMLE method measured by the RMSE and MAE is calculated using

$$Rel_{R,m} = \frac{(RMSE_{\hat{\alpha}_p} - RMSE_{\hat{\alpha}_m})}{RMSE_{\hat{\alpha}_p}}, \tag{2.10}$$

$$Rel_{M,m} = \frac{(MAE_{\hat{\alpha}_p} - MAE_{\hat{\alpha}_m})}{MAE_{\hat{\alpha}_p}}. \tag{2.11}$$

The relative improvements for the BC-2 ($Rel_{R,bc2}, Rel_{M,bc2}$) and BC-3 ($Rel_{R,bc3}, Rel_{M,bc3}$) methods can also be calculated using (2.10) and (2.11). Positive values of Rel will indicate that the method (MMLE, BC-2, BC-3) is an improvement over the standard method (MLE), while negative values will indicate that the method does not improve over the standard method.

Table 2.2 shows the relative improvement for the shape parameter using MAE and RMSE for $m = 1000$ replications for each triplet of $\{\beta, p, n\}$. In all cases, the relative improvement in the bias is positive over the profile MLE method when using the MMLE, BC-2, and BC-3 methods as measured by MAE and RMSE. In general, the relative improvement tends to decrease as the sample size increases for both MAE and RMSE. The BC-2 and BC-3 methods tend to outperform the MMLE method, but this is not always the case. For example, with $\beta = 0.5$ and $p = 70$ when $n = 20$ the BC-2 method shows similar performance with MMLE when measured by MAE (0.120 vs. 0.120) while the BC-3 method shows a decrease in MAE (0.109 vs 0.120). However, both the BC-2 and BC-3 show decreases when measured by RMSE (0.168 and 0.138 vs. 0.175). In most other cases the BC-2 and BC-3 methods improve the relative improvement over the MMLE method. All of the values in this table are positive, indicating that the three methods (MMLE, BC-2, and BC-3) can be applied successfully to the the generalized Type I censoring mechanism.

Table 2.2: Relative Improvement of MAE and RMSE for Weibull shape parameter (β) using MLE, MMLE, BC-2, and BC-3 for Generalized Type I Censored Data. ($\alpha = 100$) (MAE ($Rel_{M,\cdot}$) // RMSE ($Rel_{R,\cdot}$))

β	p	n	MMLE	BC-2	BC-3
0.5	30	20	0.040 // 0.069	0.061 // 0.092	0.061 // 0.092
		30	0.049 // 0.065	0.049 // 0.074	0.049 // 0.074
		50	0.016 // 0.026	0.016 // 0.038	0.016 // 0.026
	50	20	0.060 // 0.098	0.068 // 0.115	0.068 // 0.109
		30	0.041 // 0.069	0.051 // 0.077	0.051 // 0.069
		50	0.027 // 0.050	0.027 // 0.050	0.027 // 0.050
	70	20	0.120 // 0.175	0.120 // 0.168	0.109 // 0.138
		30	0.051 // 0.114	0.051 // 0.114	0.059 // 0.098
		50	0.030 // 0.068	0.040 // 0.068	0.040 // 0.061
1.0	30	20	0.047 // 0.070	0.089 // 0.133	0.094 // 0.133
		30	0.041 // 0.058	0.075 // 0.099	0.075 // 0.099
		50	0.017 // 0.028	0.035 // 0.048	0.035 // 0.048
	50	20	0.063 // 0.091	0.093 // 0.136	0.097 // 0.130
		30	0.041 // 0.068	0.061 // 0.094	0.061 // 0.091
		50	0.021 // 0.037	0.028 // 0.048	0.028 // 0.048
	70	20	0.109 // 0.161	0.123 // 0.178	0.117 // 0.155
		30	0.063 // 0.107	0.070 // 0.116	0.074 // 0.107
		50	0.026 // 0.064	0.032 // 0.068	0.037 // 0.068
2.0	30	20	0.067 // 0.081	0.109 // 0.153	0.106 // 0.149
		30	0.041 // 0.059	0.078 // 0.113	0.075 // 0.110
		50	0.030 // 0.037	0.052 // 0.073	0.052 // 0.070
	50	20	0.077 // 0.100	0.129 // 0.172	0.127 // 0.165
		30	0.049 // 0.066	0.091 // 0.121	0.088 // 0.117
		50	0.029 // 0.044	0.055 // 0.077	0.055 // 0.075
	70	20	0.094 // 0.147	0.147 // 0.204	0.133 // 0.177
		30	0.058 // 0.097	0.090 // 0.134	0.088 // 0.123
		50	0.026 // 0.052	0.040 // 0.069	0.040 // 0.067

Table 2.3 shows the relative improvement for the scale parameter using the MAE and RMSE for $m = 1000$ replications for each triplet of $\{\beta, p, n\}$. In all cases, the relative improvement in the bias is negative over the profile MLE method when using the MMLE, BC-2, and BC-3 methods as measured by MAE and RMSE. As with the shape parameter

estimates, the (magnitude of the) relative improvement tends to decrease as the sample size increases for both MAE and RMSE, but with a few exceptions. In terms of relative improvement the BC-2 and BC-3 methods tend to do worse (i.e. have a greater magnitude) than the MMLE method for MAE and RMSE. As the percent censored increases or the shape value decreases, the relative improvement tends to worsen across all three methods. Contrary to the results above for the shape value, all of the values in this table are negative indicating that while the MMLE, BC-2 and BC-3 methods reduce the bias in the shape parameter estimates, they increase the bias in the scale parameter estimates when using a generalized Type I censoring mechanism.

Table 2.3: Relative Improvement of MAE and RMSE for Weibull scale parameter (α) using MLE, MMLE, BC-2, and BC-3 for Generalized Type I Censored Data. (α = 100) (MAE ($Rel_{M,\cdot}$) // RMSE ($Rel_{R,\cdot}$))

β	p	n	MMLE	BC-2	BC-3
0.5	30	20	-0.045 // -0.057	-0.975 // -1.61	-0.953 // -1.556
		30	-0.029 // -0.037	-0.751 // -1.166	-0.745 // -1.154
		50	-0.018 // -0.021	-0.685 // -0.929	-0.683 // -0.926
	50	20	-0.27 // -0.383	-1.965 // -4.472	-1.71 // -3.732
		30	-0.16 // -0.247	-1.902 // -8.068	-1.791 // -7.388
		50	-0.082 // -0.114	-0.883 // -1.351	-0.867 // -1.322
	70	20	-5.171 // -11.597	-317.518 // -845.546	-87.878 // -221.187
		30	-1.059 // -1.771	-15.803 // -89.477	-11.42 // -70.123
		50	-0.351 // -0.517	-1.485 // -3.295	-1.338 // -3.018
1.0	30	20	-0.017 // -0.018	-0.703 // -0.841	-0.698 // -0.835
		30	-0.01 // -0.011	-0.618 // -0.754	-0.616 // -0.752
		50	-0.006 // -0.006	-0.514 // -0.569	-0.513 // -0.568
	50	20	-0.128 // -0.183	-1.046 // -3.876	-0.966 // -3.361
		30	-0.071 // -0.096	-0.922 // -1.304	-0.902 // -1.272
		50	-0.045 // -0.057	-0.495 // -0.644	-0.49 // -0.635
	70	20	-0.718 // -1.234	-2.399 // -6.574	-1.699 // -4.365
		30	-0.332 // -0.519	-1.411 // -3.721	-1.209 // -3.03
		50	-0.168 // -0.245	-0.623 // -0.846	-0.586 // -0.796

Continued on next page

Table 2.3 – *Continued from previous page*

2.0	30	20	-0.005 // -0.004	-0.408 // -0.434	-0.407 // -0.433
		30	-0.003 // -0.003	-0.38 // -0.393	-0.38 // -0.392
		50	-0.002 // -0.001	-0.41 // -0.447	-0.408 // -0.447
	50	20	-0.037 // -0.049	-0.734 // -0.93	-0.715 // -0.898
		30	-0.025 // -0.031	-0.575 // -0.675	-0.57 // -0.667
		50	-0.017 // -0.02	-0.551 // -0.59	-0.55 // -0.588
	70	20	-0.298 // -0.506	-1.476 // -5.376	-1.245 // -4.309
		30	-0.172 // -0.247	-0.788 // -1.187	-0.732 // -1.085
		50	-0.092 // -0.127	-0.597 // -0.727	-0.581 // -0.704

2.4 Oversampling Methodology

As the previous section indicates, the profile likelihood methods can successfully reduce the bias in the shape parameter with a generalized Type I censoring mechanism, but does not ensure a reduction in the bias of the scale parameter. This section proposes a methodology to reduce the bias in the scale parameter, and thus the overall bias in a Weibull distribution using an oversampling process akin to SMOTE. The proposed methodology is presented in the form of a simulation study.

1. Data Generation: Generate R samples of data D_i of sample size n for $i \in \{1, \ldots, R\}$ from a given (known) shape β and scale α. To ensure stability in later parameter estimates, ensure that the percent censored, pc_1, will be taken according to the the values of T_C shown in Table 2.1.

2. Parameter Estimation: Estimate the shape $\hat{\beta}_i$ and scale $\hat{\alpha}_i(\hat{\beta}_i)$, for each sample $i \in \{1, \ldots, R\}$. This paper will use the BC-3 method described in Section 2.2.3, but other methods can be used.

3. Oversampling: For each point p in the $\mathcal{N} \times \mathcal{C}$ grid, over-sample using the modified SMOTE method described in Section 2.2.4. Repeat the modified SMOTE oversampling K times, using j neighbors, and for each point calculate estimates for $\hat{\alpha}'_{ikp}(\hat{\beta}_i|t')$ using

(2.2). The value $t' = \{t, t_n, t_c\}$ represents the updated data where t is the original data, t_n is the synthetic data for the non-censored data values, and t_c is the synthetic data from the censored data values. The sets $\mathcal{N}$ and $\mathcal{C}$ are non-negative integers, representing the total amount of oversampling for the non-censored and censored values in the data, D_i, respectively. For this paper, $\mathcal{N}, \mathcal{C} \in \{0, 10, \ldots, 100\}$ yielding a grid consisting of 121 points.

4. Measure Improvement: For each data set $i \in \{1, \ldots, R\}$ calculate the mean scale value

$$\overline{\hat{\alpha}}_{ip} = \frac{\sum_{k=1}^{K} \hat{\alpha}'_{ikp}}{K}$$

at each point $p \in \mathcal{N} \times \mathcal{C}$. Then use $\overline{\hat{\alpha}}_{ip}$ to calculate the K-L divergence

$$KL_{ip} = D_{KL}\left(\alpha, \beta, \overline{\hat{\alpha}}_{ip}, \hat{\beta}_i\right) \tag{2.12}$$

at each point p for each data set i. Next, calculate the difference between the K-L divergence with no oversampling and (2.12) at each point

$$\delta_{ip} = KL_{i\{0,0\}} - KL_{ip} \ , \tag{2.13}$$

for each data set i. Note that the value for $\delta_{i,p}$ can be positive or negative. Positive values will correspond to an improvement in the distribution (positive improvement) while negative values will correspond to the opposite of an improvement in the distribution (negative improvement), as measured by the K-L divergence. The K-L divergence with no oversampling is defined as

$$KL_{i\{0,0\}} = D_{KL}\left(\alpha, \beta, \hat{\alpha}_i, \hat{\beta}_i\right).$$

To measure the expected improvement for oversampling at each point, calculate

$$\bar{\delta}_p = \frac{\sum_{i=1}^{R} \delta_p}{R}.$$

The set of points p^* where

$$\bar{\delta}_{p^*} - t_{\alpha, R-1} \cdot s_{\delta_{p^*}} > 0$$

are the set of points where oversampling will improve, in expectation, the overall distribution for a given confidence level α. The value $s_{\delta_{p^*}}$ is the standard deviation of (2.13) for each p and $t_{\alpha,R-1}$ is the critical value of the $t-$distribution at the significance level α with $R-1$ degrees of freedom.

2.5 Numerical Simulation

A Monte-Carlo simulation is presented in this section to show the efficacy of the method proposed in Section 2.4. A value of $j = 4$ neighbors is used in the modified SMOTE method, where 2 smaller and 2 larger values are chosen when calculating the interpolated synthetic point. Values for this study are $R = 1000$, $K = 200$, $\alpha = 100$, $\beta = \{0.5, 1.0, 2.0\}$, $pc = \{30, 50, 70\}$ and $n = \{20, 30, 50\}$. Each generated data set uses a value for T_C as indicated in Table 2.1 for a given shape and expected percent censored value. The BC-3 method for parameter estimation will be used for this simulation.

Figures 2.2 - 2.4 show the points in the $\mathcal{N} \times \mathcal{C}$ grid associated with positive improvement for $\beta = 0.5, 1.0$, and 2.0, respectively, and various values of n and pc. The rows, as moving from top to bottom, represent sample sizes of $n =$ 20, 30, and 50, while the columns, as moving from left to right, represent percent censored values of $pc =$ 30, 50, 70. For each sub-figure the horizontal axis represents the amount of oversampling using the non-censored data and the vertical axis represents the amount of oversampling using the censored data.

In the case where $\beta = 0.5$ (Figure 2.2), there is a clear pattern for each of the percent censored values (i.e. each column). The pattern remains for each percent censored value as the sample size increases (i.e. each row). When there is $\sim 30\%$ censoring, the points in the grid that show positive improvement tend to rely on the non-censored values more than the censored values in creating the synthetic data. This can be seen in the approximate 'line' that is less than 45 degrees. As the sample size increases the magnitude of the maximum expected amount of improvement tends to decrease; as one moves down the first column the maximum value of improvement goes from (approximately) 0.038 to 0.022 to 0.016 nats. When there is $\sim 50\%$ censoring, improvements tend to occur along a 45 degree 'line', where

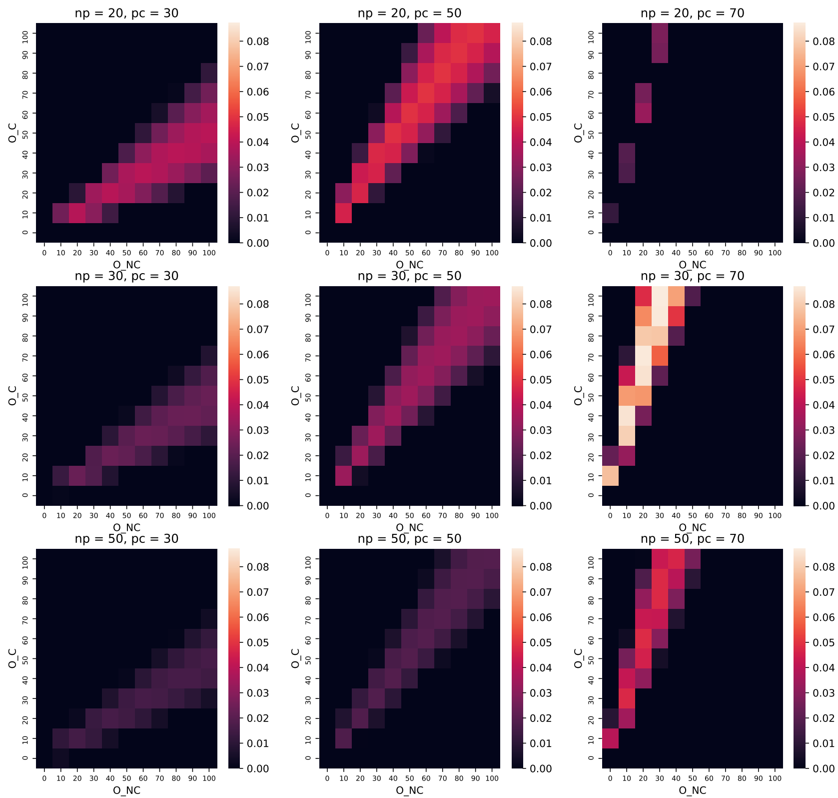

Figure 2.2: Improvement in K-L divergence for $\beta = 0.5$. Each row shows an increasing sample size (from top to bottom: 20, 30, 50) while columns show an increasing percent censored (from left to right: 30%, 50%, 70%). ($\beta = 0.5, \alpha = 100, R = 1000, K = 200$)

there is equal amount of reliance upon non-censored and censored data. Again, there tends to be a decrease in the maximum expected amount of improvement as one moves down the second column, but there is also a potential to see an overall higher increase in the improvement when compared to the lower percent censored values. Finally, when there is $\sim 70\%$ censoring the improvements appear to occur along the 'line' that is greater than 45 degrees indicating improvement when relying on the censored values as opposed to the non-censored values when using the modified SMOTE algorithm. The potential for improving the K-L divergence is higher when compared to lesser percent censored data for sample sizes of 30 and 50 (not for a sample size of 20), but there appears to be less oversampling points in the $\mathcal{N} \times \mathcal{C}$ grid where there is a positive improvement.

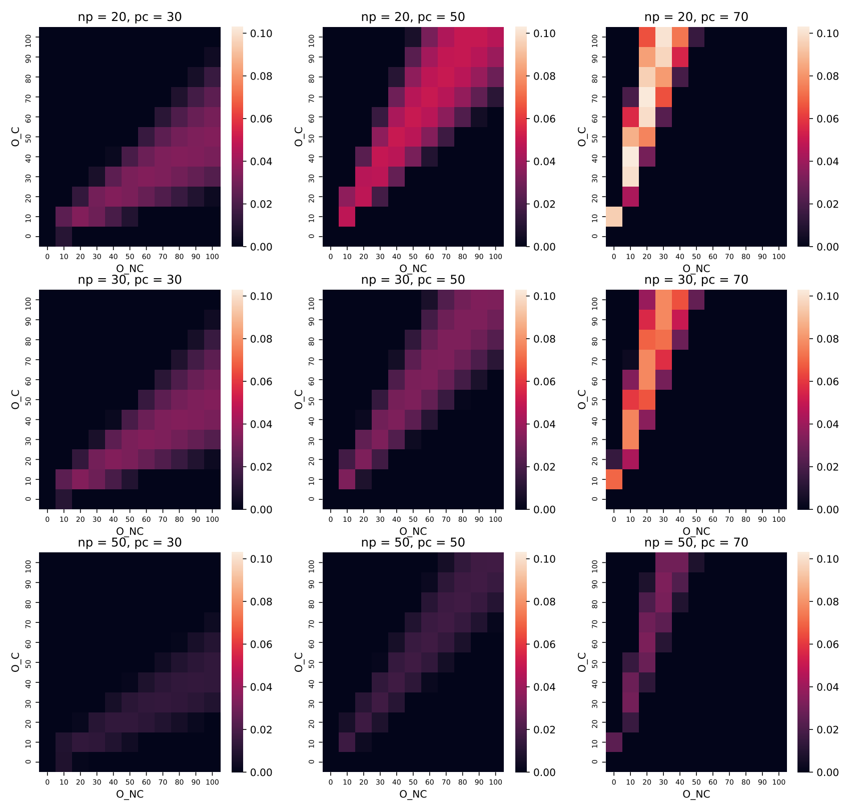

Figure 2.3: Improvement in K-L divergence for $\beta = 1.0$. Each row shows an increasing sample size (from top to bottom: 20, 30, 50) while columns show an increasing percent censored (from left to right: 30%, 50%, 70%). ($\beta = 1.0, \alpha = 100, R = 1000, K = 200$)

In the cases of $\beta = 1.0$ (Figure 2.3) and $\beta = 2.0$ (Figure 2.4), there are many of the same insights as with $\beta = 0.5$. For instance, as the sample size increases the maximum expected amount of improvement decreases. Likewise, as the percent censored increases, the potential to improve the maximum expected K-L divergence increases. The magnitudes of

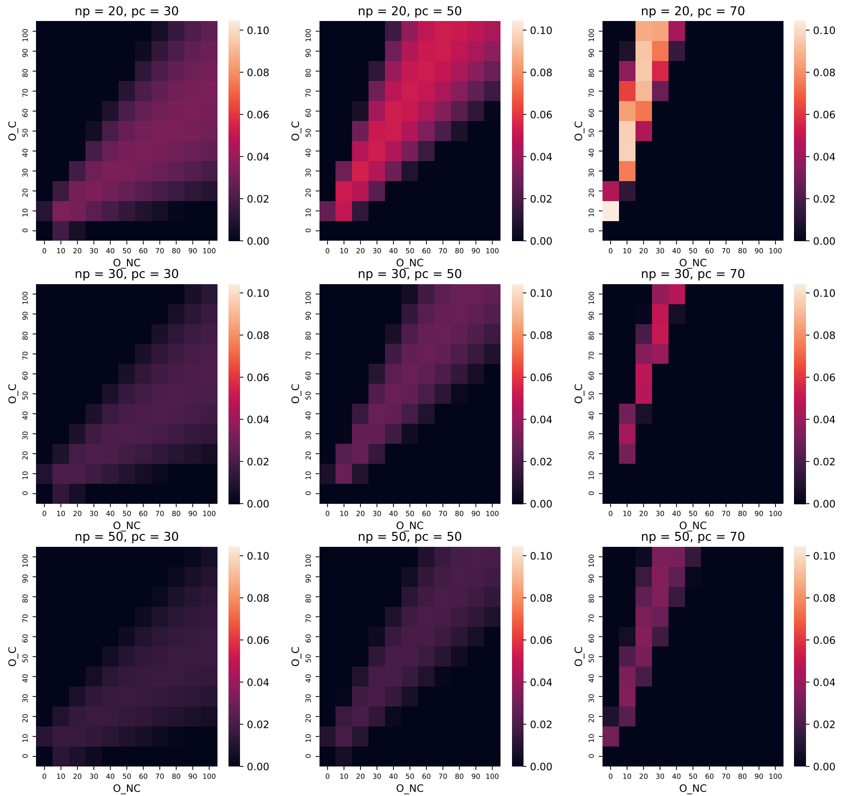

Figure 2.4: Improvement in K-L divergence for $\beta = 2.0$. Each row shows an increasing sample size (from top to bottom: 20, 30, 50) while columns show an increasing percent censored (from left to right: 30%, 50%, 70%). ($\beta = 2.0, \alpha = 100, R = 1000, K = 200$)

the maximum expected improvement are of roughly the same magnitude across all values of β, with the one possible exception in the case of $\beta = 0.5, np = 20$, and $pc = 70$. With $\beta = 2.0$ there appears to be a larger region of expected improvement when compared to other values of β, particularly when $pc = 30$ or 50 for all sample sizes.

2.6 Case Study

This case study uses *integrated-circuit memory* data that is comprised of an introduction data and end-of-life (EOL) data if known. The data is assumed to not have any *evolutionary parametric drivers* [97]. The procurement lifetime is defined as the difference between the EOL date and the introduction date.

The data consists of 1143 observations where the introduction date for the first part is 1 January 2000. The data was extracted on 29 August 2019, and this date is the effective censoring date. At the censoring date, the data consists of 518 non-censored and 625 censored observations; approximately 54% censored data. Using the profile MLE method, the Weibull parameter estimates have a shape estimate of 2.042 and a scale estimate of 7047 days (or slightly more than 19 years), while the BC-3 method provides a shape estimate of 2.039 and a scale estimate of 6853 days (or slightly less than 19 years). Figure 2.5 provides the average scale parameter estimates for the points in the $\mathcal{N} \times \mathcal{C}$ oversampling grid using $K = 200$, where the origin (lower-left square) shows the BC-3 scale estimate.

Using the middle plot in the bottom row of Figure 2.4, one would expect the best oversampling strategy to have an approximately equal oversampling of censored and non-censored values. Figure 2.5 shows that if only the censored data is oversampled 100 times, the estimated scale parameter is 7420. If only the non-censored data is oversampled 100 times, the estimated scale parameter is 6649. In Figure 2.5, the scale estimates on the diagonal show that the oversampling-based estimates at $O_{NC} = O_C > 0$ tend to be slightly greater than the estimate from the BC-3 method (at $O_{NC} = O_C = 0$). In other words, the oversampling result suggests that a scale of 6853 days is likely an underestimated value. Therefore, one can either increase the estimate based on Figure 2.5 to reduce the potential bias or interpret the subsequent forecasting based on a scale of 6927 days with a caution on the underestimated scale. In practical terms, the underestimation of the scale parameter means that a part may be forecasted to become obsolete 100-200 days early (i.e. range of the scale parameter is approximately 6900 to 7100 days as given by the values on the diagonal in Figure 2.5.

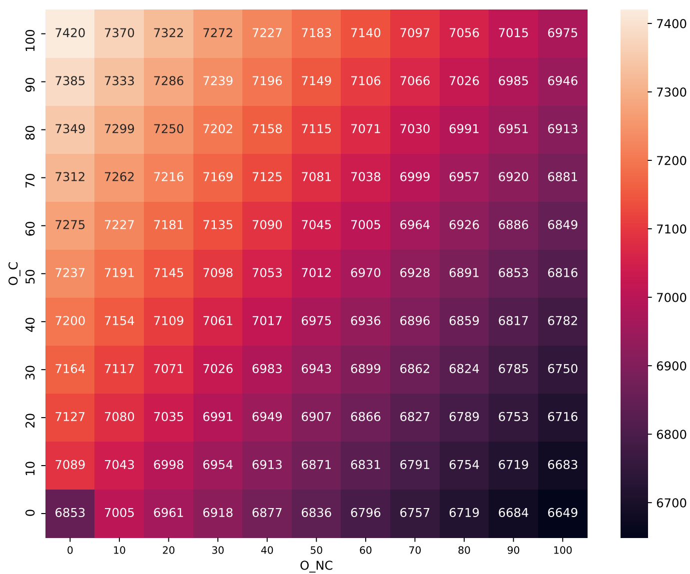

Figure 2.5: Weibull scale parameter estimates for integrated-circuit memory data using the proposed oversampling methodology. Units for the scale values presented are in days.

2.7 Conclusion

This work has shown that three profile likelihood methods (i.e. MMLE, BC-2, BC-3) minimize the bias in the shape estimates for a Weibull distribution when compared to the standard profile MLE for the generalized Type I censoring mechanism. However, using these methods will induce a bias that is larger than the profile MLE estimate (see Table 2.3). As expected, the amount of bias tends to be larger as the sample size is smaller and/or the percent censored is larger. The generalized Type I censoring considered in this study assumes a uniform distribution for introduction dates and the Weibull distribution for the item lifetimes but can be extended to other distributions as necessary. The analysis in 2.8 can be used as a framework to account for different distributions by exchanging values for the introduction and procurement lifetime dates.

The results in Section 2.5 show that the bias in the scale parameter can be decreased as evidenced by a decrease in the K-L divergence. The general pattern points to a reliance on oversampling synthetic data from the non-censored data when the percent censored is low, relying more on censored data when the percent censored is high, and relying on both censored and non-censored data when the percent censored is moderate. These results are promising to solve the problem of estimating a probability distribution with smaller sample sizes and higher levels of censoring. Extending this method to a case study with only a single data set can provide a modeler a range of reasonable values to consider as shown in Section 2.6, despite not knowing the true parameter values.

2.8 Expected Value of Percent Censored for Generalized Type I Censoring

The current lifetime T_i as discussed in Section 2.2 consists of a lifetime, $L_i \sim f_L(\theta_L)$, and an introduction date, $D_i \sim f_D(\theta_D)$, where f_L, θ_L are the PDF and parameters of the lifetime and f_D, θ_D are the PDF and parameters of the introduction date. The random variable T_i represents a value that dictates the obsolescence status of the item, relating the introduction date, procurement lifetime, and the censoring time. The expected value of a random item being censored (non-obsolete) is given by:

$$\begin{aligned}\mathbb{E}[\text{item being censored}] &= \mathbb{E}\left[\mathbb{I}(T_i \geq T_C)\right] \\ &= 1 \cdot P(T_i \geq T_C) + 0 \cdot P(T_i < T_C) \\ &= P(T_i \geq T_C). \end{aligned} \tag{2.14}$$

where $\mathbb{I}(\cdot)$ is the indicator function. Rewriting (2.14) using a convolution yields

$$\begin{aligned}P(T_i \geq T_C) &= 1 - F_{T_i}(T_C) \\ &= 1 - F_{L_i+D_i}(T_C) \\ &= 1 - \iint\limits_{l+d<T_C} f_{D_i}(d) f_{L_i}(l) \mathrm{d}d\, \mathrm{d}l \\ &= 1 - \int_0^{\infty} \int_0^{T_C - l} f_{D_i}(d) f_{L_i}(l) \mathrm{d}d\, \mathrm{d}l\end{aligned}$$

$$
\begin{aligned}
&= 1 - \int_0^\infty \left(\int_0^{T_C - l} f_{D_i}(d)\mathrm{d}d \right) f_{L_i}(l)\mathrm{d}l \\
&= 1 - \int_0^\infty F_{D_i}(T_C - l) f_{L_i}(l)\mathrm{d}l, \\
&= 1 - \int_0^{T_C} F_{D_i}(T_C - l) f_{L_i}(l)\mathrm{d}l + \int_{T_C}^\infty F_{D_i}(T_C - l) f_{L_i}(l)\mathrm{d}l \\
&= 1 - \int_0^{T_C} F_{D_i}(T_C - l) f_{L_i}(l)\mathrm{d}l, \qquad (+ \quad 0)
\end{aligned} \tag{2.15}
$$

where F_{T_i} $(= F_{L_i + D_i})$ is the cumulative distribution function (CDF) of the random variable T_i $(= L_i + D_i)$, F_{D_i} is the CDF of D_i, and $f_L(l)$, $f_{D_i}(d)$ are the PDFs of L_i and D_i, respectively. For arbitrary distributions of D_i and L_i, (2.15) can be solved numerically.

As this paper has assumed a uniform distribution for the introduction dates, F_D, on the interval $[0, T_C]$, and a Weibull distribution with shape parameter β and scale parameter α, (2.15) can be further simplified. Using the uniform distribution's CDF on the interval $[0, T_C]$,

$$
F_D(T - l) = \frac{T - l}{T},
$$

the Weibull PDF

$$
f_L(l) = \frac{\beta}{\alpha} \left(\frac{l}{\alpha} \right)^{\beta - 1} e^{-\left(\frac{l}{\alpha}\right)^\beta},
$$

and the Weibull CDF

$$
F_L(l) = 1 - e^{-\left(\frac{l}{\alpha}\right)^\beta},
$$

(2.15) becomes

$$
\begin{aligned}
P(T \geq T_C) &= 1 - \int_0^{T_C} \frac{T_C - l}{T_C} f_L(l)\mathrm{d}l \\
&= 1 - \int_0^{T_C} \left(1 - \frac{l}{T_C} \right) f_L(l)\mathrm{d}l \\
&= 1 - \int_0^{T_C} f_L(l)dl + \int_0^{T_C} \frac{l}{T_C} \left(\frac{\beta}{\alpha} \left(\frac{l}{\alpha} \right)^{\beta - 1} e^{-\left(\frac{l}{\alpha}\right)^\beta} \right) \mathrm{d}l \\
&= 1 - \left(1 - e^{-\left(\frac{T_C}{\alpha}\right)^\beta} - 0 \right) + \frac{\beta}{\alpha^\beta\, T_C} \int_0^{T_C} l^\beta e^{-\left(\frac{l}{\alpha}\right)^\beta} \mathrm{d}l \\
&= e^{-\left(\frac{T_C}{\alpha}\right)^\beta} + \frac{\beta}{\alpha^\beta\, T_C} \int_0^{T_C} l^\beta e^{-\left(\frac{l}{\alpha}\right)^\beta} \mathrm{d}l.
\end{aligned} \tag{2.16}
$$

Thus the expected value of an item being censored is the same as the probability of it being censored and is given by equation (2.16).

The expected value of the number of parts being obsolete out of n parts has a binomial distribution where a success (censored) will occur with probability $p = \mathbb{E}[\text{item being censored}]$, and a failure (not censored) will occur with probability $q = 1 - p$. The expected number of successes (# censored) is

$$\mathbb{E}[\#\ \text{censored}] = np.$$

The expected percent censored is

$$\mathbb{E}[\%\ \text{censored}] = \frac{\mathbb{E}[\#\ \text{censored}]}{n} = p,$$

which is the same as (2.16).

Chapter 3

SIMULATING AVAILABILITY RISK AT THE SYSTEM LEVEL

This chapter presents the manuscript accepted for publication by the *International Journal of Production Research* [108].

3.1 Abstract

Many enterprise systems are comprised of parts with shorter product lifetimes than the system lifetime. Managing the availability of the parts in the supply chain to ensure uninterrupted operation of the system is non-trivial and can be costly in terms of capital and resources. A DMSMS (Diminishing Manufacturing Sources and Material Shortages) issue is the loss, or impending loss, of a manufacturer because the manufacturer discontinues production or support of needed parts. Proactive DMSMS requires the ability to forecast part availability in the marketplace under varying conditions. This paper goes beyond part-level forecasting by developing a framework to estimate availability risk at the system level. The proposed framework quantifies and compares availability risk for multiple parts in a system using a finite-source capacitated queuing model. Two availability risk metrics are defined: the fraction of time with no vendor parts available and the time until a part will be unavailable in the market. The metrics are demonstrated in scenarios that a DMSMS practitioner is likely to experience. The results demonstrate that the framework can be used to inform proactive DMSMS decisions by providing a measurement of the risk in the logistics system which supports cost and resource allocation trade-offs.

3.2 Introduction

The sustainment of long-life production and logistic systems can be adversely affected by part unavailability in the supply chain. Diminishing Manufacturing Sources and Material Shortages (DMSMS) is a subset of Supply Chain Risk Management (SCRM) that evaluates the manufacturing, supply, and demand risks associated with long-life systems. Conducting proactive DMSMS management is a non-trivial exercise as competing and limited budgets will often constrain the decision space for a supply chain analyst.

Proactive DMSMS requires an ability to forecast obsolescence risks for components and requires a process for articulating, reviewing, and updating the system status. Conversely, reactive DMSMS management is driven by part unavailability issues and can lead to costly solutions in order to keep a larger system in operation. DMSMS risk can be quantified via material risk index (MRI) [19, 104] and technology (or design) refresh planning [69, 107, 128]. While MRI studies tend to identify risk via probabilistic means, technology refreshes quantify the cost of proactive vs. reactive mitigation approaches. As such, these tools support a proactive DMSMS mitigation approach and allow for better management of the logistics surrounding production and logistic systems. This paper provides inputs to improve the efficacy of these tools.

Previous studies provide forecasts for procurement life-cycles, or the length of time a particular part is available from an original equipment manufacturer (OEM), but no studies have sufficiently provided a framework for evaluating aggregated risk across multiple parts [90]. Other studies have pointed out the need to take into account the product life-cycle curve of a technology [78, 106] and the size of the marketplace [89, 121]. An understanding of a system-level unavailability risk, or its propensity to be non-procureable in the market, is the first step in moving towards proactive DMSMS within the broader logistic system. Proactive DMSMS approaches must consider system-level availability risk, individual part procurement lifetimes, and also account for market size.

[45] identifies that the majority of SCRM research in the past has been focused on

'mathematical and stochastic optimization' and states that simulation modeling in SCRM remains 'under-explored'. [41] echo this refrain in their breakdown of published studies where the majority (57 of 119) include some form of mathematical programming or the newsvendor model while only a smaller number (10 of 119) included some form of simulation. They propose five risks associated with SCRM, including macro risk, demand risk, manufacturing risk, supply risk, and infrastructural risk. DMSMS seeks to address important elements of manufacturing risk (as a function of product obsolescence, design change, and technological change) and supply risk (as a result of the effects of single supply sourcing).

The primary contribution of this paper is casting the DMSMS management problem into a novel queuing modeling framework that compares availability risk at the system level taking into account the number of alternative parts in a market. Two availability risk metrics are proposed that allow for implementing the queuing modeling framework as a discrete event simulation (DES) model to quantify and compare the availability risk for the system. The modeling framework starts from a finite-source capacitated queuing model for each configuration part as an element of a bill of materials (BOM). Each queuing model takes into account the procurement lifetime distributions for that particular part type and the number of tracked parts (or market size) over time for individual technologies.

The remainder of this paper is as follows: Section 3.3 discusses work relevant to DMSMS issues; Section 3.4 discusses the modeling framework; Section 3.5 presents two scenarios that identify and highlight specific DMSMS issues answered by the proposed modeling framework; Section 3.6 discusses insights from the simulation results, provides recommendations for future work, and provides a summary of findings.

3.3 Related Work

This section discusses the background materials related to the modeling framework: a definition for DMSMS, resolution options available to analysts, previous models that have aggregated DMSMS risk over a system, forecasting methods used in other studies to predict procurement lifetimes, and the product life-cycle curve. This study defines a system, or assembly, as the collection of components consisting of sub-parts or sub-assemblies as defined in a BOM [90].

The U.S. Department of Defense (DoD) defines DMSMS as 'the loss, or impending loss, of manufacturers or suppliers of items, raw materials, or software' [23]. At its heart, DMSMS issues are supply chain issues not related to the transportation or exchange of parts, but rather related to the ability to acquire or procure a part. Obsolescence is an example of a potential DMSMS issue that deals with the loss of original manufacturers, suppliers, or raw materials [99], but obsolescence does not always become a DMSMS issue. Mitigation options include using existing stock, lifetime buys, substitution, aftermarket purchase, developing a new source (emulation), extending production, repair, refurbishment, reclamation, and re-design [23, 26, 69, 106, 129]. [43] provide a promising framework to measure and account for the 'circular economy', which refers to solutions such as repairs, refurbishment, and reclamation. Similarly, [26] use a newsvendor model evaluating decisions regarding remanufacturing. Using these resolution options can mitigate the risk of an obsolescence issue.

DMSMS management strategies can be broken down into three categories: reactive, proactive, and strategic [94]. Reactive DMSMS management is characterized by actions taken after a DMSMS event has occurred and tends to be associated with higher life-cycle costs. Proactive DMSMS management creates obsolescence forecasts and takes into account obsolescence mitigation options such as lifetime buys, etc. Strategic DMSMS management uses a combination of reactive mitigation methods and planned technology refreshes to find the optimal strategies that minimize overall life-cycle costs. A similar breakdown is provided by [114] but labels them 'Levels 1-3'. Some of the potential benefits of performing proactive or strategic DMSMS management (as opposed to reactive) include the following: improved budget allocation, improved operational availability, and better design refresh guidelines for system modification [104]. Forecasting availability risk of multiple parts in a system will provide a proactive management tool that can also inform strategic DMSMS management.

Two strategic management tools identified in the DMSMS literature are using material risk indices (MRI) and technology (or design refresh) planning. A MRI calculates a risk score for specified parts from the BOM of a system. Typically, this risk is measured in the likelihood of becoming obsolete [90]. The score is often combined with other data, specifically cost and consumption rates to evaluate a cost at risk related to obsolescence [104]. [19] identify that the number of manufacturers (“alternate suppliers”) as an input to the MRI function, but do not specify how to account for market size. The models presented in this paper provide a method to account for the number of manufacturers in the market. The second tool, technology refresh planning, is often used to identify optimal strategies (or sequences) of technology refreshes (or other DMSMS mitigation options) that minimize overall cost [69, 107, 128]. These tools are similar to the standard age-replacement strategies [15, 102], but differ in that DMSMS tools focus on the procurement issues of a part as opposed to the reliability or wear-out of a part. This study does not directly address cost, but rather focuses on improving the prediction of procurement lifetimes in the presence of form/fit/function (F3) replacements in the market. This study assumes that the cost to identify a F3 replacement is minimal compared to other mitigation options, such as redesigning a new system or conducting a technology refresh.

The majority of DMSMS-centric studies have focused on component-level or individual part-level forecasts as opposed to system-level or assembly-level forecasts [90]. Many only consider electronic part obsolescence and do not account for mechanical or software obsolescence. Determining the procurement lifetime behavior of individual parts is a fundamental aspect of proactive and strategic DMSMS management and are used in the models presented in this paper. The product life-cycle curve has been used to describe how a technology moves through various stages throughout its lifetime and is closely related to part availability. Most of the literature describes between four to six stages of the product life-cycle curve to describe changing markets [87]. The life-cycle curves are usually presented as a bell-shaped curve although the actual curves may take on different shapes in reality. An example product life-cycle curve is shown in Figure 3.2. Examples of models that determine the procurement life-cycles include: estimates of product lifetimes using sales and the number of entrants into the market [9]; a data mining-based approach using sales volume data resulting in estimates of a time window of obsolescence [101]; an obsolescence forecasting model using sales data and primary and secondary attributes to provide a window of obsolescence [106]; machine learning models including random forests, neural networks, and support vector machines to compute the risk of a part being obsolete or to predict the date of obsolescence [47]. Using these aforementioned methods to describe the procurement lifetimes for individual parts can be used in the models developed in this paper to describe the procurement lifetimes of individual parts.

In the production research literature, there is a dearth of DMSMS-specific research. However, there are many fields that are relevant to DMSMS. One issue that this paper addresses is the idea of reserve capacity in a supply chain. [68] consider reserve capacity to counter disruption risk at the part level with a risk mitigation inventory, but they do not consider alternate manufacturers or vendors as mitigation techniques. Additionally, their study focuses on a single-part, single-location system, whereas this study aims to evaluate risk for multi-part production and logistic systems. Another related often-studied aspect in production research is determining the optimal number of suppliers. [42] identify multiple-sourcing as a driver of a resilient supply chain. A few studies recommend closely tracking sole source configuration parts [23, 89], and this implies that sole source equates to higher levels of risk for the system. Previous work evaluates the optimal number of suppliers while accounting for disruptions [12, 45, 58]. In general, dual-sourcing tends to outperform single-sourcing while multi-sourcing typically shows diminished returns [41]. Other studies evaluate the optimal stocking values of individual parts or items that have decaying field lives [80, 110] but do not consider the cases where parts do not have a decaying demand signal or have time-changing market sizes. These studies make assumptions that the suppliers (and parts) will continue to be available in the market and account for disruptions. This paper provides models to bridge the gap to account for the risk where a market has varying numbers of suppliers.

Another field related to DMSMS issues is that of considering perishable items in mathematical models. In DMSMS terms, the availability of an individual manufacturer can be thought of as a perishable item; when a manufacturer ceases producing parts in the market, it can be considered perished. [5] identify three main ways to model the lifetimes of perishable components: fixed lifetime; age-dependent lifetimes; and time- or inventory-dependent deterioration rates. In their review of the literature, they state that there have been very few models that consider multiple items as well as multiple warehouses. Some of the earliest studies have evaluated order quantities where the commodities have fixed lifetimes [34], while later studies have expanded to allow for stochastic demands but still consider fixed lifetimes [6]. The model presented in this paper does not consider demands, but is based on stochastic procurement lifetimes.

Other studies have outlined suggestions to improve DMSMS management. [89] offer strategies to assess obsolescence risk using the number of manufacturers, years to end of life (YTEOL), available stock, consumption rates and criticality assessments. The YTEOL methods use a point estimate for procurement lifetime and does not take uncertainty into account. This study not only accounts for the number of manufacturers but also includes uncertainty in procurement lifetime estimates. These two items are used to model the behavior of the life-cycle curve and provide metrics for measuring the availability.

3.4 Modeling the Availability Risk Framework

A proactive DMSMS management model must have the ability to forecast availability for individual parts. In addition, the model must be able to account for all tracked parts. To achieve this, this section provides a novel way to model DMSMS availability as a finite-source capacitated queuing model. The framework is linked to the product life-cycle curve by modeling the number of vendor parts available over time. Two availability risk metrics and DES modeling frameworks are presented.

3.4.1 Queuing Models in DMSMS

A BOM identifies the components and materials comprising a system. These BOMs 'list all the sub-assemblies, component parts, and raw materials that go into an end item' [86]. These sub-assemblies and component parts are not actual parts, but specify the requirements or specifications for parts that are to be procured and used from manufacturers. These specifications will be referred to collectively as *configuration parts* (CPs). They are sometimes referred to as *drawing numbers*. Likewise, the actual procurable parts from manufacturers will be referred to as *vendor parts* (VPs). For each configuration part, an analyst will typically track a number of vendor parts, up to and including all the approved and tracked parts which is referred to as 'market size'.

Before describing the modeling framework, the notation for a queuing model is introduced. A queuing model consists of customers who arrive to a system and are served by servers. The model is usually represented using Kendall's notation: $A/B/m/K/n/Di$, where A describes the inter-arrival time distribution, B is the service time distribution, m is the number of servers, K is the system capacity, n is the population size or number of sources, and Di is the queue discipline [111]. Some possible values for A and B include M for an exponential distribution, D for deterministic values, and G for general distributions.

The modeling framework represents the market size as a *finite-source capacitated queuing model*, where the number of servers, the system capacity, and the population size are all equal (i.e. $m = K = n$). In DMSMS terms, if there are K tracked vendor parts in the market for a configuration part, the number of servers, system capacity, and population size will be set to K for a finite-source capacitated queuing model. This assumption models the reality that there is usually a finite, and assumed known, number of manufacturers in the market. The inter-arrival time is the delay between successive part introductions into the market, or lag, by a manufacturer. A vendor part's procurement lifetime is the amount of time that a manufacturer will be available in the market and is described by the service time distribution. Parametric or non-parametric probability distributions can be used to describe the inter-arrival and procurement lifetimes and can be estimated from observational data or subject matter expert (SME) input. Some of the distributions identified in previous DMSMS studies include the Weibull distribution [97] and the triangular distribution [32, 100]. The latter is often recommended for DMSMS practitioners as it allows for easy interpretation since it is defined over a specified range with the option for a non-symmetric mode value. Possible methods for estimating procurement lifetimes are described in [9,47,97,101,106]. The queue discipline, Di, is not relevant in a finite-source capacitated queuing model framework and the queuing notation will simplify to $A/B/m/K/n$. Figure 3.1 shows an example system (System A) with multiple configuration parts $i \in \{1, \ldots, n\}$ and vendor parts $j \in \{1, \ldots, K_i\}$, where each configuration part will have K_i tracked vendor parts. The underlying birth-death process for a configuration part will have the following inter-arrival λ_k and service rates μ_k when there are $k \in \{0, 1, \ldots, K\}$ active vendor parts

$$\lambda_k = (K - k)\lambda, \quad 0 \leq k \leq K$$
$$\mu_k = k\mu, \qquad\quad 0 \leq k \leq K,$$

under the assumption of homogeneous (or similar) and independent vendor parts, where each vendor part has the same inter-arrival λ and service μ rates.

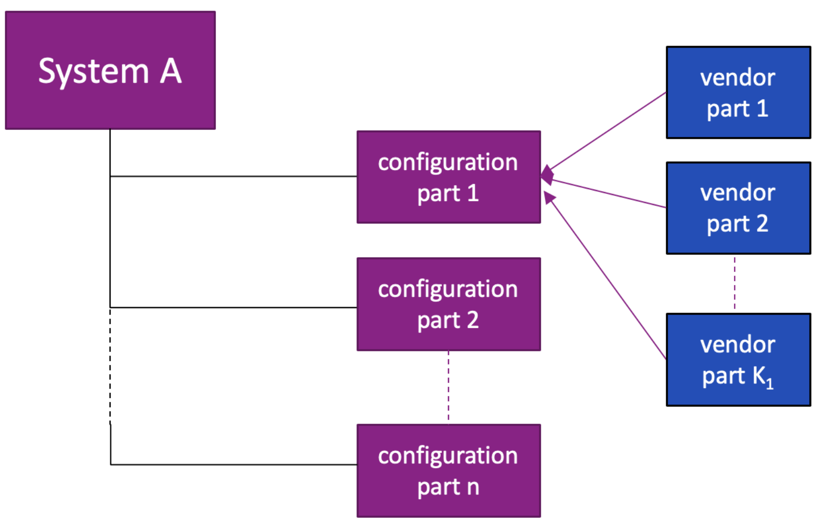

Figure 3.1: Conceptual model of a queuing modeling framework in a DMSMS context. Each configuration part is modeled as a finite-source capacitated queue where vendor parts arrive in the queuing system (become procurable in the market for the configuration part) and leave the queuing system (become obsolete/unavailable in the market).

3.4.2 Market Size and Number of Manufacturers

[78] note that the number of manufacturers (and thus vendor parts) change in the market as a technology moves through various stages of the product life-cycle curve. The introduction stage has only a few manufacturers, whereas the growth and maturity stages experience a greater number of manufacturers. However, the number of manufacturers tends to taper off as the technology moves towards obsolescence. As the technology continues through the decline, phase-out, and obsolescence stages, the number of manufacturers decreases. Figure 3.2 shows the product life-cycle curve that is discussed in [78,87,106]. Overlaid on this figure is an example of how the number of manufacturers may change over a product life-cycle. In this example, as the technology is in the *maturity* stage it has a maximum of five vendor parts in the market; in the *decline* stage it can has a maximum of three vendor parts in the market; and finally in the *phase-out* stage a maximum of one vendor part in the market.

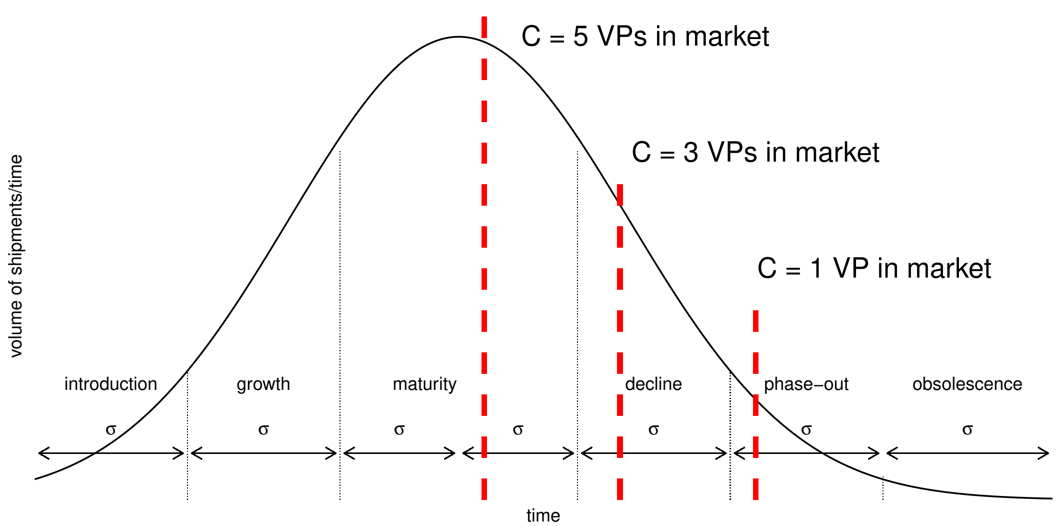

Figure 3.2: Linking the product life-cycle curve with the queuing simulation model framework. In this example, there are 5 vendor part (VPs) in the maturity stage, 3 VPs in the decline stage, and 1 VP in the phase-out stage.

The modeling framework estimates availability risk by accounting for the changing number of manufacturers (and vendor parts). This study assumes that the term *vendor part* is synonymous with *manufacturer* which implies that each manufacturer produces only one vendor part. This assumption allows for independence between vendor parts. In actuality, one manufacturer could produce multiple vendor parts for a configuration part. A case using this modeling framework is provided in Section 3.5.1. The actual number of vendor parts or manufacturers can be acquired using market survey data or historical records.

3.4.3 Availability Risk Metrics and Models

A scarcity of vendor parts from an OEM leads to an increasing level of availability risk, which leads to a decrease in the operational capability of the production system. In order to move towards practicing proactive DMSMS management, it is important to minimize instances where there are no procurable vendor parts in the market. After assigning a level of risk to each configuration part, comparing the availability risk metrics for each configuration part can inform decisions regarding optimal resource allocation to mitigate DMSMS issues. This paper develops two risk metrics to quantify vendor part availability. The first risk metric is the *fraction of time with zero vendor parts available*, P_Z. The second risk metric is the *time until obsolescence*, T_Z. Each risk metric is suited for a particular type of analysis and assumptions and two DES models are developed to capture two predominant ways of thinking about DMSMS/obsolescence dynamics. The first, Model P_Z, will use the metric P_Z to measure availability risk and will use a fixed number of tracked vendor parts that experience gaps in market arrival. The second, Model T_Z, will use the metric T_Z to measure availability risk starting with an initial number of tracked vendor parts that may become obsolete and not replaced (related to a decreasing market). Model P_Z can be used to inform MRI studies, while Model T_Z can be used to replace the simpler, single-part procurement lifetime estimates in technology refresh strategies.

Model P_Z

The first model provides a framework to evaluate the availability metric, P_Z. In DMSMS terms, P_Z is important as it indicates the extent that there will be no available vendor parts for procurement. This model assumes a fixed number of tracked vendor parts over a (usually shorter) time period of interest and time-lag between successive introductions of vendor parts. This time-lag is represented by a positive inter-arrival time; if the the inter-arrival time was equal to zero, P_Z would be equal to zero since vendor parts would always be available. Each configuration part $i \in \{1, \dots, n\}$ is initialized as a finite-source, capacitated queuing system with no assumptions regarding the distributions for inter-arrival and procurement lifetimes. A configuration part with a larger estimate of P_Z will be considered more risky.

In reality, it is unlikely that a manufacturer will stop making a part and not offer a client a replacement part, assuming that the manufacturer will continue to want the client's business. [101] shows an example of monolithic flash memory that increases memory size over time. Although each specific flash memory part may have different procurement lifetimes as the technology advances, the parts will most likely have a F3 replacement. For example, when a specific flash memory becomes obsolete, a flash memory with larger memory is usually available. These replacements fall in the category of an approved item or simple substitution. Model P_Z assumes that the number of tracked vendor parts remains the same, but accounts for a slight lag between introductions of successive vendor parts from the same manufacturer.

A graphical example showing one replication of Model P_Z is shown in Figure 3.3. The simulation starts with both vendor parts available. The first vendor part (VP1) becomes obsolete at time t_2 and a replacement part is back on the market at time t_4, but is off of the market again at time t_5. The second vendor part (VP2) becomes obsolete at time t_1 and a replacement part is back on the market at time t_3 and remains on the market until time T. Throughout the time frame, there are two vendor parts in the intervals $[0, t_1]$ and $[t_4, t_5]$; one vendor part in the intervals $[t_1, t_2]$, $[t_3, t_4]$, and $[t_5, T]$; and zero vendor parts in the interval $[t_2, t_3]$. For each replication $r \in \{1, \dots, R\}$, $P_{Z,i}^{(r)}$ is calculated by taking the amount of time represented by the interval with zero vendor parts and dividing it by the simulation time period, T, for each configuration part $i \in \{1, \ldots, n\}$.

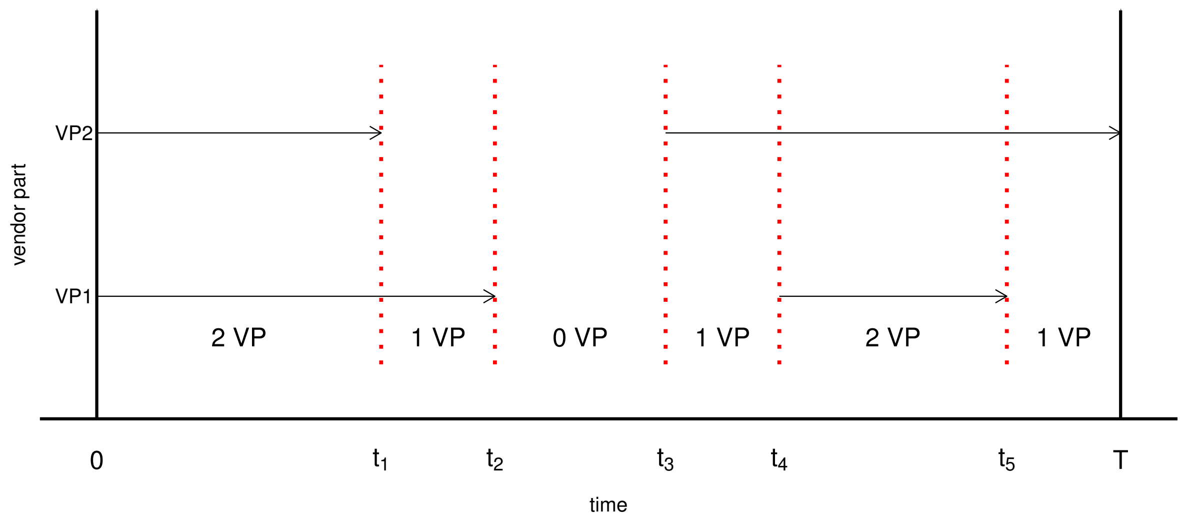

Figure 3.3: Model P_Z example. For each replication, the fraction of time with zero vendor parts, $P_{Z,i}^{(r)}$, is calculated by dividing the total amount of time with zero vendor parts by the total simulation time. In this example, this consists of the amount of time represented between the two red dashed lines annotated by the '0 VPs' divided by T.

Estimates of P_Z for each configuration part, namely, the sample *mean* fraction of time with zero vendor parts available, $\bar{P}_{Z,i}$, and the sample *median* fraction of time with zero vendor parts available, $\tilde{P}_{Z,i}$, are calculated. Consider a particular configuration part which has K_i vendor parts. For each vendor part $j \in \{1, 2, \ldots, K_i\}$ and each simulation replication $r \in \{1, 2, \ldots R\}$, define

$$v_{j,r}(t) = \begin{cases} 0, & \text{if available at time } t \\ 1, & \text{if unavailable at time } t, \end{cases} \tag{3.1}$$

which indicates whether or not vendor part j is available at time t, resulting in a set of K_i piece-wise defined functions. For each replication, $r \in \{1, 2, \ldots R\}$, the fraction of time for configuration part i having zero vendor parts available is given by:

$$P_{Z,i}^{(r)} = \frac{1}{T} \int_0^T \prod_{j=1}^{K_i} v_{j,r}(t)\; dt. \tag{3.2}$$

Note that the integrand will be 0 if any of the K_i vendor parts are available at any time $t \in [0, T]$. The sample mean of all replications is given by:

$$\bar{P}_{Z,i} = \frac{1}{R} \sum_{r=1}^{R} P_{Z,i}^{(r)}. \tag{3.3}$$

The sample median of all replications can be found by ordering all results of $P_{Z,i}^{(r)}$, and identifying the proper ordered value depending upon whether R is odd or even:

$$\tilde{P}_{Z,i} = \begin{cases} \text{(odd): } \left(\frac{R+1}{2}\right)^{th} \text{ordered value} \\ \text{(even): mean of} \left(\frac{R}{2}\right)^{th} \text{ and } \left(\frac{R}{2}+1\right)^{th} \text{ordered values.} \end{cases} \tag{3.4}$$

To estimate the availability risk in terms of the fraction of time with zero vendor parts P_Z a DES algorithm is developed. A few parameters must be set prior to using the DES. A list of n configuration parts can include all or a subset of parts from a BOM. For each configuration part, the number of tracked vendor parts K_i, inter-arrival distribution Λ_i, and procurement lifetime distribution Ω_i are required for $i \in \{1, \ldots, n\}$. The inter-arrival and procurement lifetime distributions can be estimated from observational data or SME input (recall the discussion in Section 3.4.1 and see [9, 47, 97, 101, 106]). The run length (T) is the length of simulated time for each replication of the simulated model and corresponds to the time frame that an analyst is interested in. This must be set to appropriate units, for example months, quarters, or years according to the desired time frame. Finally, the number of replications (R) is an integer value, usually large enough to gain insights out of the simulation but not so large that the simulation is unable to run in a timely manner. Under the Model P_Z assumptions, the number of tracked vendor parts K_i will remain fixed over the entire time period $t \in [0, T]$. The DES algorithm for Model P_Z is given by:

for replication **do** $r \in \{1, \ldots, R\}$

    for VP **do** $j \in \{1, \ldots, \kappa\}$

3: $l \leftarrow$ VP proc. lifetime from Ω_i

4: $L_j \leftarrow l$

5: $v_{j,r}(t) \leftarrow 0, \ \forall t \in [0, T]$

6: **end for**

7: $ind \leftarrow \arg\min_{1 \le j \le \kappa}\{L_j\}$

8: **while** $L_{ind} < T$ **do**

9: $a \leftarrow$ VP inter-arrival time from Λ_i

10: $l \leftarrow$ VP proc. lifetime from Ω_i

11: $v_{ind,r}(t) \leftarrow 1, \ \forall t \in [L_{ind}, L_{ind} + a)$

12: $L_{ind} \leftarrow L_{ind} + a + l$

13: $ind \leftarrow \arg\min_{1 \le j \le \kappa}\{L_j\}$

14: **end while**

15: **record** $P_{Z,i}^{(r)}$ for each CP $i \in \{1, \ldots, n\}$

16: **end for**

17: **return** $\bar{P}_{Z,i}, \tilde{P}_{Z,i}$ for each CP $i \in \{1, \ldots, n\}$

The algorithm iterates through each of R replications (line 1). At the outset of each replication each of κ vendor parts is initialized, where the total number of vendor parts is bounded by the sum of all configuration part capacities. This allows for the instances where some configuration parts share the same vendor parts, i.e. $\kappa \le \sum_{i=1}^{n} K_i$ (the equality holds when no configuration parts share the same vendor parts). Each vendor part is initialized by generating a procurement lifetime random variate l from Ω_i (line 3), setting the procurement lifetime L_j (line 4), and setting each to available (line 5). The algorithm identifies the first obsolescence event, indicated by the minimum procurement lifetime (line 7). If the earliest obsolescence event is before the run time T, then two random variates are generated for the inter-arrival and procurement lifetimes from Λ_i and Ω, respectively (lines 9, 10). The availability status of the vendor part is set to unavailable between the obsolescence time and the lag time (line 11) and the next obsolescence event for the vendor part is updated by adding the two random variates to the current time (line 12). The next obsolescence event is identified (line 13) and the while loop will continue until time T. The fraction of time with no vendor parts available is recorded for replication r (line 15), and once all replications are complete the estimates for P_Z are returned using (3.3) and (3.4) for each configuration part $i \in \{1, \ldots, n\}$ (line 17).

Model T_Z

The second model provides a framework to estimate the availability risk metric, *time until obsolescence*, T_Z. Whereas P_Z is the fraction of time with no vendor parts available, T_Z estimates the time when there will be no vendor parts available. Model T_Z assumes that if a tracked vendor part becomes obsolete and there is no F3 replacement, the DMSMS manger will not be able to replace it with another part in the market. Unlike the risk metric P_Z, a larger value for T_Z is considered less risky.

In Model T_Z, each configuration part is initialized as a finite-source capacitated queuing system with no assumptions regarding the procurement lifetimes but with inter-arrival times equal to zero.

Since the model assumes that an analyst will not actively seek a replacement for a vendor part, the process can be considered a *pure-death* process as the number of tracked vendor parts will only decrease over time [92]. At the end of a vendor part's procurement lifetime there is a probability b_i of the vendor part becoming obsolete. This represents a Bernoulli trial with probability b_j that the vendor part will not have a F3 replacement and a probability of $1 - b_j$ that the vendor part will have a F3 replacement. This models the reality of a manufacturer that stops making a vendor part, but will either have a F3 replacement, or decide to stop creating a vendor part according to the specifications outlined by the configuration part. A vendor part that is certain to have a replacement will have $b_i = 0$, whereas a vendor part that is certain to not have a replacement will have $b_i = 1$. (Note: in terms of a Bernoulli trial, a success is defined as a vendor part leaving the market.) Model T_Z assumes there is no time-lag in successive introductions to the market for a replacement vendor part, thus the inter-arrival times are set to exactly zero to allow the model to account for this assumption.

A graphical example showing the results for one replication of Model T_Z is shown in Figure 3.4 for a time period $[0, T]$. The simulation starts with three vendor parts available. The first vendor part becomes obsolete at time t_2 after only two life-cycles (denoted by the arrowheads), indicating that a F3 replacement was available after the first life-cycle but not after the second. The second vendor part (VP2) becomes obsolete at time t_3 after three life-cycles, indicating that there were F3 replacements after the first and second life-cycles. The third vendor part (VP3) becomes obsolete at time t_1 after only one life-cycle indicating that there was not a F3 replacement. The time until obsolescence, $T_Z^{(r)}$, is recorded at t_3 as this is the earliest time where all tracked vendor parts have left the marketplace with no replacements, indicating obsolescence.

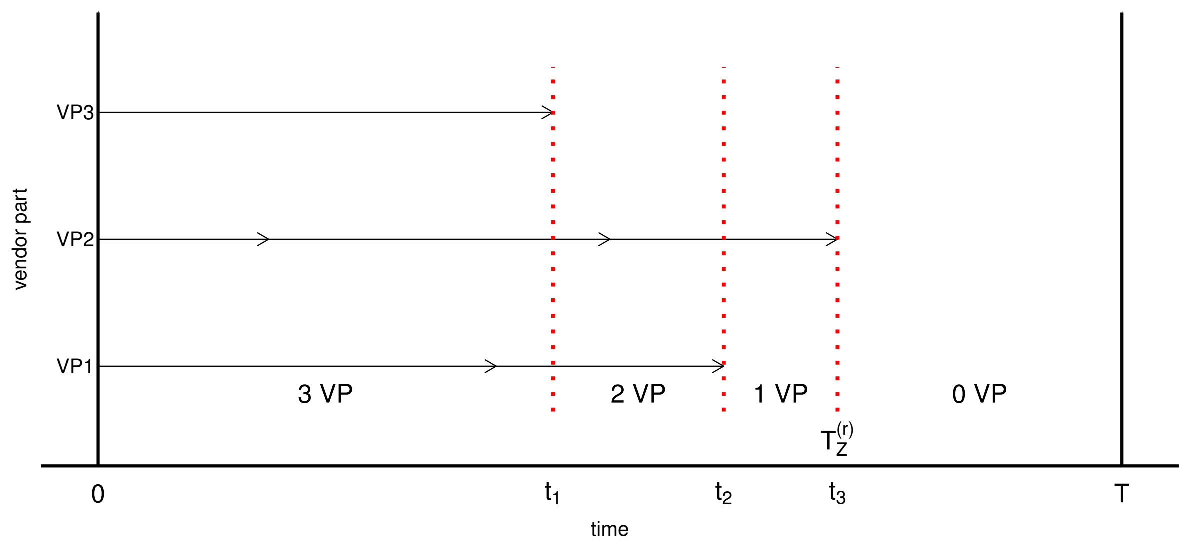

Figure 3.4: Model T_Z example. For each replication, the time until obsolescence, $T_{Z,i}^{(r)}$, is recorded when there are zero tracked vendor parts in the marketplace for the first time. In this example, $T_{Z,i}^{(r)} = t_3$.

The output from the DES can be used to estimate T_Z for each configuration part, using the sample mean time until obsolescence $\bar{T}_{Z,i}$ and the sample median time until obsolescence $\tilde{T}_{Z,i}$. Using $v_{i,r}$ as defined in (3.1), the time until obsolescence, for each replication, is given by:

$$T_{Z,i}^{(r)} = \int_0^T \left(1 - \prod_{j=1}^{K_i} v_{j,r}(t)\right) dt. \tag{3.5}$$

The sample mean time until obsolescence, $\bar{T}_{Z,i}$, and the sample median time until obsolescence over all replications $\tilde{T}_{Z,i}$ can be estimated by exchanging $T_{Z,i}^{(r)}$ for $P_{Z,i}^{(r)}$ in (3.3) and (3.4), respectively:

$$\bar{T}_{Z,i} = \frac{1}{R}\sum_{r=1}^{R} T_{Z,i}^{(r)}, \tag{3.6}$$

$$\tilde{T}_{Z,i} = \begin{cases} \text{(odd): } \left(\frac{R+1}{2}\right)^{th} \text{ordered value} \\ \text{(even): mean of} \left(\frac{R}{2}\right)^{th} \text{ and } \left(\frac{R}{2}+1\right)^{th} \text{ordered values.} \end{cases} \tag{3.7}$$

To estimate availability risk in terms of T_Z requires a list of n configuration parts, the number of tracked vendor parts K_i, procurement lifetime distribution Ω_i, run length (T), and the number of replications (R) as defined in Model P_Z. Since Model T_Z does not assume a lag between successive part introductions, the inter-arrival distributions will not be used. The DES algorithm for Model T_Z is given by:

for replication **do** $r \in \{1, \ldots, R\}$
    for VP **do** $j \in \{1, \ldots, \kappa\}$
        $l \leftarrow$ VP proc. lifetime from Ω_i
        $L_j \leftarrow l$
        $v_{j,r}(t) \leftarrow 0,\ \forall t \in [0, T]$
    end for
    $ind \leftarrow \arg\min_{1\le j\le\kappa}\{L_j\}$
    while $L_{ind} < T$ **do**
        $u \leftarrow \text{Bernoulli}(b_j)$

10: **if** $u = 1$ **then**
11: $v_{ind,r}(t) \leftarrow 1,\ \forall t \in [L_{ind}, T]$
12: $L_{ind} \leftarrow T$
13: **else**
14: $l \leftarrow$ VP proc. lifetime from Ω_i
15: $L_{ind} \leftarrow L_{ind} + l$
16: **end if**
17: $ind \leftarrow \arg\min_{1 \leq j \leq \kappa}\{L_j\}$
18: **end while**
19: **record** $T_{Z,i}^{(r)}$ for each CP $i \in \{1, \ldots, n\}$
20: **end for**
21: **return** $\bar{T}_{Z,i}, \tilde{T}_{Z,i}$ for each CP $i \in \{1, \ldots, n\}$

The algorithm iterates through each of R replications (line 1). Each of the κ vendor parts is initialized by generating a procurement lifetime random variate l from Ω_i (line 3), setting the procurement lifetime L_j (line 4), and setting each to available (line 5). The algorithm identifies the first obsolescence event, indicated by the minimum procurement lifetime (line 7). When a vendor part becomes obsolete at a time less than T, the result of a Bernoulli trial determines if there is a F3 replacement part with probability of success of b_j (line 9). If the Bernoulli trial results in a success, i.e. the vendor part becomes obsolete, then the availability of the vendor part is set to unavailable for the remainder of the run time. To simulate a reduction in the number of tracked vendor parts, the next obsolescence event for vendor part j is set to T (line 11). If the Bernoulli trial is not a success, the next obsolescence event for vendor part j is determined by generating another random variate (line 14) and added to the current time (line 15). The next obsolescence event is identified (line 17) and the while loop will continue until time T. The fraction of time with no vendor parts available is recorded for replication r (line 19), and once all replications are complete the estimates for T_Z are returned using (3.6) and (3.7) for each configuration part $i \in \{1, \ldots, n\}$ (line 21).

3.5 Model Applications and Results

This section evaluates two scenarios simulating availability risk of configuration parts that represent typical DMSMS issues. The first scenario models the availability risk between two configuration parts with varying levels of *churn* under Model P_Z and Model T_Z assumptions, where *churn* is defined as the rate at which new products arrive to the marketplace and replace older products. A vendor part with a slower churn rate will have longer procurement lifetimes. The second scenario analyzes the impact on availability when a configuration part is in various stages of the product life-cycle curve, also using Model P_Z and Model T_Z assumptions. Both scenarios model a period of $T = 10$ years (120 months).

The expected values of P_Z and T_Z are analytically derived in Appendices 3.7 and 3.8 under Markovian assumptions and assume exponential inter-arrival and procurement lifetimes. Additionally, the expected values of T_Z are modeled using a Bernoulli trial at the end of each vendor part's procurement lifetime, and assume independence between the procurement lifetime and Bernoulli trials. The results for $\mathbb{E}[P_Z]$ and $\mathbb{E}[T_Z]$ are used for verification of the simulation results for the base scenarios and used to compare to extensions of the base scenarios.

All scenarios will use Tukey's honestly significant difference (HSD) test (also known as Tukey's range test) to test for differences between the means of pairs of different configuration parts [116]. This paper uses $R = 1000$ replications for each of the scenarios as the simulated market size is relatively small. To determine statistically significant differences between larger systems (or markets), it is recommended to start with 30 or 50 replications and observe the results of the Tukey HSD test. Then increase the total number of replications by the factor of $\mathcal{M}$ to reduce the observed standard error by approximately the factor of $\sqrt{\mathcal{M}}$ based on the central limit theorem.

3.5.1 Scenario 1 - Varying Procurement Lifetime Distributions

This scenario allows for the comparison of configuration parts comprised of vendor parts with different churn rates. The base model simulates two configuration parts where the vendor parts for the first configuration part (CP 1) have a larger mean procurement lifetime (smaller churn) than the vendor parts associated with the second configuration part (CP 2). This model assumes independent configuration parts each with independent, homogeneous vendor parts. An extension to the base model is also explored, where multiple configuration parts are comprised of non-homogeneous vendor parts.

Model P_Z

In this scenario, CP 1 will have a slower rate of churn with a mean procurement lifetime of 24 months, while CP 2 will have a higher rate of churn with a mean procurement lifetime of 12 months. At the end of their procurement lifetimes, successive vendor parts will arrive to the market with a mean lag time of 12 months. Both CP 1 and CP 2 are initialized as finite-source capacitated queuing systems written as $M/M/K_i/K_i/K_i$ with a maximum of $K_i = 3, i \in \{1, 2\}$ independent vendor parts in the market. The model assumes that the number of maximum vendor parts remains the same over the time period. Table 3.1 shows the parameters for the first scenario under the Model P_Z assumptions. The values λ and μ are the inter-arrival rate and procurement lifetime rate, respectively. The expected value of P_Z is derived in Appendix 3.7, under these assumptions.

The graphical results of 1000 replications for the first scenario over a ten-year period ($T = 10$) are shown in Figure 3.5a. Additionally, the sample means $\bar{P}_Z$, sample medians $\tilde{P}_Z$, and the expected values $\mathbb{E}[P_Z]$, for both configuration parts are calculated using (3.3), (3.4), and as described in Appendix 3.7, respectively, and shown in Table 3.3.

Table 3.1: Churn comparison configuration part parameters for Model P_Z.

Parameter	CP 1 (slower churn)	CP 2 (quicker churn)
mean inter-arrival time	12.0 months ($\lambda = 1.0$/year)	12.0 months ($\lambda = 1.0$ / year)
mean procurement life	24.0 months ($\mu = 0.5$ / year)	12.0 months ($\mu = 1.0$ / year)
# tracked vendor parts	3	3

Model T_Z

As with Model P_Z, CP 1 will have a lower rate of churn and has a mean procurement lifetime of 24 months and CP 2 will have a quicker rate of churn with a mean procurement lifetime of 12 months. Both configuration parts are initialized as finite-source capacitated queuing systems written as $G/M/K_i/K_i/K_i$ with three initial vendor parts and the inter-arrival time equal to 0 with 50% probability of no additional arrival. In other words, at the end of a vendor part's procurement lifetime, the probability of a manufacturer producing a suitable F3 replacement part is 0.5 for both configuration parts. Thus, the number of maximum vendor parts decreases over time, thereby modeling a market that is reducing in size. Table 3.2 shows the parameters under the Model T_Z assumptions. The expected value of T_Z is derived analytically under these assumptions in Appendix 3.8.

The graphical results of 1000 replications for the first scenario over a ten-year period ($T = 10$) are shown in Figure 3.5b. The sample mean $\bar{T}_Z$ and the sample median $\tilde{T}_Z$ is the earliest time with zero vendor parts available for both configuration parts is calculated using (3.6) and (3.7), while the expected value $\mathbb{E}[T_Z]$ is calculated as described in Appendix 3.8. These values are shown in Table 3.3.

Table 3.2: Churn comparison configuration part parameters for Model T_Z.

Parameter	CP 1 (slower churn)	CP 2 (quicker churn)
mean procurement life	24.0 months ($\mu = 0.5$ / year)	12.0 months ($\mu = 1.0$ / year)
# tracked vendor parts	3	3
probability of no F3 replacement [a]	0.5	0.5

[a]or probability of success in terms of Bernoulli trial

Scenario 1 Results

The results from the first scenario provide an analyst the ability to compare relative availability risk for two configuration parts with differing rates of churn (for homogeneous vendor parts). As expected, the configuration part with a greater churn rate exhibits higher availability risk and risk variability, both in terms of P_Z, Figure 3.5a, and T_Z, Figure 3.5b. Table 3.3 provides point estimates for the mean and median with 95% confidence intervals for availability risk. The Tukey HSD test indicates there is a difference between the means of CP 1 and CP 2 at the $\alpha = 0.05$ significance level for both models. The confidence intervals presented are individual and calculated using the central limit theorem.

Under the Model P_Z framework, the expected value, sample mean, and sample median for P_Z are *lower* for CP 1 compared to CP 2. The mean and median are indicated in Figure 3.5a with the green triangle and vertical line inside the box, respectively. This implies that the availability risk, in terms of P_Z, is much greater for CP 2 than CP 1. Although the mean procurement life for individual vendor parts in CP 1 is double that of CP2, when accounting for market size the expected value of availability risk is more than three times higher for CP 2 (0.033 vs 0.114). When accounting for all tracked vendor parts to be available initially, the risk over a ten-year period is nearly ten times higher for the median estimates for P_Z for

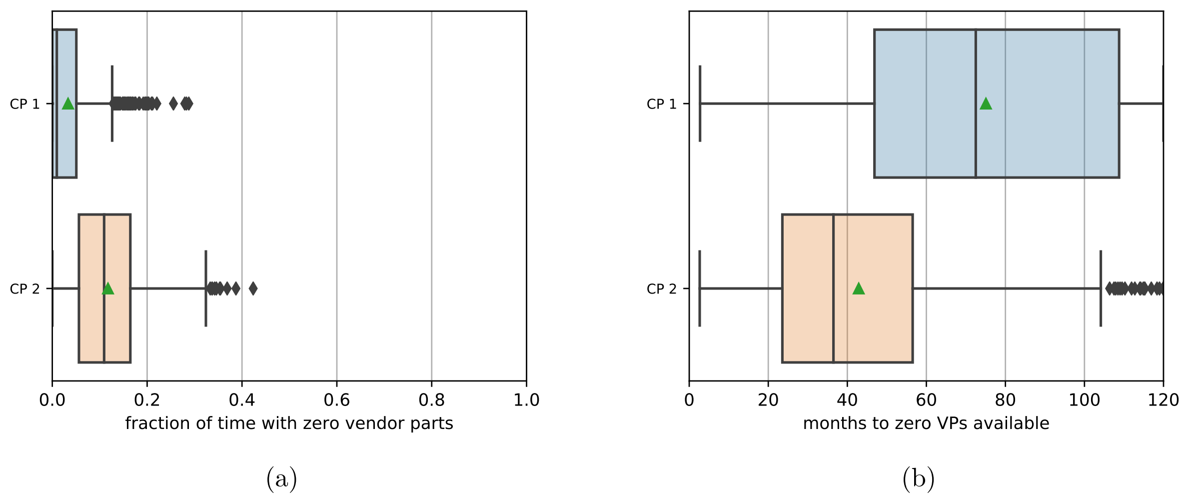

Figure 3.5: Comparison of P_Z (a) and T_Z (b) for two configuration parts with different levels of churn. Simulation uses 1000 replications modeling a 10-year time frame. The green triangle represents the mean value while the center vertical line within the box shows the median value.

CP 2 than CP 1.

Under the Model T_Z framework, the expected value, sample mean, and sample median of T_Z for CP 1 are *higher* than for CP 2, as evidenced in Figure 3.5b and Table 3.3, indicating a higher level of risk for CP 2, in terms of T_Z. The expected value of T_Z for CP 1 is roughly 1.7 times higher than CP 2 (76.7 months vs. 43.5 months), whereas the median value estimate is roughly 2 times higher (72.5 months vs. 36.5 months). The sample mean, $\bar{T}_Z$, is close to the expected value of the time until obsolescence, $\mathbb{E}[T_Z]$, as expected by the law of large numbers. Although this scenario only shows a comparison between two configuration parts, this analysis can be extended to compare larger numbers of configuration parts and dependencies as explored in the Section 3.5.2.

Table 3.3: Churn comparison results for P_Z and T_Z estimates for $R = 1000$ and $T = 10$ years. Estimates are shown with 95% confidence intervals.

Availability risk metric	CP 1 (slower churn)	CP 2 (quicker churn)
$\mathbb{E}[P_Z]$ [a]	0.033	0.114
$\bar{P}_Z$ [a]	0.033 (0.030, 0.036)	0.117 (0.112, 0.122)
$\tilde{P}_Z$ [a]	0.010 (0.006, 0.013)	0.109 (0.101, 0.116)
$\mathbb{E}[T_Z]$ [b]	76.7	43.5
$\bar{T}_Z$ [b]	75.1 (73.0, 77.2)	42.9 (41.3, 44.5)
$\tilde{T}_Z$ [b]	72.5 (69.7, 75.9)	36.5 (34.8, 38.4)

[a] expected value/sample mean/sample median of fraction of zero vendor parts available

[b] expected value/sample mean/sample median of time until obsolescence (months)

Extending Scenario 1 - Dependent Configuration Parts with Non-homogeneous Vendor Parts

This scenario represents the case where a configuration part may share multiple non-homogeneous vendor parts. Also, the vendor parts in the market can be approved for multiple configuration parts. In this extension to Scenario 1, the market still consists of six vendor parts, but these are associated with four configuration parts each with a capacity of three vendor parts. The configuration parts consist of the same vendor parts shown in Table 3.1 (for Model P_Z) or Table 3.2 (for Model T_Z). The four configuration parts consist of: three vendor parts with a slower churn and none with a quicker churn ('S3Q0' – the same as CP 1 in Scenario 1); two vendor parts with a slower churn and one with a quicker churn ('S2Q1'); one vendor part with a slower churn and two with a quicker churn ('S1Q2'); and three vendor parts with a quicker churn and none with a slower churn ('S0Q3' – the same as CP 2 in Scenario 1).

The results shown in Figures 3.6a and 3.6b and Table 3.4 account for dependencies among the configuration parts. The configuration parts 'S3Q0' and 'S0Q3' yield similar results as shown in Section 3.5.1. The configuration parts 'S2Q1' and 'S1Q2' have availability risk that is between 'S3Q0' and 'S0Q3', as one should expect; there is more risk associated with having more vendor parts with a quicker churn. Although it is hard to detect looking at Figure 3.6, there is a slight non-linear relationship as the combination of quick and slow churn vendor parts changes. The Tukey HSD test indicates that there is a significant difference between all pairs of means.

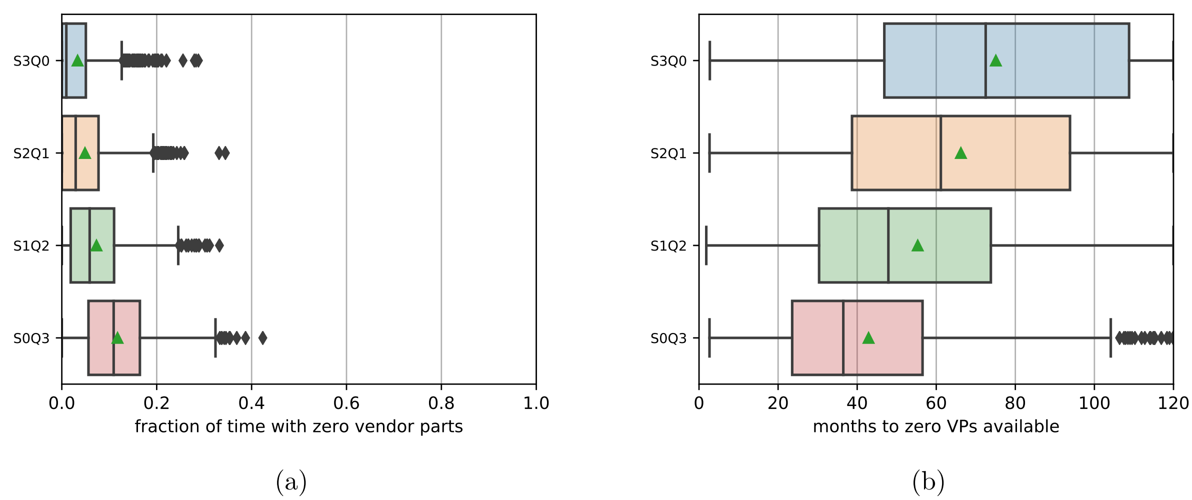

Figure 3.6: Comparison of P_Z(a) and T_Z (b) for four configuration parts with shared vendor parts. Simulation uses 1000 replications modeling a 10-year time frame. The green triangle represents the mean value while the center vertical line within the box shows the median value.

While the base models ('S3Q0' and 'S0Q3') can be verified using the analytic derivations

Table 3.4: Results for the comparison of P_Z and T_Z for four configuration parts with shared vendor parts for $R = 1000$ and $T = 10$ years. Estimates are shown with 95% confidence intervals.

Availability risk metric	S3Q0	S2Q1	S1Q2	S0Q3
$\mathbb{E}[P_Z]$ [a]	0.033	—	—	0.114
$\bar{P}_Z$ [a]	0.033	0.049	0.073	0.117
	(0.030, 0.036)	(0.045, 0.052)	(0.069, 0.077)	(0.113, 0.122)
$\tilde{P}_Z$ [a]	0.010	0.029	0.059	0.109
	(0.006, 0.013)	(0.026 0.035)	(0.053 0.064)	(0.101 0.116)
$\mathbb{E}[T_Z]$ [b]	76.7	—	—	43.5
$\bar{T}_Z$ [b]	75.1	66.2	55.3	42.9
	(73.0, 77.2)	(64.2, 68.3)	(53.3, 57.3)	(41.3, 44.5)
$\tilde{T}_Z$ [b]	72.5	61.2	47.9	36.5
	(69.7, 75.9)	(58.2, 64.3)	(45.7, 50.6)	(34.8, 38.4)

[a] expected value/sample mean/sample median of fraction of zero vendor parts available

[b] expected value/sample mean/sample median of time until obsolescence (months)

for $\mathbb{E}[P_Z]$ and $\mathbb{E}[T_Z]$ under the assumptions of homogeneous vendor parts, calculating the risks for 'S2Q1' and 'S1Q2' requires more involved analyses. As the behaviors of the vendor parts and configuration parts become more complex, analytic derivations become intractable and simulation is required to get estimates of the level of risk for a configuration part. In terms of the algorithms shown in Sections 3.4.3 and 3.4.3, the value for κ is less than total sum of capacities for all configuration parts, i.e. $\kappa \leq \sum_{i=1}^{n} K_i$. Since the vendor parts are assumed to operate independently, the appropriate changes to calculating the risk P_Z will occur in lines 15 and 17 in Section 3.4.3 and lines 19 and 21 in Section 3.4.3.

3.5.2 Scenario 2 - Changing Market Size

This scenario models the availability risk for a single configuration part as it transitions through the various stages of the life-cycle curve (Figure 3.2). A base model is presented where a single configuration part has tracked vendor parts and the base model is verified analytically. The number of tracked vendor parts represents the configuration part being in different stages of the life-cycle curve, as described in Figure 3.2. Generally speaking, a configuration part with more initially tracked vendor parts corresponds to the *maturity* stage, while fewer vendor parts could correspond to the *decline* or *phase-out* stages. An extension to the simple model is presented with three cases of time- and state-dependent vendor part behavior representing typical DMSMS issues.

Model P_Z and Model T_Z Parameters for Base Model

The parameters for the second scenario under the Model P_Z assumptions are the same as those for CP 1 shown in Table 3.1, but with $k = 1, 2, \ldots, 5$ of initially tracked vendor parts. There are five instantiations for the configuration part, where the number of initial vendor parts ranges from one to five and they remain in the market, albeit with a lag between successive introductions. The parameters for the second scenario under the Model T_Z assumptions are the same as those for CP 1 shown in Table 3.2 but with $k = 1, 2, \ldots, 5$ initially tracked vendor parts. This model also creates five instantiations of single configuration part with one through five initially tracked vendor parts in the marketplace but the number of vendor parts in the market is assumed to decrease over time.

Figures 3.7a and 3.7b show the results of 1000 replications over a ten-year period ($T = 10$) for the second scenario for Models P_Z and T_Z, respectively. Additionally, the expected values, sample means, and sample medians for P_Z and T_Z are shown in Table 3.5, where CP 1-k represents the cases where the configuration part has $k = 1, 2, \ldots, 5$ initially tracked vendor parts.

Scenario 2 Results

The results from the second scenario allow an analyst to quantify the risk for a single configuration part in various stages of the product life-cycle, as a function of initially tracked vendor parts that either remain fixed (Model P_Z) or are allowed to decrease over time (Model T_Z). This results in a risk metric that can be used to understand the trade-offs associated with part tracking. For example, an analyst can then decide to take proactive DMSMS mitigation measures such as developing a new source through emulation or extending production of a current vendor part to ensure the number of tracked vendor parts remains at a certain level. The Tukey HSD test indicates that the means were not significantly different for only one pair of configuration parts for Model P_Z (CP 1-4 vs. CP 1-5), but indicates that the means are all different for Model T_Z (at the significance level of $\alpha = 0.05$).

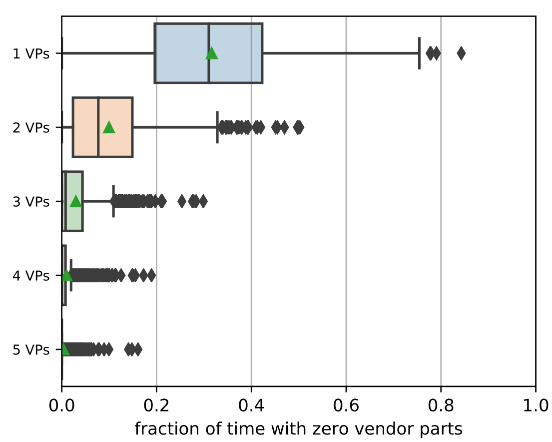

(a)

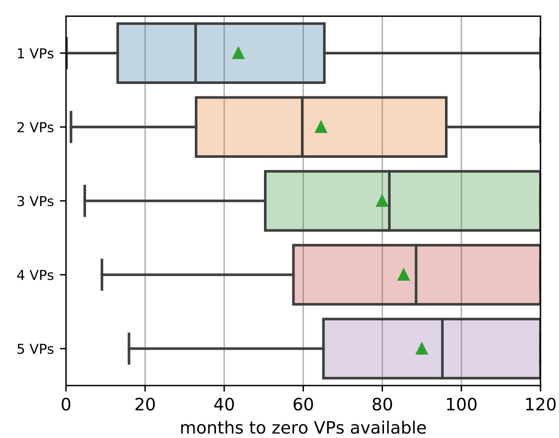

(b)

Figure 3.7: Comparison of P_Z (a) and T_Z (b) for one configuration part with various initially tracked vendor parts. Simulation uses 1000 replications modeling a 10-year time frame. The green triangle represents the mean value while the center vertical line within the box shows the median value.

Table 3.5: Results for the comparison of P_Z and T_Z for one configuration part with various tracked vendor parts for $R = 1000$ and $T = 10$ years. Estimates are shown with 95% confidence intervals.

Availability risk metric	CP 1-1	CP 1-2	CP 1-3	CP 1-4	CP 1-5
$\mathbb{E}[P_Z]$ [a]	0.311	0.100	0.033	0.011	0.003
$\bar{P}_Z$ [a]	0.316	0.100	0.030	0.010	0.004
	(0.306, 0.326)	(0.094, 0.106)	(0.027, 0.033)	(0.009, 0.011)	(0.003, 0.005)
$\tilde{P}_Z$ [a]	0.310	0.077	0.008	0	0
	(0.296, 0.326)	(0.070, 0.086)	(0.005, 0.011)	(0, 0)	(0, 0)
$\mathbb{E}[T_Z]$ [b]	44.1	64.3	76.7	85.2	91.4
$\bar{T}_Z$ [b]	43.6	64.5	79.9	85.4	90.0
	(41.3, 45.9)	(62.2, 66.8)	(77.8, 82.1)	(83.4, 87.4)	(88.2, 91.8)
$\tilde{T}_Z$ [b]	32.8	59.7	81.8	88.5	95.2
	(29.2, 36.7)	(56.7, 63.0)	(77.6, 85.7)	(83.6, 93.7)	(91.0, 99.0)

[a] expected value/sample mean/sample median of fraction of zero vendor parts available

[b] expected value/sample mean/sample median of time until obsolescence (months)

The results for Model P_Z (Table 3.5 and Figure 3.7a) show the expected value $\mathbb{E}[P_Z]$, sample mean $\bar{P}_Z$, and sample median $\tilde{P}_Z$ all *decrease* as the number of tracked vendor parts increases from one to five. Figure 3.7b and Table 3.5 provide the results for Model T_Z, where the expected value, $\mathbb{E}[T_Z]$, sample mean, $\bar{T}_Z$, and sample median, $\tilde{T}_Z$, all *increase* as the number varies from one to five initially tracked vendor parts. The sharpest increase in risk occurs when the vendor parts decrease from 2 to 1. As one considers tracking additional vendor parts, there are diminishing returns in the amount of availability risk. For example, the diminishing returns predicted from Model T_Z's results indicate a roughly twenty month increase in T_Z when tracking two vendor parts instead of one, but only a ten month increase in T_Z when tracking three vendor parts instead of two. This finding can inform decisions to proactively mitigate future DMSMS issues by increasing the number of vendor part sources by providing a measure of the mitigated risk.

Extending Scenario 2 - Time- and State-dependent Cases

This extension of the second scenario presents three cases where the vendor part procurement lifetimes are not assumed to be stationary, but rather have time- or state-dependence. The first two cases model a diminishing procurement lifetime over time. The first case reduces a vendor part's procurement lifetime via an exponential decay function

$$L_j \leftarrow l e^{-\mathcal{D}t}, \tag{3.8}$$

where $\mathcal{D} > 0$ is the decay constant and t is the current time in the simulation, $0 \leq t \leq T$. To account for this change, the algorithms in Sections 3.4.3 and 3.4.3 will update line 4 with (3.8).

The second case models the increasing probability of there being no F3 replacement in the market, in other words, increasing the Bernoulli trial probability of success, b_j, for VP $j = 1, \ldots, \kappa$ over time. A way to model this is to use a linear function with the starting probability (β_1) and the probability at the end of the time frame (β_2):

$$b_j \leftarrow \beta_1 + \frac{\beta_2 - \beta_1}{T} t, \tag{3.9}$$

where $0 \leq \beta_1 < \beta_2 \leq 1$. To account for this change the Model T_Z algorithm in Section 3.4.3 is modified by inserting (3.9) between lines 8 and 9.

The third case models the supply chain situation where sole/single manufacturers are relied upon to provide critical vendor parts, usually via contractual means. This can be modeled by using a state-dependent function that scales the procurement lifetime by a (positive) scalar value in the event where there is only one manufacturer in the market:

$$L_{ind} \leftarrow L_{ind} + \mathcal{S}^{\mathbb{1}(V(t)=1)}\, l, \tag{3.10}$$

where $\mathcal{S} > 1$ represents the amount of scaling that is expected when there is a sole manufacturer, and $\mathbb{1}(\cdot)$ is the indicator function. $V(t)$ is defined as the number of manufacturers in the market, which can be expressed using $v_{j,r}$ from (3.1) in Section 3.4.3:

$$V(t) = \sum_{j=1}^{\kappa} (1 - v_{j,r}(t)) \,.$$

Updating line 15 in the Model T_Z algorithm in Section 3.4.3 to (3.10) will allow this phenomenon to be modeled. To account for the instance where there is only one vendor part available at the beginning of the simulation, line 4 should also be updated with

$$L_j \leftarrow \mathcal{S}\, l.$$

The extensions to Scenario 2 present the findings in terms of Model T_Z. The results would be similar for Model P_Z for (3.8) and (3.10), but there is no direct interpretation for (3.9). The results shown below assume a rate of decay of $\mathcal{D} = 0.025$; the beginning probability β_1 is 50% while the ending probability β_2 is 90%; and the procurement lifetime will double when there is only one vendor part in the marketplace, i.e. $\mathcal{S} = 2$. The parameters $\mathcal{D}, \beta_1, \beta_2$, and $\mathcal{S}$ can be calibrated by fitting the appropriate historical data in practice. Also, the functional forms in (3.8), (3.9), and (3.10) can be updated to better fit the available data. These additions can be combined with the first scenario for added modeling realism when comparing multiple configuration parts.

The results for the extension of Scenario 2 are shown in Figure 3.8 and Table 3.6. The top element in each figure is an instantiation of the configuration parts shown in Section 3.5.2 for comparison. In all instances, the decaying procurement lifetime case ('CP-d') and the increasing Bernoulli parameter case ('CP-b') show decreases in the mean and median values of T_Z, indicating increased risk. Likewise, modeling the single vendor case ('CP-s') shows increases in the mean and median values of T_Z, indicating reduced risk.

The number of initially tracked vendor parts affects the degree of the impact of the cases. For example, when the simulation starts with only one vendor part, the mean T_Z for the decay case decreases by almost nine months compared to the base model but the impact

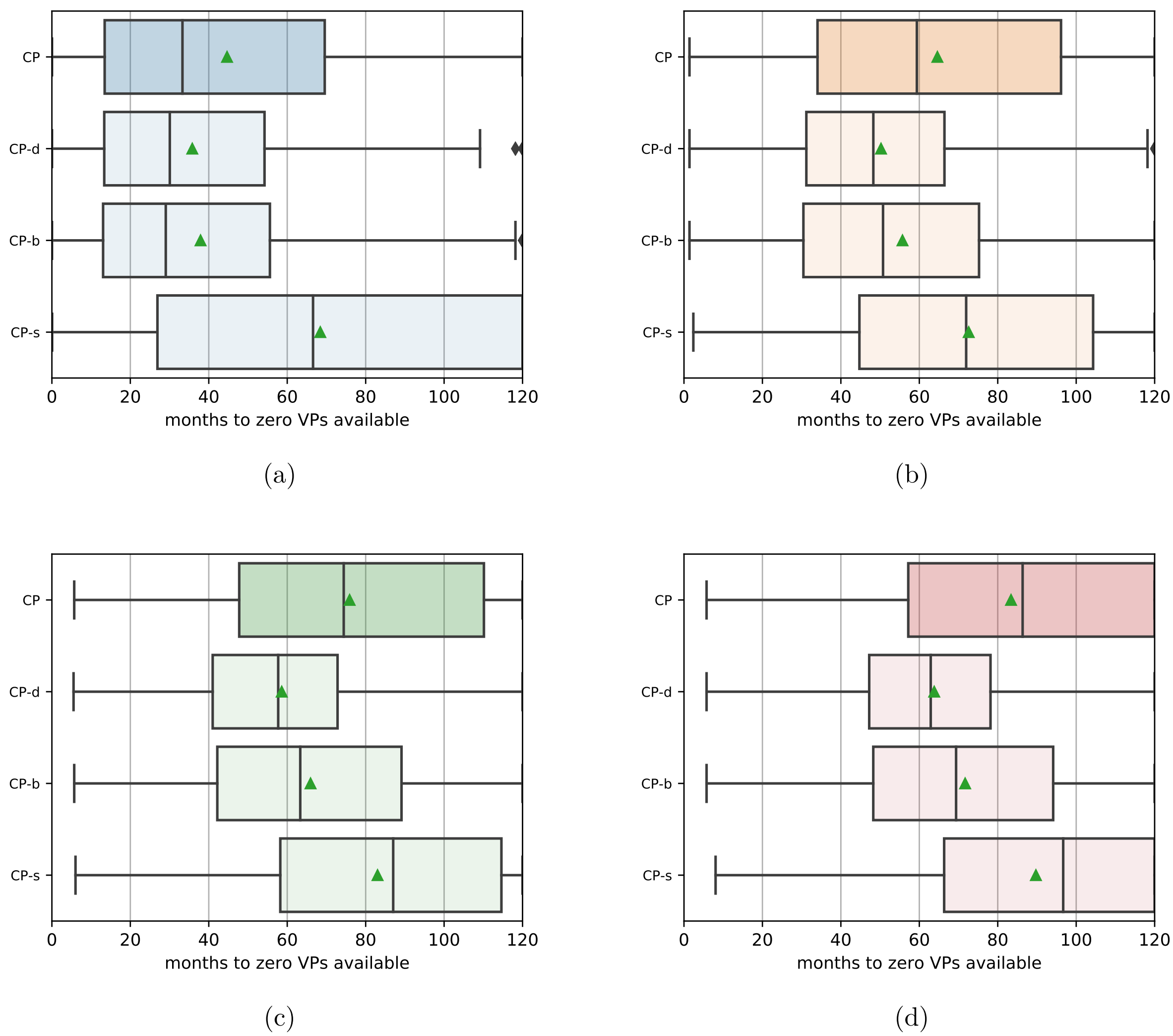

Figure 3.8: Effects on the T_Z risk metric when accounting for time- and state-dependent cases for (a) one initial vendor part, (b) two initial vendor parts, (c) three initial vendor parts, and (d) four initial vendor parts. Simulation uses 1000 replications modeling a 10-year time frame. The green triangle represents the mean value while the center vertical line within the box shows the median value.

Table 3.6: Results for the T_Z risk metric when accounting for time- and state-dependent with one through four initial vendor parts in the marketplace for $R = 1000$ and $T = 10$ years. Estimates are shown with 95% confidence intervals.

Initial VPs	Availability risk metric	CP	CP-d	CP-b	CP-s
1	$\bar{T}_Z$[a]	44.7 (42.3, 47.0)	35.8 (34.1, 37.5)	37.9 (36.0, 40.0)	68.4 (65.7, 71.1)
	$\tilde{T}_Z$[b]	33.3 (29.7, 36.0)	30.0 (28.1, 33.3)	29.0 (27.2, 31.6)	66.6 (59.4, 71.9)
2	$\bar{T}_Z$[a]	64.6 (62.4, 66.9)	50.2 (48.6, 51.8)	55.7 (53.7, 57.7)	72.6 (70.5, 74.7)
	$\tilde{T}_Z$[b]	59.4 (55.4 63.3)	48.3 (46.2, 50.7)	50.8 (48.4, 52.9)	71.9 (69.2, 76.0)
3	$\bar{T}_Z$[a]	75.9 (73.8, 78.0)	58.6 (57.1, 60.1)	65.9 (64.1, 67.8)	83.0 (81.1, 85.0)
	$\tilde{T}_Z$[b]	74.4 (71.8, 77.7)	57.7 (55.9, 59.3)	63.3 (60.1 65.7)	87.0 (83.6, 90.9)
4	$\bar{T}_Z$[a]	83.4 (81.4, 85.4)	63.8 (62.4, 65.2)	71.7 (69.9, 73.5)	89.7 (87.9, 91.6)
	$\tilde{T}_Z$[b]	86.3 (82.0 89.5)	62.9 (61.0 64.3)	69.4 (66.8 71.7)	96.7 (93.3 100.7)

[a] sample mean time until obsolescence (months)

[b] sample median time until obsolescence (months)

is increased to more than twenty months when starting with four vendor parts. There are similar effects for the median T_Z values for the decay case and the mean and median T_Z values in the increasing Bernoulli parameter case. For the chosen values of $\mathcal{D}, \beta_1$, and β_2, the decay model tends to have a greater impact on the value of T_Z than the case of changing the Bernoulli trial parameter value. On the contrary, when looking at the single vendor case the changes in the estimates for T_Z are larger when there is only one vendor part in the market but decrease as the number of initial vendor parts increases. The fixed timeline ($T = 10$) used in this DES affects the mean values. One must be aware of the choice of T in specific applications.

3.6 Discussion and Conclusion

The proposed modeling framework provides a proactive DMSMS management method that is capable of quantifying and comparing availability risk across configuration parts with multiple vendor parts in a production or logistic system. Both availability risk metrics, P_Z and T_Z, provide the ability to quantify availability risk on a system level and can be used as inputs to currently used DMSMS tools. The first scenario estimates the risk for two configuration parts with different procurement lifetimes and provides a comparison. The second scenario quantifies the risk for a single configuration part in various stages of the product life-cycle. Extensions to both scenarios highlight the modeling framework's ability to handle common DMSMS issues, in particular, inter-dependencies among vendor parts and time- and state-dependent procurement lifetimes.

This modeling framework is implemented assuming exponentially distributed procurement lifetimes and inter-arrival times which are conducive to a) theoretical analyses as shown in the appendices and to b) comparison and verification of the simulation results. However, such distributional assumptions can be relaxed in practice to use distributions more fitting to historical data. Procurement lifetimes of individual vendor parts are at the heart of DMSMS management and can be estimated using a variety of methods as discussed by [97] among others. In cases where data is missing or insufficient, SME knowledge and inputs can be used to validate the procurement lifetime distributions. Future work may account for supply disruptions discussed by [12], [45], and [58] by making similar extensions as those in Section 3.5.2.

In a world of finite resources, the proposed modeling framework describing the availability risk of a system can be used to inform decisions regarding optimal resource allocation. Future work could evaluate various policies involving the actions taken by decision makers and their associated costs using this modeling framework. The results can be used to proactively inform DMSMS issue resolution scheduling.

3.7 Mathematical Analysis for $\mathbb{E}[P_Z]$

For an $M/M/k/k/k$ system as described by Model P_Z, one can derive the expected value for the *fraction of time with zero vendor parts available*, $\mathbb{E}[P_Z]$. The infinitesimal generator matrix Q of the underlying continuous-time Markov chain (CTMC) is given as

$$Q = \begin{bmatrix} -k\lambda & k\lambda & 0 & \cdots & 0 & 0 & 0 \\ \mu & -(\mu + (k-1)\lambda) & (k-1)\lambda & \cdots & 0 & 0 & 0 \\ 0 & 2\mu & -(2\mu + (k-2)\lambda) & (k-2)\lambda & 0 & 0 & 0 \\ \vdots & \vdots & \vdots & \ddots & \vdots & \vdots & \vdots \\ 0 & 0 & 0 & \cdots & (k-1)\mu & -((k-1)\mu + \lambda) & \lambda \\ 0 & 0 & 0 & \cdots & 0 & k\mu & -k\mu \end{bmatrix},$$

where each entry q_{s_1,s_2} is the transition rate of going from state s_1 to s_2 for $s_1,\ s_2 \in \{0, 1, \ldots, k\}$.

The expected value of P_Z can be calculated by using (3.2) from Section 3.4.3. Letting

$X(t) \in \{0, 1, \ldots, k\}$ represent the CMTC state for $t \in [0, T]$, the expected value of P_Z is

$$\begin{aligned}
\mathbb{E}\left[P_{Z,i}^{(r)}\right] &= \mathbb{E}\left[\frac{1}{T}\int_0^T \prod_{j=1}^{K_i} v_{j,r}(t)dt\right] \\
&= \mathbb{E}\left[\frac{1}{T}\int_0^T \mathbb{1}(X(t)=0)dt\right] \\
&= \frac{1}{T}\int_0^T \mathbb{E}\left[\mathbb{1}(X(t)=0)\right]dt \\
&= \frac{1}{T}\int_0^T P(X(t)=0)dt \\
&= \frac{1}{T}\int_0^T P_{k,0}(t)dt
\end{aligned} \tag{3.11}$$

where $P_{k,0}(t)$ is the probability of being in the zeroth state at time t, given a starting state of k vendor parts available at $t = 0$ ($X(0) = k$). The probability $P_{k,0}(t)$ can be calculated by taking the $(k, 0)^{th}$ entry of the matrix exponential, $\exp(Qt)$.

A general form to solve for $\exp(Qt)$ is found by substituting $Q = UDU^{-1}$ using eigendecomposition, where U is the eigenvector matrix and D is the diagonal matrix consisting of the eigenvalues of Q, d_i for $i \in \{1, \ldots, n\}$. Letting $\boldsymbol{d}(t) = diag(\exp(Dt)) = [e^{d_1 t}, e^{d_2 t}, \cdots, e^{d_n t}]'$ yields the general form:

$$\begin{aligned}
\exp(Qt) &= U\exp(Dt)U^{-1} \\
&= \begin{bmatrix} U[0,:] \\ U[1,:] \\ \vdots \\ U[k,:] \end{bmatrix} \begin{bmatrix} e^{d_0 t} & 0 & \cdots & 0 \\ 0 & e^{d_1 t} & \cdots & 0 \\ \vdots & \vdots & \ddots & 0 \\ 0 & 0 & 0 & e^{d_k t} \end{bmatrix} \begin{bmatrix} U^{-1}[:,0] & U^{-1}[:,1] & \cdots & U^{-1}[:,k] \end{bmatrix} \\
&= \begin{bmatrix} u_{00}e^{d_0 t} & u_{01}e^{d_1 t} & \cdots & u_{0k}e^{d_k t} \\ u_{10}e^{d_0 t} & u_{11}e^{d_1 t} & \cdots & u_{1k}e^{d_k t} \\ \vdots & \vdots & \ddots & \vdots \\ u_{k0}e^{d_0 t} & u_{k1}e^{d_1 t} & \cdots & u_{kk}e^{d_k t} \end{bmatrix} \begin{bmatrix} U^{-1}[:,0] & U^{-1}[:,1] & \cdots & U^{-1}[:,k] \end{bmatrix} \\
&= \begin{bmatrix} U[0,:] \odot \boldsymbol{d}(t) \\ U[1,:] \odot \boldsymbol{d}(t) \\ \vdots \\ U[k,:] \odot \boldsymbol{d}(t) \end{bmatrix} \begin{bmatrix} U^{-1}[:,0] & U^{-1}[:,1] & \cdots & U^{-1}[:,k] \end{bmatrix}
\end{aligned}$$

$$= \begin{bmatrix} (U[0,:] \odot \boldsymbol{d}(t)) \bullet U^{-1}[:,0] & (U[0,:] \odot \boldsymbol{d}(t)) \bullet U^{-1}[:,1] & \cdots & (U[0,:] \odot \boldsymbol{d}(t)) \bullet U^{-1}[:,k] \\ (U[1,:] \odot \boldsymbol{d}(t)) \bullet U^{-1}[:,0] & (U[1,:] \odot \boldsymbol{d}(t)) \bullet U^{-1}[:,1] & \cdots & (U[1,:] \odot \boldsymbol{d}(t)) \bullet U^{-1}[:,k] \\ \vdots & \vdots & \ddots & \vdots \\ (U[k,:] \odot \boldsymbol{d}(t)) \bullet U^{-1}[:,0] & (U[k,:] \odot \boldsymbol{d}(t)) \bullet U^{-1}[:,1] & \cdots & (U[k,:] \odot \boldsymbol{d}(t)) \bullet U^{-1}[:,k] \end{bmatrix},$$

where $\odot$ is the Hadamard product (or element-wise product) and $\bullet$ is the dot product. The terms $U[m,:]$ and $U[:,n]$ refer to the m^{th} row and n^{th} column of matrix U, respectively, and u_{mn} refers to the m^{th} row and n^{th} column entry of matrix U. Thus,

$$P_{k,0}(t) = \exp(Qt)[k,0] = (U[k,:] \odot \boldsymbol{d}(t)) \bullet U^{-1}[:,0]. \tag{3.12}$$

Substituting (3.12) into (3.11) yields:

$$\mathbb{E}\left[P_{Z,i}^{(r)}\right] = \frac{1}{T}\int_0^T (U[k,:] \odot \boldsymbol{d}(t)) \bullet U^{-1}[:,0]dt. \tag{3.13}$$

The numerical results of (3.13), tailored to the specific scenarios, are shown in Tables 3.3-3.5.

3.8 Mathematical Analysis for $\mathbb{E}[T_Z]$

In Model T_Z, under the conditions mentioned above, one can analytically derive the expected value for the *time to obsolescence*, $\mathbb{E}[T_Z]$. The random variable, $Y_{ij} = X_{ij1} + X_{ij2} + \ldots + X_{ijL}$, is the total procurement lifetime over all life-cycles for vendor part j and associated with configuration part i. The random variable L is defined as the number of life-cycles until a vendor part is not procurable (obsolete) and is considered a stopping time for Y_{ij}. Each X_{ijl} for $j \in \{1,\ldots,K_i\}$ and $l \in \{1,\ldots,L\}$ is assumed to be *iid* across all life-cycles and all vendor parts associated with configuration part i. Under these assumptions, let the common distribution of X_{ijl} for any j and any l to be denoted as the distribution of X_i. It is also assumed that $X_i, i \geq 1$, and L are independent. For a configuration part i with one tracked vendor part, Wald's equation yields

$$\begin{aligned} \mathbb{E}\left[Y_{ij}\right] &= \mathbb{E}\left[\sum_{l=1}^{L} X_{ijl}\right] \\ &= \mathbb{E}[X_i]\mathbb{E}[L] \\ &= \frac{\mu_{X_i}}{b_i}, \end{aligned}$$

where μ_{X_i} is the expected value of X_i. Since the random variable L is the number of Bernoulli trials until a success, it has a geometric distribution with probability of success b_i, and $\mathbb{E}[L] = \frac{1}{b_i}$.

Using the moment generating function (MGF), one can see that Y_{ij} is exponentially distributed:

$$
\begin{aligned}
M_{Y_{ij}}(t) &= \mathbb{E}\left[\exp\left(tY_{ij}\right)\right] \\
&= \mathbb{E}\left[\mathbb{E}\left[\exp\left(tY_{ij}\right)|L\right]\right] \\
&= \sum_{l=1}^{\infty}(1-\mu_{X_i}t)^{-l}b_i(1-b_i)^{l-1} \qquad (3.14) \\
&= \frac{b_i}{1-b_i}\sum_{l=1}^{\infty}\left(\frac{1-b_i}{1-\mu_{X_i}t}\right)^l \qquad (3.15) \\
&= \frac{b_i}{1-b_i}\cdot\frac{1-b_i}{b_i-\mu_{X_i}t} \qquad (3.16) \\
&= \frac{\frac{b_i}{\mu_{X_i}}}{\frac{b_i}{\mu_{X_i}}-t}. \qquad (3.17)
\end{aligned}
$$

In (3.14), it is noted that $Y_{ij}|L$ follows an Erlang distribution and used its MGF defined for $t < 1/\mu_{X_i}$. Noting the sum of a geometric series in (3.15), the equality in (3.16) follows for $t < b_i/\mu_{X_i}$. The expression in (3.17) is the MGF of an exponential distribution with rate, $B_i = \frac{b_i}{\mu_{X_i}}$. This result is intuitive because of the memoryless property of both exponential and geometric distributions.

For a configuration part with K_i tracked vendor parts for $K_i > 1$, T_{Z_i} is equal to $\max\{Y_{i1}, Y_{i2}, \ldots, Y_{iK_i}\}$ for configuration part i. The cumulative distribution function (CDF) of T_{Z_i} is then

$$
\begin{aligned}
F_{T_{Z_i}}(t) &= P(T_{Z_i} \leq t) \\
&= P(\max\{Y_{i1}, Y_{i2}, \ldots, Y_{iK_i}\} \leq t) \\
&= \prod_{j=1}^{K_i} P(Y_{ij} \leq t) \\
&= \left(1-\exp\left(-B_i t\right)\right)^{K_i}.
\end{aligned}
$$

Taking the first derivative of $F_{T_{Z_i}}(t)$ and using the binomial theorem gives us the probability density function (PDF) of T_{Z_i},

$$\begin{aligned} f_{T_{Z_i}}(t) &= \frac{d}{dt} F_{T_{Z_i}}(t) \\ &= \frac{d}{dt} \left(1 - \exp\left(-B_i t\right)\right)^{K_i} \\ &= \frac{d}{dt} \sum_{j=0}^{K_i} (-1)^j \binom{K_i}{j} \left(e^{-jB_i t}\right) \\ &= \sum_{j=1}^{K_i} (-1)^{j+1} \binom{K_i}{j} (jB_i) \left(e^{-jB_i t}\right). \end{aligned}$$

Since the simulation run length, T, is an upper bound on T_{Z_i}, a new random variable T'_{Z_i} is introduced:

$$T'_{Z_i} = \begin{cases} T_{Z_i}, & T_{Z_i} < T \\ T, & T_{Z_i} \geq T. \end{cases}$$

The expected value of T'_{Z_i} is given by

$$\begin{aligned} \mathbb{E}[T'_{Z_i}] &= \mathbb{E}[T'_{Z_i} \mid T_{Z_i} < T] P(T_{Z_i} < T) + \mathbb{E}[T'_{Z_i} | T_{Z_i} \geq T] P(T_{Z_i} \geq T) \\ &= \int_0^T t \cdot f_{T'_{Z_i} | T_{Z_i} < T}(t) dt \cdot P(T_{Z_i} < T) + T \cdot (1 - P(T_{Z_i} < T)). \end{aligned} \tag{3.18}$$

The conditional PDF $f_{T'_{Z_i}|T_{Z_i}<T}(t)$ can be found by taking the derivative of the conditional CDF

$$\begin{aligned} F_{T'_{Z_i}|T_{Z_i}<T}(t) &= P(T'_{Z_i} \leq t | T_{Z_i} < T) \\ &= \frac{P(\{T'_{Z_i} \leq t\} \cap \{T_{Z_i} < T\})}{P(T_{Z_i} < T)} \\ &= \frac{P(T_{Z_i} \leq t) \mathbb{1}(t < T) + P(T_{Z_i} < T) \mathbb{1}(t \geq T)}{P(T_{Z_i} < T)} \\ &= \begin{cases} \frac{P(T_{Z_i} \leq t)}{P(T_{Z_i} < T)}, & t < T \\ 1, & t \geq T. \end{cases} \end{aligned}$$

Thus, the conditional PDF is

$$f_{T'_{Z_i}|T_{Z_i}<T}(t) = \frac{d}{dt}F_{T'_{Z_i}|T_{Z_i}<T}(t) = \begin{cases} \frac{f_{T_{Z_i}}(t)}{P(T_{Z_i}<T)}, & t < T \\ 0, & t \geq T. \end{cases} \tag{3.19}$$

Substituting (3.19) into (3.18) yields

$$\begin{aligned}
\mathbb{E}[T'_{Z_i}] &= \int_0^T t \cdot \frac{f_{T_{Z_i}}(t)}{P(T_{Z_i} < T)} dt \cdot P(T_{Z_i} < T) + T \cdot (1 - P(T_{Z_i} < T)) \\
&= \int_0^T \left(\sum_{j=1}^{K_i} (-1)^{j+1} \binom{K_i}{j} (jB_i) \left(t \cdot e^{-jB_i t}\right) \right) dt + T \cdot \left(1 - \left(1 - e^{-B_i T}\right)^{K_i}\right) \\
&= \left(\sum_{j=1}^{K_i} (-1)^{j+1} \binom{K_i}{j} (jB_i) \int_0^T \left(t \cdot e^{-jB_i t}\right) dt \right) + T \cdot \left(1 - \left(1 - e^{-B_i T}\right)^{K_i}\right) \\
&= \left(\sum_{j=1}^{K_i} (-1)^{j+1} \binom{K_i}{j} (jB_i) \cdot \left(\frac{e^{-jB_i T}(-jB_i T - 1)}{(-jB_i)^2} + \frac{1}{(-jB_i)^2} \right) \right) + \\
&\qquad\qquad\qquad\qquad T \cdot \left(1 - \left(1 - e^{-B_i T}\right)^{K_i}\right) \\
&= \left(\sum_{j=1}^{K_i} (-1)^j \binom{K_i}{j} \frac{e^{-jB_i T}(jB_i T + 1) - 1}{(jB_i)} \right) + T \cdot \left(1 - \left(1 - e^{-B_i T}\right)^{K_i}\right).
\end{aligned} \tag{3.20}$$

Equation (3.20) can be calculated for given values of μ_{X_i}, b_i, K_i, T. As the number of replications, R, tends to infinity $\bar{T}_{Z,i}$ in (3.6) will converge to $\mathbb{E}[T'_{Z_i}]$ for the i^{th} configuration part by the law of large numbers. The results of (3.20) are shown in Tables 3.3-3.6.

Chapter 4

OPTIMAL TECHNOLOGY REFRESH STRATEGIES FOR STRATEGIC DMSMS MANAGEMENT

This chapter presents research that was accepted for publication in the *Proceedings of the 2019 Winter Simulation Conference* [107]. The paper identified an optimal technology refresh strategy using a ranking and selection method for a finite horizon. New work that uses a rolling horizon is added.

Abstract

The effects of Diminishing Manufacturing Sources and Material Shortages (DMSMS) can be excessively costly if not addressed in a timely manner. A strategic DMSMS management method that seeks to minimize the overall life-cycle cost of a system, e.g. an aircraft or ship, is presented. The goal is to select an optimal scheduling of technology refreshes over a fixed lifetime, using lifetime buys (LTBs) as the mitigation option. A DMSMS-specific cost model is constructed that accounts for costs of multiple, diverse parts in a system and multiple technology refreshes. This study compares the optimal technology refresh strategy when using a ranking and selection (R&S) method with a rolling horizon (RH) framework, which uses a global optimization method at each decision period, for a complex cost function dependent upon varying refresh costs. In a simulation case study for a system with a ten-year lifetime, the R&S method tends to recommend less technology refreshes than the RH framework as the technology refresh costs increase. A visual model is presented for the R&S method which provides the ability to quickly compare other feasible strategies.

4.1 Introduction

For sustainment dominated systems, where the system lifetime is much larger than the constituent sub-parts of the system, accounting for diminishing manufacturing sources and material shortages (DMSMS) issues in life-cycle planning is critical. If these systems are managed poorly, sustainment costs can dominate operational costs and diminish the operational readiness of the system. Alternatively, retiring large systems and replacing them with newer systems can be extremely costly and should be avoided unless absolutely necessary. To keep military platforms operationally effective and relevant, it is necessary to evaluate the trade-offs between complete system redesigns and other lower cost alternatives. One of the goals of DMSMS management is evaluation, identification, and implementation of the most cost-effective strategy while ensuring operational effectiveness. The primary contribution of this chapter is providing the optimal technology refresh strategies for a system with a ten-year lifetime, using an R&S method versus using a RH framework that uses a global optimization model at each decision stage (i.e. each year) and comparing the results from each. A secondary contribution of this chapter is providing a method to visualize strategies and their associated costs for easy comparison and is described in Section 4.5.

DMSMS management can be thought of as consisting of three facets: reactive, proactive, and strategic [7]. Reactive DMSMS management occurs after a part has become obsolete or is known to become obsolete in the near future. At the disposal of the DMSMS manager are a multitude of reactive options to mitigate DMSMS issues such as using existing stock, using approved parts, part substitutions, extending production, developing new sources, lifetime buys (LTBs), and technology refreshes [7, 23]. LTBs are a mitigation technique where a DMSMS manager purchases a large enough quantity of the parts to sustain the product until the next scheduled technology refresh or the planned end of life. LTBs are also referred to as “life-of-need”, “bridge”, “last-time”, and “life-of-type” buys. Proactive DMSMS management forecasts the risk for components and uses reactive options to mitigate obsolescence issues [94].

Strategic DMSMS management is defined as a "mix of reactive mitigation approaches and [planned technology] refreshes that minimizes life-cycle costs" [94]. A technology refresh is a predictable process for replacing old technology with new assets to avoid technology obsolescence, to save money by improving system efficiency, and to reduce failures and downtime. Other terms for technology refreshes are "design refresh", "redesign", and "technology insertion". This chapter considers strategic DMSMS management plans that use a sequence of planned technology refreshes with LTBs as the intermediate mitigation option between technology refreshes.

An optimal DMSMS management plan minimizes the overall cost of a platform over the operational lifetime. Modeling technology refresh decisions can be accomplished using a equipment replacement model, first introduced by Bellman which seeks the "optimal procedure for replacing old equipment with new" [11]. Bellman [11] evaluated the optimal equipment policy under an infinite horizon as a finite horizon model may introduce end-of-study (boundary) effects [35]. However, there are cases where a finite horizon model may be appropriate, for instance, when equipment is contracted for a period of time or when equipment and technology are acquired for a very specific use [38]. A strong case for the use of a finite horizon can be made in Department of Defense (DoD) applications, where equipment such as aircraft, naval vessels, trucks, etc., will have a (somewhat) definitive life-cycle.

This study will consider a complex system consisting of multiple parts with LTBs as a mitigation strategy over the finite, ten-year lifetime. The sequence of decisions made at each time period is considered a strategy represented by the vector, $y \in Y$ of length $T-1$, where Y is the set of feasible strategies. Each element y_t in the vector y is either a 0 or a 1, where $y_t = 1$ indicates a planned refresh at year t. For each time period, a decision maker must decide whether or not to schedule a technology refresh each year over the system's planned lifetime T. This can be translated into a finite horizon program, given by:

$$\begin{aligned} \min_{y \in Y} \quad & Z(y) \\ s.t. \quad & y_t \in \{0,1\} \\ & t \in \{1, 2, \ldots, T-1\} \end{aligned} \tag{4.1}$$

where the strategy y is a vector of length $T-1$. The term $Z(y)$ is the cost associated with the strategy y; for the R&S method it is defined as the expected cost, $Z(y) \stackrel{\text{def}}{=} \mathbb{E}[C(y)]$, as the method will allow for stochasticity, while the RH framework will assume deterministic costs defining $Z(y) \stackrel{\text{def}}{=} C(y)$. The result of solving (4.1) is an optimal strategy defined as

$$y^* \stackrel{\text{def}}{=} \arg\min_{y \in Y} \; Z(y),$$

informing the decision maker of an optimal scheduling of technology refreshes using LTBs as a mechanism to fill any shortages.

Two example strategies are shown in Figure 4.1 to help visualize how LTBs can be used with a strategy. The red, dashed lines represent the years with a planned technology refresh. Arrows represent the procurement lifetime of a part, or the time that a part is available for procurement in the marketplace. If a part becomes obsolete prior to a planned refresh, these shortfalls must be covered by a LTB purchase, indicated by the boxes. Costs are incurred at a planned technology refresh (vertical dashed red lines) and LTBs (boxes). The purchase quantity of the LTB must be large enough to ensure there are sufficient quantities available to meet demand until the next planned technology refresh or planned system obsolescence. The figure on the left depicts a strategy ($\langle 001000100 \rangle$) with two technology refreshes. Costs for this strategy are incurred at the planned refresh years (years three and seven) and to cover the demands represented by the LTB boxes. The figure on the right depicts a strategy ($\langle 000001000 \rangle$) with one technology refresh. This strategy only incurs one technology refresh cost at year six for the technology refresh, but will incur greater LTB costs since there is a greater amount of time to cover the LTB periods.

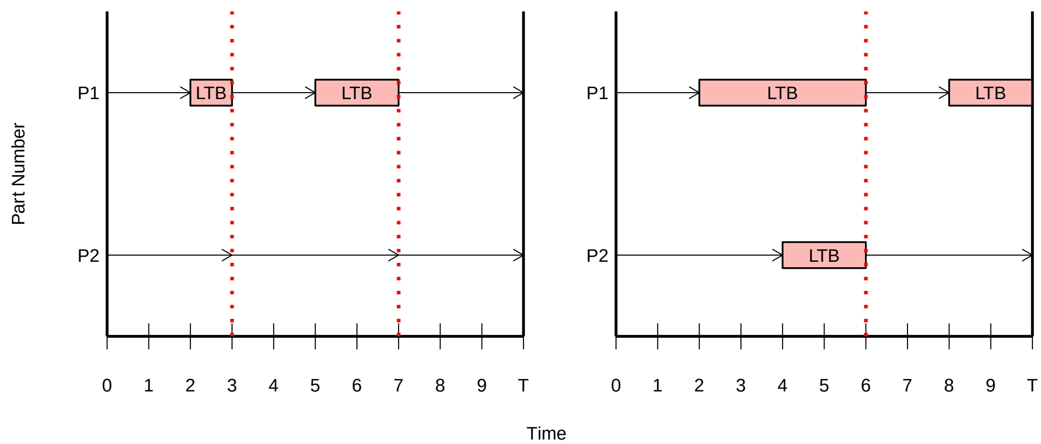

Figure 4.1: An example two-part (P1 and P2) system with two proposed redesign strategies. The figure on the left depicts a strategy with two technology refreshes; the figure on the right illustrates a strategy with one technology refresh. Technology refreshes are represented by red dashed lines, LTBs by boxes, and procurement lifetimes by arrows.

4.2 Related Literature

This section will provide an overview of previous studies related to strategic DMSMS management. These include how other studies have attempted to address strategic DMSMS management, outline a simple cost function using LTBs and technology refreshes, and provide an overview of R&S methods and the RH framework.

4.2.1 Strategic DMSMS Background

Other studies have evaluated the use of LTBs and technology refreshes as part of strategic DMSMS management. One study compares three strategies, programmed technology refreshes, LTBs, and re-engineering (which is defined as reactive measures other than LTBs) using a Monte-Carlo simulation [117]. They recommend programmed technology refreshes as the most cost effective, but condition their findings on the reliability characteristics used in their model. Whereas these authors evaluate three different mitigation options (separately), this dissertation will evaluate a combination of the two options they evaluated (LTB and technology refreshes).

Another study uses graph theory and mixed integer programming with a combination of LTB and technology refreshes [69]. They seek an optimal strategy over a fixed lifetime for a system with multiple parts. They seek to find an optimal schedule for a single technology refresh using a deterministic model. This chapter will follow a similar methodology, but will allow multiple technology refreshes and compare the results of a deterministic model and the the stochastic R&S method in calculating the life-cycle costs.

One must consider using a DMSMS specific cost function when solving (4.1). Feng et al. [32] and Teunter and Fortuin [113] present net-present value (NPV) models that evaluate the effect of the LTB quantities on the ability to support a system. The models search for an optimal LTB size for multiple parts in a system to minimize the overall life-cycle cost, accounting for LTBs, technology refreshes, holding, stock-out, and salvage costs. However, the models evaluate the effects of the overall life-cycle cost for a single, fixed technology refresh date. This dissertation seeks to evaluate life-cycle costs for multiple combinations of refresh dates, taking into account various operational time-frames. A simpler cost model is presented by Bartels et al. [7], that is based on previous work by Porter [83]. The Porter model is a net present value model that considers the refresh cost and LTB costs for a single technology refresh date. The formulation by [83] is given by:

$$C = C_{TR} + C_{LTB} \tag{4.2}$$

where the total cost, C, is given by the costs associated with a technology refresh, C_{TR}, and the costs associated with LTBs, C_{LTB}. The cost for a technology refresh is given by:

$$C_{TR} = \exp(-rY_R)c_R, \tag{4.3}$$

where c_R is the technology refresh cost in year 0; r is the discount rate; and Y_R is the year of the technology refresh (> 0).

The cost associated with a LTB is given by:

$$C_{LTB} = \begin{cases} 0, & \text{when } t = 0 \text{ or if } Y_R = 0, \\ c\sum_{t=1}^{Y_R} d_t, & \text{for } Y_R > 0, \end{cases} \tag{4.4}$$

where t is the year after obsolescence; c is the price of the obsolete part in the year of the LTB ($t = 0$); d_t is the demand at time t. The model in (4.2) assumes that the part under consideration is obsolete at the beginning of the simulation ($t = 0$), whereas this dissertation will allow parts to be procureable. In the DMSMS literature, multiple studies have sought to minimize overall life-cycle costs for a system but a majority of these studies only evaluate single component DMSMS risk and not DMSMS risk at the aggregate or system level [90]. This paper expands the cost model provided by [7] in Section 4.3.1 to account for systems composed of multiple parts and multiple technology refreshes over a fixed timeline.

4.2.2 Ranking and Selection

Ranking and Selection (R&S) methods seek to find an optimal arrangement with respect to a value of interest (i.e. cost). In terms of DMSMS, this is often identifying the strategy with minimal cost over a set of alternative strategies. Popular R&S methods involve using an indifference zone (IZ) which identifies the optimal strategy within a "smallest difference worth detecting" at a given confidence level [36]. In terms of DMSMS the IZ is the dollar amount that the decision maker is indifferent to regarding the total cost; i.e. they consider the differences to be negligible. The IZ value will change depending upon the context of the problem, the tolerance of the procurement life distributions, and budget constraints. Two main R&S methods are used in the case of unknown and unequal variances of the value of interest: two-stage and fully sequential methods. An example of the first method is presented by Nelson, Swann, Goldsman, and Song (NSGS) and an example of the second is Kim and Nelson (KN) [36]. Both methods begin by replicating all strategies an equal number of times then creating a subset of the most promising strategies. The NSGS method determines the number of additional samples required for each strategy in the sub-set of the most promising strategies and then identifies an optimal strategy. Instead of performing a batch update as with the NSGS method, the KN method iteratively samples each strategy in this sub-set once and removes less promising strategies until the sub-set only includes one member. For the NSGS method, the independence assumption is satisfied by ensuring independent simulation replications and the central limit theorem reasonably satisfies the normality assumption when using the sample mean to estimate the value of interest in (4.1). Current work in this field revolves mostly around computational efficiency as the number of alternatives is “large”, where “large” is on the order of one-million alternatives [74, 76]. For this paper, the NSGS method is used as it is straightforward to implement and supports the DMSMS example in Section 4.4.

4.2.3 Rolling Horizon Framework

An RH framework seeks to find the optimal solution for the first (or current) period, under the current state, before moving on to the next period. At the next period, the optimal solution is calculated, given that the optimal set of decisions has been made up until that point [14]. Many studies that use an RH framework identify the current optimal solution by using a fixed horizon but the solution can be sub-optimal as there may be some end-of study effects induced by choosing a finite horizon [35]. To mitigate choosing a sub-optimal strategy, oftentimes it is sufficient to pick a finite horizon that is large enough to minimize the end-of-study effects. One study in particular evaluated the expected cost error when using a finite horizon to estimate an infinite horizon [4].

This chapter will use an RH framework using a method presented by [53] which solves for each period’s optimal decision. The method converts an infinite horizon problem into a global optimization problem to identify the current period’s optimal decision. This method is explained in more detail in Section 4.3.3.

4.3 Simulation Model Development

This section updates the cost functions (4.3) and (4.4) and provides a DMSMS specific application of the NSGS method RH framework.

4.3.1 Updated Cost Function

The model in (4.2) assumes that the part goes obsolete at the beginning of the time period ($t = 0$) and seeks to find an optimal time to conduct a single refresh after that time. This paper considers the case where multiple parts of a system are non-obsolete at the beginning of the simulation (but can be allowed to be obsolete, if necessary). The technology refresh and LTB cost functions for a system with N parts, over a finite horizon $[0, T]$, are given by:

$$C_{TR} = \sum_{t=1}^{T-1} y_t \exp(-rt)\ c_R, \tag{4.5}$$

$$C_{LTB} = \sum_{t=1}^{T-1} \sum_{i=1}^{N} y_t \exp\left(-rZ_{ti}(y)\right) c_i d_i S_{ti}(y) + \sum_{i=1}^{N} \exp\left(-rZ_{Ti}(y)\right) c_i d_i S_{Ti}(y), \tag{4.6}$$

respectively, where:

- c_R is the cost of a single refresh;
- c_i is the per-item cost of part i;
- d_i is the demand, per unit time, of part i;
- r is the discount factor rate, $r \geq 0$;
- $S_{ti}(y)$ is a random variable for the shortage time for part i for a planned refresh at time t. The shortage time is defined as the time gap between when a part is no longer procurable (obsolete) and the next planned refresh time. Given a procurement lifetime for part i, X_i, and the time of the previous planned technology refresh, $t_{prev} \in [0, t)$, the shortage time is defined as $S_{ti}(y) = \max\{0, t - X_i - t_{prev}\}$;

- and $Z_{ti}(y)$ is a random variable for the time at which part i becomes obsolete in the time period before t, but after the previous planned refresh. This time can be calculated with: $Z_{ti}(y) = t - S_{ti}(y)$.

(Note that the last term in (4.6) represents the LTB cost that will allow the system to operate up until time T. Since it is assumed that there will not be a technology refresh at time T, the sum in (4.5) only includes $t = 1, \ldots, T-1$. Also note $t \in \mathbb{N}$, but $X_i, S_{ti}(y), Z_{ti}(y) \in \mathbb{R}_{\geq 0}$.)

The costs from planned technology refreshes in (4.5) will incur a discounted cost when $y_t = 1$, at time t. Likewise, LTB costs will be incurred when $y_t = 1$ and when part i is obsolete, as indicated by $Z_{ti}(y)$. Obsolete parts will be purchased at a discounted cost at the time when part i actually becomes obsolete, $Z_{ti}(y)$. The amount purchased is given by the demand rate, d_i, multiplied by the shortage time, $S_{ti}(y)$. The values for the item cost, item demand, and refresh costs are assumed to be fixed in this model, but could be allowed to be dependent upon the current time, t. Updating (4.2), using the technology refresh costs in (4.5) and LTB costs in (4.6), the cost function, $C(y)$, is given by:

$$C(y) = \sum_{t=1}^{T-1} y_t \exp(-rt)\, c_R + \sum_{t=1}^{T-1} \sum_{i=1}^{N} y_t \exp(-rZ_{ti}(y)) c_i d_i S_{ti}(y) + \sum_{i=1}^{N} \exp(-rZ_{ti}(y)) c_i d_i S_{ti}(y). \tag{4.7}$$

Figure 4.2 shows an example system with three parts and two planned technology refresh dates, $t = a, b$ where $0 < a < b < T$. Prior to time a, part 1 and part 2 (P1, P2) experience obsolescence for that particular part. This difference between the planned technology refresh time and the time of obsolescence is given by $S_{a,1}$ and $S_{a,2}$ for parts P1 and P2, respectively. Similarly, the shortages before time b are represented by S_{bi} and shortages before time T are given by $S_{ti}(y)$. The LTB costs will only be incurred when $S_{ti}(y) > 0$ and technology refresh costs at time a and b.

4.3.2 DMSMS Applications of the NSGS Method

Simulating the estimated values to approximately solve (4.1) will involve some randomness in each set of samples. The NSGS method ensures the probability of correctly selecting the

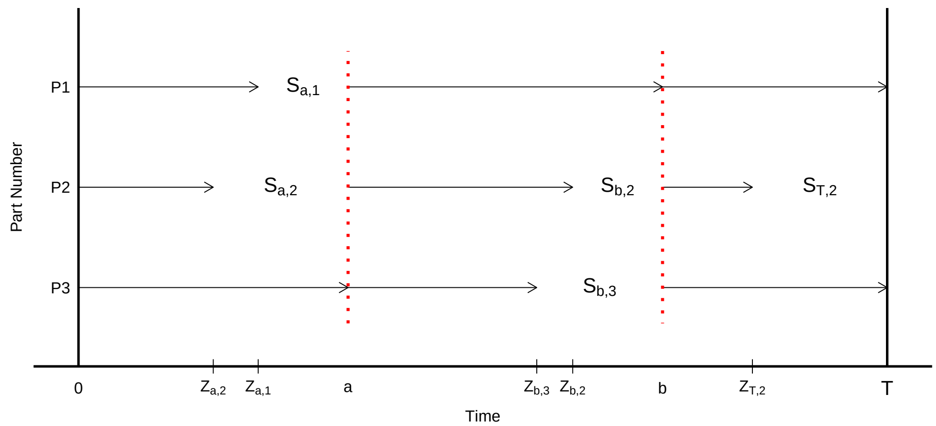

Figure 4.2: Example of a system consisting of three parts (P1, P2, P3) with two technology refresh dates, a and b, where $0 < a < b < T$. LTB costs are incurred when values for $S_{ti}(y)$ are positive and technology refresh costs at the red dashed lines.

optimal strategy, within an indifference zone, is greater than or equal to an overall confidence level $(1 - \alpha)$ under the aforementioned assumptions. The overall significance level is defined as $\alpha = \alpha_0 + \alpha_1$, where α_0 and α_1 are the first stage and second stage significance levels, respectively. The first stage identifies a set of promising strategies, subject to the indifference zone, with a probability of at least $(1 - \alpha_0)$ of containing the optimal strategy. The second stage consists of sampling the promising set of strategies for an appropriate amount of additional samples to ensure correctly identifying an optimal strategy at a confidence level of at least $(1 - \alpha_1)$. A DMSMS application of the NSGS algorithm is as follows:

1. Select the first and second stage confidence levels, $1 - \alpha_0, 1 - \alpha_1$, such that the overall significance level is $\alpha = \alpha_0 + \alpha_1$. Also, choose a practically significant difference (IZ) parameter, δ, for k strategies. Set $t = t_{(1-\alpha_0)^{1/(k-1)}, n_0 - 1}$ which is the $(1 - \alpha_0)^{1/(k-1)}100$ percentile of the t-distribution with $n_0 - 1$ degrees of freedom. Also set h equal to Rinott's constant, which will be discussed below.

2. Evaluate the cost $C(y)_{ij}$, n_0 times for each strategy $(i = 1, 2, \ldots, k; j = 1, 2, \ldots, n_0)$.

3. Compute the first stage sample mean $\overline{C(y)}_i^{(1)}$ and sample variance S_i^2 of the costs for each of the k strategies. Calculate a weighted t statistic for each paired combination of strategies:

$$W_{ii'} = t \left(\frac{S_i^2 + S_{i'}^2}{n_0} \right)^{1/2}, \text{ for } i \neq i'.$$

4. Identify the set of strategies that are not significantly greater than the others. The set is identified by $I = \{i : 1 \leq i \leq k \text{ and } \overline{C(y)}_i^{(1)} \leq \overline{C(y)}_{i'}^{(1)} + (W_{ii'} - \delta)^+, \forall i' \neq i\}$.

5. If the set I only has one strategy, stop and record that strategy as the best. If not, calculate the total number of replications required for the second stage for each $i \in I$:

$$N_i = \max \left\{ n_0, \left\lceil \left(\frac{hS_i}{\delta} \right)^2 \right\rceil \right\}, \tag{4.8}$$

where $\lceil \; \rceil$ is the ceiling function.

6. Take $N_i - n_0$ additional replications for each strategy $i \in I$ and calculate the second stage sample means:

$$\overline{C(y)}_i^{(2)} = \frac{1}{N_i} \sum_{j=1}^{N_i} C(y)_{ij}, \quad i \in I.$$

7. Select the best system with the smallest $\overline{C(y)}_i^{(2)}$.

Rinott's constant in Step 1 can be found in tables shown in [36]. For those values outside of these tables, it is necessary to numerically calculate the value of h that gives the solution to:

$$\int_0^\infty \int_0^\infty \left[\Phi \left(\frac{h}{\sqrt{\nu(1/p + 1/q)}} \right) f_\nu(p) \right]^{k-1} f_\nu(q) \, \mathrm{d}q\mathrm{d}p = 1 - \alpha_1, \tag{4.9}$$

where Φ is the cumulative distribution function of the standard normal distribution, $f_\nu(y)$ is the probability density function of the chi-squared distribution with $\nu = k - 1$ degrees of freedom. Bechhofer et al. [10] present FORTRAN code to find a numerical solution to (4.9), which was later converted into Java by Ni [76]. The latter version was converted into Python for computational use in this dissertation.

4.3.3 DMSMS Applications of the RH Framework

Solving an infinite horizon problem coupled with a rolling horizon framework, the optimal sequence of technology refresh decisions can be compared with the NSGS method for a finite horizon. The rolling horizon framework will solve for the optimal solution at each time period, conditioned on the optimal sequence of previous decisions, using an infinite horizon optimization (IHO) problem. The method presented by [53] transforms the infinite sequence of binary decisions (to conduct a technology refresh or not) to the Cantor set on the interval $[0, 1/2]$. This is accomplished by mapping the infinite sequence y' to $x \in [0, 1/2]$, using a base-3 expansion:

$$x(y') = \sum_{t=1}^{\infty} \frac{y'_t}{3^t}, \quad \forall y' \in Y', \tag{4.10}$$

with $y'_t \in \{0, 1\}$ and $Y' = \prod_{t=1}^{\infty}\{0, 1\}$ for $t \in \{1, 2, \ldots\}$. If an optimal solution, x^*, for minimizing the cost is in the interval $[0, 1/6]$, then the optimal first decision is to not conduct a technology refresh; if x^* is in the interval $[1/3, 1/2]$, then a technology refresh is optimal in the first decision. This can be seen by mapping the strategies where all of the decisions are 0's, the first decision is a 0 followed by all 1's, the first decision is a 1 followed by all 0's, and where all decisions are 1's, respectively:

$$x(0\bar{0}) = 0, \qquad x(0\bar{1}) = 1/6, \qquad x(1\bar{0}) = 1/3, \qquad x(1\bar{1}) = 1/2.$$

Under the rolling horizon framework, after the first period decision is identified the process repeats and is conditioned on the optimal previous period decisions.

Since (4.10) uses an infinite sequence, the values cannot truly be calculated. However, one can calculate the optimal next period decision by removing the end-of-study effects by choosing a finite horizon that is large enough, under the assumptions of discounted costs and a Hölder continuity condition.

Using the base-3 idea above, an optimal first period decision can be identified by first identifying a set of sample points Q_j with a spacing no greater than Δ_j and a set of truncation horizons T_j. The sample points and truncation horizons are chosen such that Δ_j decreases and T_j increases as $j \to \infty$. The algorithm begins with the initial set of sample points Q_0 and truncation horizon T_0. For each set of sample points in $[0, 1/6]$ and $[1/3, 1/2]$, a lower bound $\bar{f}_0[a, b]$ and an upper bound $\underline{f}_0[a, b]$ are calculated at the truncated horizon. These lower and upper bounds take into account: 1) Estimating an infinite horizon with a finite horizon; and 2) Using a piece-wise linear extension in the interval $[a, b]$ for sample points that may not match up directly with a strategy under the base-3 expansion. (Additional details on how this is accomplished can be found in the original paper [53]). As such, the algorithm is conducted by the following:

1. Calculate $\bar{f}_j[0, 1/6]$, $\underline{f}_j[0, 1/6]$, $\bar{f}_j[1/3, 1/2]$, and $\underline{f}_j[1/3, 1/2]$.

2. If $\bar{f}_j[0, 1/6] \geq \underline{f}_j[1/3, 1/2]$ and $\bar{f}_j[1/3, 1/2] \geq \underline{f}_j[0, 1/6]$, go to step 1 and repeat with a new set of sample points Q_{j+1} and a new truncation horizon T_{j+1}.

3. If $\bar{f}_j[0, 1/6] < \underline{f}_j[1/3, 1/2]$ then the first period decision is to not conduct a technology refresh. If $\bar{f}_j[1/3, 1/2] < \underline{f}_j[0, 1/6]$ then the first period decision is to conduct a technology refresh.

In addition to a discounting (or interest) rate r, the RH framework also uses a growth rate γ, and a maximum-increase cost scalar B. From these three values, terms related to the Hölder continuity function are calculated: $\beta = (1 + \gamma)/(1 + r), 0 < \alpha \leq \min\{\log_3(1/\beta), 1\}, M = 4B/(1 - \beta)$. These values will be reported in Section 4.4 for the simulation study.

4.4 Simulation Study

This section presents a simulation study to highlight the use of the two approaches in DMSMS applications. The scenario is that of a DMSMS manager wishing to explore possible strategies for a current system being replaced by a newer system ten years ($T = 10$) from now, assuming they only consider the LTB option to mitigate any obsolescence issues. A simple, five-part system is presented with expected procurement lifetimes, demands, and costs of the individual parts. In order to explore all alternatives, this simulation study will enumerate all $k = 2^{T-1} = 512$ strategies for the NSGS method, representing all exhaustive strategies in a time frame of 10 years.

4.4.1 Scenario Parameters

The procurement lifetime, X_i, for part $i \in \{1, ..., k\}$ is assumed to be exponentially distributed with a mean procurement lifetime of μ_{X_i} for the NSGS method. As the RH framework is deterministic, the mean value will be used for the procurement lifetime. The values for the parameters of the mean procurement lifetime (in months), annual demand, and the per-item cost are shown in Table 4.1.

Table 4.1: Parameters for simple, five-part system.

	mean proc. lifetime (μ_{X_i})	annual demand (d_i)	per-item cost (c_i)
part 1	24	2000	\$3
part 2	36	1000	\$6
part 3	36	500	\$12
part 4	48	200	\$50
part 5	60	100	\$75

Uncertainty in the LTB costs is captured by the exponentially distributed procurement lifetimes for all five parts and assumes that the annual demands and per-item costs remain fixed. Future models can allow uncertainty in the annual demand and per-item costs if desired. For the NSGS method, the discount rate is set to 10%, $r = 0.10$; refresh costs C_R are \$10,000, \$100,000, and \$500,000, with IZ values of δ =\$50,000, \$100,000, and \$300,000, respectively. In this example, the first IZ value represents the manager being indifferent to costs equal to five technology refreshes; the second IZ value being indifferent to one technology refresh; and the final IZ value to three-fifths of a technology refresh. In reality, these values should be discussed iteratively with the DMSMS manager and should be proportionate with the manager's preference structure. The overall significance level is set at $\alpha = 0.1$, with $\alpha_0 = \alpha_1 = 0.05$; and the sample size in the first stage is set to 30 replications, $n_0 = 30$.

For the RH framework, the discount rate is also set to 10%, the growth rate is 0%, and the maximum-increase scalar $B = \$720,000$. These correspond with values of $\beta = 0.\overline{90}$, $\alpha = 0.086755$, and $M = 31,680$. The RH framework will consider more refresh costs of \$10,000, \$100,000, \$200,000, \$300,000, \$400,000, and \$500,000. Additionally, the truncation horizon is set to $T_j = 20 + j$ and the spacing is set to $\Delta_j = 1/(80(j + 1) + 20)$.

4.4.2 NSGS Method Simulation Results

The results when using the NSGS method for refresh costs of \$10,000, \$100,000, and \$500,000 with their respective IZ values are shown in Table 4.2. The technology refresh and IZ costs, mean costs, strategies, total number of technology refreshes ($\sum_t y_t$), and the second stage number of replications, N_i, are shown. The six strategies with the lowest sample mean cost values are shown in each table for comparison.

With a lower technology refresh cost of \$10,000 with a decision maker indifferent to five technology refreshes, the top section in Table 4.2 indicates that it is preferable to avoid LTBs and to conduct a refresh every year. The set of competitive strategies identified in the first stage includes 45 alternatives ($|I| = 45$), but after second stage sampling only seven other strategies' mean costs are within the IZ of the optimal value. Of these, six have eight technology refreshes and one has seven refreshes. The overall total number of replications is 33,435 for both stages.

Table 4.2: NSGS simulation results for various technology refresh costs and IZ values.

\$ TR / \$ IZ	mean cost	strategy	$\sum_t y_t$	N_i
\$10,000 / \$50,000	\$723,464	⟨111111111⟩	9	140
	\$745,028	⟨111111110⟩	8	226
	\$757,010	⟨111110111⟩	8	308
	\$759,787	⟨111101111⟩	8	222
	\$760,304	⟨111111011⟩	8	260
	\$763,959	⟨111111101⟩	8	256
\$100,000 / \$100,000	\$2,012,328	⟨000100100⟩	2	612
	\$2,013,061	⟨001001000⟩	2	310
	\$2,029,043	⟨000100010⟩	2	383
	\$2,032,522	⟨000101000⟩	2	386
	\$2,045,531	⟨001010000⟩	2	190
	\$2,047,271	⟨001000100⟩	2	190
\$500,000 / \$300,000	\$3,562,830	⟨000000000⟩	0	30
	\$3,928,527	⟨000001000⟩	1	30
	\$3,998,173	⟨000000100⟩	1	30
	\$4,002,652	⟨000010000⟩	1	30
	\$4,138,701	⟨000000010⟩	1	30
	\$4,218,997	⟨000100000⟩	1	30

When a decision maker is indifferent to one technology refresh with a moderate cost of \$100,000, the middle section in Table 4.2 indicates that the optimal strategy is to conduct a technology refresh twice, at years four and seven. The set of second stage strategies includes 53 alternatives ($|I| = 53$) with 20 strategies within the IZ of the optimal value after second stage sampling. Of these, one strategy recommends one refresh, ten recommend 2 refreshes, and nine recommend three refreshes. The total number of replications is 34,372.

When a decision maker is indifferent to 3/5 of a technology refresh with a higher cost of \$500,000, the bottom section in Table 4.2 indicates that it is preferable to not conduct any technology refreshes and to only rely on LTB options to remedy any obsolescence issues. For this particular set of parameters, the optimal strategy does not recommend any additional second stage samples ($|I| = 1$). This occurs in the case where an optimal strategy's cost is much smaller than the other alternatives (in the statistically significant sense). For comparison, the next five closest alternatives all have only one recommended technology refresh, but were outside of the indifference zone.

The total number of samples for each part N_i for $i \in I$ is a function of the IZ parameter, the standard deviation of the samples, and the number of initial samples as indicated by (4.8). As the desired confidence level increases, or the indifference to cost decreases, the number of second stage samples will generally increase. The combination of these parameters must be chosen with an understanding of the practical implications to identify an optimal strategy.

4.4.3 RH Framework Simulation Results

The results when using the RH framework for multiple technology refresh costs are shown in Table 4.3. The technology refresh cost, strategies, and total number of technology refreshes ($\sum_t y_t$) are shown. Unlike the NSGS method's results, the RH framework will only provide a single, optimal strategy.

Table 4.3: Rolling Horizon results for various technology refresh costs.

\$ TR	strategy	$\sum_t y_t$
\$10,000	⟨111111111⟩	9
\$100,000	⟨111111111⟩	9
\$200,000	⟨101001001⟩	4
\$300,000	⟨001001001⟩	3
\$400,000	⟨001001001⟩	3
\$500,000	⟨000000000⟩	0

Using the RH framework indicates that when technology refresh values of \$10k and \$100k a technology refresh should be conducted every year. The number of refreshes drops to four over the ten-year period when the technology refresh cost increases to \$200k and three when the cost increases to \$300k and \$400k. When the technology refresh cost is \$500k, the RH framework recommends not doing any refreshes.

It is important to point out the differences between the optimal strategies identified by the NSGS method and the RH framework. When the technology refresh cost is small (\$10k), both methods identify a strategy where one would conduct a refresh every time period. As the cost increases to \$100k, the RH framework indicates to continue to conduct a technology refresh every time period, while the number of refreshes deceases to two over the ten year time period. Finally, when the technology refresh cost is high (\$500,000), the optimal strategy is to not conduct any technology refreshes for both methods.

4.5 Visualization of Strategies

This section will present a visualization technique to assist a DMSMS manager when considering alternatives. The visualization will present the set of solutions costs calculated using the NSGS method from Section 4.4.2. Since the purpose of enumerating all strategies (when using the NSGS method) is to explore the set of alternatives, the DMSMS manager may want to consider other alternatives relative to a chosen IZ value. Tabulating the strategies can provide some insights, but if the number of strategies is large it may be difficult to compare the different sequences of technology refreshes. The visualization is based on the base-3 expansion shown in Section 4.3.3 as it also allows for a finite strategy to be mapped to the range $[0, 1/2]$ and is modified from [53].

The results shown in Table 4.2 only provide a handful of the overall strategies considered in the simulation; using the mapping in (4.10) can allow many more strategies to be plotted visually, with the capability to provide insights to alternate technology refresh schedules. Figures 4.3-4.5 show the results for the three refresh costs, \$10,000, \$100,000, and \$500,000. Figure 4.3 shows the optimal strategy (the larger red dot) near the value of $x = 1/2$, indicating a series of technology refreshes every year, which is the same result shown in Table 4.2 for a technology refresh cost of $10,0000 with an IZ value of $50,000. The seven other strategies that are within the IZ as mentioned in Section 4.4.2 can be identified by the dots below the dashed line and indicate that the first decision should be to conduct a refresh.

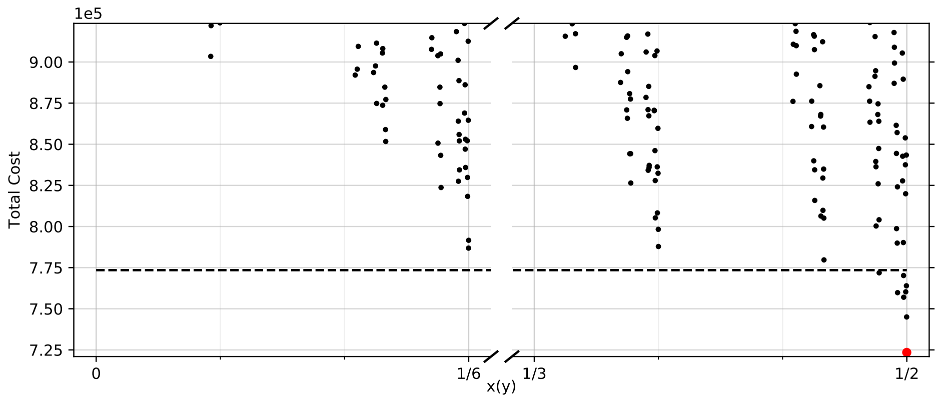

Figure 4.3: Visualization of the mean total costs of alternative strategies with a refresh cost of $10,000 with an IZ value of $50,000.

Increasing the refresh cost and IZ values to $100,000 changes the optimal first choice to not recommend a technology refresh in the first time period. Figure 4.4 shows a larger number of strategies will have a lower cost when not performing a technology refresh during the first period and the optimal time to conduct the first technology refresh is in the fourth year. The 20 strategies within the IZ value are also shown in the figure and indicate that the first decision should be to not conduct a technology refresh.

When the refresh cost is increased to $500,000 with an IZ value of $300,000, Figure 4.5 shows that relying on LTB options is ideal. The optimal minimal cost and strategy are easily seen in this figure, where the mapping $x(0 \cdots 0) = 0$ is on the far left of the figure. The figure shows the alternatives that may be included if the IZ were raised to a larger value.

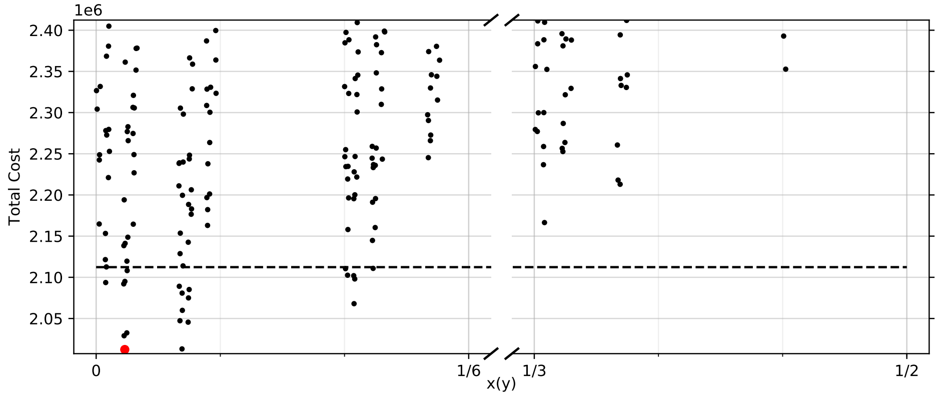

Figure 4.4: Visualization of the mean total costs of alternative strategies with a refresh cost of \$100,000 with an IZ value of \$100,000.

4.6 Discussion

This chapter compares a R&S method with a RH framework to identify the optimal strategy for strategic DMSMS management. The tabular and visual results can assist the DMSMS manager in planning the sequence of technology refreshes, particularly when exploring strategies to adopt. Actual technology refresh costs should be dictated by data while the IZ parameter should be chosen by a decision maker and tied to actual budget values.

The results in Section 4.4 provide insights to the relationship between the LTB costs and the technology refresh costs. In general, as the technology refresh costs increase, the optimal strategy will include less refreshes and rely more on LTBs. Also, the RH framework tends to provide a more conservative strategy for a given technology refresh cost. This is likely due to the fact that the IHO method using the RH framework has removed any end-of-study effects when compared with a finite horizon model. Factoring out the similar items in (4.7),

$$C(y) = \sum_{t=1}^{T-1} y_t \exp(-rt) \left[c_R + \sum_{i=1}^{N} \exp\left(rS_{ti}(y)\right) c_i d_i S_{ti}(y) \right] + \sum_{i=1}^{N} \exp\left(-rZ_{Ti}(y)\right) c_i d_i S_{Ti}(y),$$

allows for a better view of the relationship between the two costs. Since the objective is to minimize the overall costs over all strategies, there is a trade-off between the refresh costs

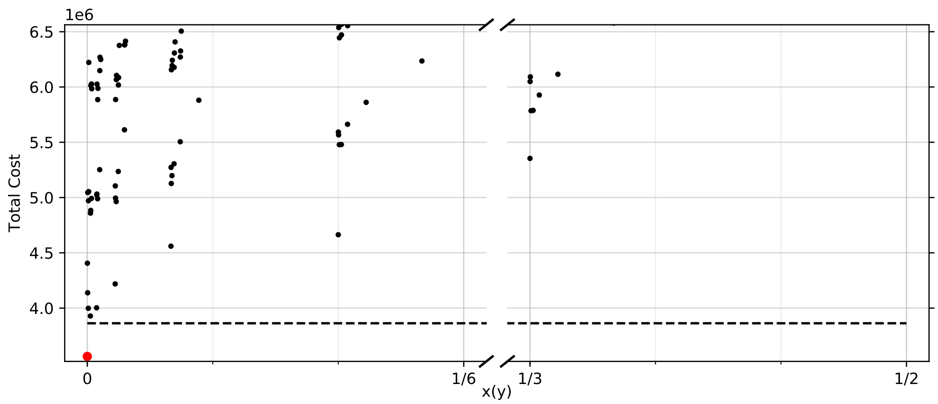

Figure 4.5: Visualization of the mean total costs of alternative strategies with a refresh cost of \$500,000 with an IZ value of \$300,000.

c_R and the LTB costs (the second term in the brackets and last term). As the number of technology refreshes ($\sum_t y_t$) increases the overall technology refresh costs will also increase; however, the overall LTB costs will tend to decrease as the shortage times ($S_{ti}(y)$) will also decrease. This trade-off between technology refresh and LTB (and other) costs is at the heart of determining optimal strategies and will be central in a real-world application. The cost function (4.7) can be expanded to accommodate additional mitigation options beyond LTBs, and additional costs such as holding, stock-out, and salvage costs. Future applications of the NSGS method to DMSMS applications can include uncertainty in the annual demand and the item costs.

Both the NSGS method and RH framework can guarantee an optimal solution (or set of solutions) even when the cost function is ill-behaved, so long as the underlying assumptions are satisfied. The costs modeled in this chapter assumed stationarity in the costs and the procurement lifetimes of the parts, but this will not be an issue with either the NSGS method or the RH framework. One limiting factor with the NSGS method is that it cannot handle a feasible set of alternatives where there are many decision periods or many decisions at each period. Using heuristic methods before using the NSGS method to identify a smaller set of strategies could be useful in reducing some strategies that would not be optimal. On the other hand, the RH framework will be able to identify an optimal strategy even if there are many decision periods or many decisions at each period. A drawback to the RH framework is that finding a set of practically significant alternatives to help shape business policies may be harder, which is one of the benefits of using the NSGS method. An area for further study includes evaluating a blended method that uses both methods, possibly where the RH framework is utilized first to identify a set of alternatives before using the NSGS method to identify a practically significant set of alternatives.

Chapter 5

CONCLUSION

This dissertation provides three mechanisms to improve proactive and strategic DMSMS management. The contribution in Chapter 2 shows that previous methods to reduce the bias in the shape parameter can be applied to generalized Type 1 censoring, and shows how oversampling, according to a SMOTE-like procedure, can reduce the bias in the scale estimates and the overall density for a Weibull distribution. Previous studies have highlighted the issues with parameter estimation when there are smaller samples sizes and/or increased levels of censoring [40, 65, 125]. The ratio of oversampling non-censored to censored values to reduce the bias is related to the level of censoring. As the censoring percentage increases, creating synthetic data by oversampling the censored values tends to increase as well. In general, there is greater potential to reduce the bias (in expectation) in the overall distribution with oversampling where there are smaller sample sizes. Identifying the points in the $\mathcal{N} \times \mathcal{C}$ grid for creating over-sampled synthetic observations is novel in that it does so for smaller sample sizes and across all levels of censoring. Although this model was represented from a DMSMS perspective, there is potential to apply this method in other contexts.

The availability models developed in Chapter 3 provide a framework to include the market size when forecasting part availability. Both models, P_Z and T_Z, are validated with analytic solutions and allow for quantification of DMSMS availability risk. The models show the varying levels of risk when comparing different parts with differing churn rates or for a single part with varying market sizes. Since the model is built upon a DES framework, the analytic solutions shown in Sections 3.7 and 3.8 can be modified as necessary to assist in numerical validation for procurement lifetimes that do not have exponential distributions. Extensions to the models explore the case where a configuration part may have non-homogeneous vendor parts and time and state-dependent cases (shortening procurement lifetimes, increasing probability of no F3 replacements, and single manufacturers). The extensions allow a modeler to provide additional realism as needed to the model, assuming they will have access to relevant data regarding part procurement lifetimes and market sizes.

The final contribution in Chapter 4 provides the DMSMS practitioner two additional methods to identify optimal technology refresh strategies when considering LTBs as a mitigation strategy. Both the NSGS method and RH framework can identify the optimal refresh solutions even if the cost functions are ill-defined. In general, the RH framework chooses the optimal decision in the current time period with a finite approximation to an infinite horizon optimization problem. This results in a strategy that will tend to be more risk-adverse and can be used to hedge against uncertainty. On the other hand, a strategy identified by the NSGS method will ensure that there are sufficient parts on hand or available to make it to the end of the ten-year period, but typically no excess parts. One benefit of the NSGS method when applied to a DMSMS application is that it identifies a handful of strategies that are within a pre-identified zone of indifference. From a decision maker's standpoint, this benefit is invaluable as it can provide a handful of options to consider when exploring options. Although the system and costs in this model are fictitious, the results shown in Chapter 4 highlight the trade-off between the LTB costs and the technology refresh costs; as the cost of a refresh increases, relative to the LTB costs incurred, there tend to be less recommended refreshes over the ten year period.

This dissertation presented the models from Chapters 2, 3, and 4 as independent. Future research and case study applications could examine the efficacy of combining the three models. For example, the bias reduction method could be integrated into the availability models to improve the individual part procurement lifetimes. Integrating the availability models into the optimal technology refresh model can improve the overall cost estimates by taking into account the market sizes for various parts when estimating the technology refresh costs.

As mentioned before, the oversampling procedure in Chapter 2 assumes the parts do not have evolutionary parametric drivers and only use the introduction date and obsolescence date or censoring date. As much as it is possible, additional efforts to more accurately and adequately track parametric drivers can help with estimating procurement lifetimes. Additional data, such as capability growth, cost, design deficiency, environmental impact, maintainability, reliability, safety, and supportability, have been identified by [18] to assist in making decisions regarding technology and redesign refreshes. This additional information can be used to improve the procurement lifetime estimates, but can also improve the availability model and optimal technology refresh planning.

BIBLIOGRAPHY

[1] Sukru Acitas, Cagdas Hakan Aladag, and Birdal Senoglu. A new approach for estimating the parameters of weibull distribution via particle swarm optimization: An application to the strengths of glass fibre data. *Reliability Engineering & System Safety*, 183:116–127, 2019.

[2] Oluwatomi Adetunji, John Bischoff, and Christopher J Willy. Managing system obsolescence via multicriteria decision making. *Systems Engineering*, 21(4):307–321, 2018.

[3] Kahkashan Afrin, Gurudev Illangovan, Sanjay S Srivatsa, and Satish TS Bukkapatnam. Balanced random survival forests for extremely unbalanced, right censored data. *arXiv preprint arXiv:1803.09177*, 2018.

[4] Jeffrey M Alden and Robert L Smith. Rolling horizon procedures in nonhomogeneous markov decision processes. *Operations Research*, 40(3-supplement-2):S183–S194, 1992.

[5] Monique Bakker, Jan Riezebos, and Ruud H Teunter. Review of inventory systems with deterioration since 2001. *European Journal of Operational Research*, 221(2):275–284, 2012.

[6] Elia Balugani, Francesco Lolli, Rita Gamberini, Bianca Rimini, and MZ Babai. A periodic inventory system of intermittent demand items with fixed lifetimes. *International Journal of Production Research*, pages 1–13, 2019.

[7] Bjoern Bartels, Ulrich Ermel, Peter Sandborn, and Michael G Pecht. *Strategies to the Prediction, Mitigation and Management of Product Obsolescence*. John Wiley & Sons, 2012.

[8] Christian Bauckhage. Computing the kullback-leibler divergence between two weibull distributions. *arXiv preprint arXiv:1310.3713*, 2013.

[9] Barry L Bayus. An analysis of product lifetimes in a technologically dynamic industry. *Management Science*, 44(6):763–775, 1998.

[10] Robert E Bechhofer, David M Goldsman, and Thomas J Santner. *Design and Analysis of Experiments for Statistical Selection, Screening, and Multiple Comparisons*. Wiley, 1995.

[11] Richard Bellman. Equipment replacement policy. *Journal of the society for industrial and applied Mathematics*, 3(3):133–136, 1955.

[12] Paul D Berger, Arthur Gerstenfeld, and Amy Z Zeng. How many suppliers are best? a decision-analysis approach. *Omega*, 32(1):9–15, 2004.

[13] Joshua M Brock, Elizabeth R Payne, Paul D Collopy, and Owen C Brown. Considering obsolescence in system design. *Procedia Computer Science*, 153:317–324, 2019.

[14] Suresh Chand, Vernon Ning Hsu, and Suresh Sethi. Forecast, solution, and rolling horizons in operations management problems: A classified bibliography. *Manufacturing & Service Operations Management*, 4(1):25–43, 2002.

[15] Chin-Chih Chang. Optimal age replacement scheduling for a random work system with random lead time. *International Journal of Production Research*, 56(16):5511–5521, 2018.

[16] Nitesh V Chawla, Kevin W Bowyer, Lawrence O Hall, and W Philip Kegelmeyer. SMOTE: Synthetic minority over-sampling technique. *Journal of Artificial Intelligence Research*, 16:321–357, 2002.

[17] Youngjun Choe. Information criterion for minimum cross-entropy model selection, 2017.

[18] Cal C Classi, David R Nowicki, Mo Mansouri, Brian J Sauser, and Wesley S Randall. A systems thinking approach to managing sustainment phase redesign planning. *Engineering Management Journal*, 30(1):68–81, 2018.

[19] William Clay, James R Morrison, Francis Wolff, Daniel J Weyer, Biman Ghosh, and David D Yellamati. A risk based methodology for managing material/product life cycle disruptions. In *2016 Annual Reliability and Maintainability Symposium (RAMS)*, pages 1–6. IEEE, 2016.

[20] DR Cox and N Reid. On the stability of maximum-likelihood estimators of orthogonal parameters. *Canadian Journal of Statistics*, 17(2):229–233, 1989.

[21] Herbert Aron David and Melvin L Moeschberger. *The Theory of Competing Risks: HA David, ML Moeschberger*. C. Griffin, 1978.

[22] Defense Standardization Program Office. *Diminishing Manufacturing Sources and Material Shortages: Cost Metrics*. U.S. Department of Defense, Fort Belvoir, VA, 2015.

[23] Defense Standardization Program Office. *SD-22 - Diminishing Manufacturing Sources and Material Shortages (DMSMS): A Guidebook of Best Practices for Implementing a Robust DMSMS Management Program*. Fort Belvoir, VA, January 2016.

[24] Marie Laure Delignette-Muller and Christophe Dutang. fitdistrplus: An R package for fitting distributions. *Journal of Statistical Software*, 64(4):1–34, 2015.

[25] Jay L Devore. *Probability and Statistics for Engineering and the Sciences*. Thomson Brooks/Cole, 7 edition, 2008.

[26] Rafael Diaz and Erika Marsillac. Evaluating strategic remanufacturing supply chain decisions. *International Journal of Production Research*, 55(9):2522–2539, 2017.

[27] Florence Ducros and Patrick Pamphile. Bayesian estimation of weibull mixture in heavily censored data setting. *Reliability Engineering & System Safety*, 180:453–462, 2018.

[28] Tommie L Ellis, Robert A Nicholson, Antoinette Y Briggs, Scott A Hunter, James E Harbison, Paul S Saladna, Michael W Garris, Robert K Ohnemus, John E O'Connor, and Steven B Reynolds. Lifting and shifting the air force retail supply system. *Journal of Defense Analytics and Logistics*, 1(2):172–184, 2017.

[29] Andrew Estabrooks, Taeho Jo, and Nathalie Japkowicz. A multiple resampling method for learning from imbalanced data sets. *Computational intelligence*, 20(1):18–36, 2004.

[30] Paul F Evangelista, Mark J Embrechts, and Boleslaw K Szymanski. Synergistic classifier fusion for security applications. In *Interservice/Industry Training, Simulation, and Education Conference (I/ITSEC)*, 2007.

[31] Tom Fawcett. ROC graphs: Notes and practical considerations for researchers. *Machine Learning*, 31(1):1–38, 2004.

[32] Dan Feng, Pameet Singh, and Peter Sandborn. Lifetime buy optimization to minimize lifecycle cost. In *Proceedings of the 2007 Aging Aircraft Conference*, 2007.

[33] Alberto Fernández, Salvador Garcia, Francisco Herrera, and Nitesh V Chawla. Smote for learning from imbalanced data: progress and challenges, marking the 15-year anniversary. *Journal of artificial intelligence research*, 61:863–905, 2018.

[34] Brant E Fries. Optimal ordering policy for a perishable commodity with fixed lifetime. *Operations Research*, 23(1):46–61, 1975.

[35] Archis Ghate. Infinite horizon problems. *Wiley Encyclopedia of Operations Research and Management Science*, 2010.

[36] David Goldsman. A practical guide to ranking and selection methods. In *The Operations Research Revolution*, pages 89–110. INFORMS, 2015.

[37] D. F. Gross, J. M. Shortie, and J. Thompson. *Fundamentals of Queueing Theory*. John Wiley and Sons, Hoboken, NJ, 4 edition, 2013.

[38] Joseph C Hartman and Alison Murphy. Finite-horizon equipment replacement analysis. *IIE transactions*, 38(5):409–419, 2006.

[39] Dennis R Helsel. *Statistics for Censored Environmental Data Using Minitab and R*, volume 77. John Wiley & Sons, 2011.

[40] Hideo Hirose. Bias correction for the maximum likelihood estimates in the two-parameter weibull distribution. *IEEE Transactions on Dielectrics and Electrical Insulation*, 6(1):66–68, 1999.

[41] William Ho, Tian Zheng, Hakan Yildiz, and Srinivas Talluri. Supply chain risk management: a literature review. *International Journal of Production Research*, 53(16):5031–5069, 2015.

[42] Seyedmohsen Hosseini, Dmitry Ivanov, and Alexandre Dolgui. Review of quantitative methods for supply chain resilience analysis. *Transportation Research Part E: Logistics and Transportation Review*, 125:285–307, 2019.

[43] Mickey Howard, Peter Hopkinson, and Joe Miemczyk. The regenerative supply chain: a framework for developing circular economy indicators. *International Journal of Production Research*, pages 1–19, 2018.

[44] Guiping Hu and Bopaya Bidanda. Modeling sustainable product lifecycle decision support systems. *International Journal of Production Economics*, 122(1):366–375, 2009.

[45] Dmitry Ivanov. Simulation-based ripple effect modelling in the supply chain. *International Journal of Production Research*, 55(7):2083–2101, 2017.

[46] Kateřina Janurová and Radim Briš. A nonparametric approach to medical survival data: Uncertainty in the context of risk in mortality analysis. *Reliability Engineering & System Safety*, 125:145–152, 2014.

[47] Connor Jennings, Dazhong Wu, and Janis Terpenny. Forecasting obsolescence risk and product life cycle with machine learning. *IEEE Transactions on Components, Packaging and Manufacturing Technology*, 6(9):1428–1439, 2016.

[48] Connor Jennings, Dazhong Wu, and Janis Terpenny. Receiver operating characteristic analysis for forecasting obsolescence risk. In *IIE Annual Conference. Proceedings*, pages 722–727. Institute of Industrial and Systems Engineers (IISE), 2017.

[49] Jeasu Jeon and So Young Sohn. Product failure pattern analysis from warranty data using association rule and weibull regression analysis: A case study. *Reliability Engineering & System Safety*, 133:176–183, 2015.

[50] Renyan Jiang. A novel parameter estimation method for the weibull distribution on heavily censored data. *Proceedings of the Institution of Mechanical Engineers, Part O: Journal of Risk and Reliability*, pages 1–10, 2019.

[51] Kailash C Kapur and Michael Pecht. *Reliability Engineering*. John Wiley & Sons, 2014.

[52] Matthew R Kennedy and David A Umphress. An agile systems engineering process: The missing link? *CrossTalk: The Journal of Defense Software Engineering*, 24(3):16–20, 2011.

[53] Seksan Kiatsupaibul, Robert L Smith, and Zelda B Zabinsky. Solving infinite horizon optimization problems through analysis of a one-dimensional global optimization problem. *Journal of Global Optimization*, 66(4):711–727, 2016.

[54] Herbert E Kierulff. The replacement decision: Getting it right. *Business Horizons*, 50(3):231–237, 2007.

[55] Seong-Joon Kim, Byeong Min Mun, and Suk Joo Bae. A cost-driven reliability demonstration plan based on accelerated degradation tests. *Reliability Engineering & System Safety*, 183:226–239, 2019.

[56] John P Klein and Melvin L Moschberger. *Survival Analysis: Techniques for Censored and Truncated Data*. Springer, New York, NY., 2003.

[57] Solomon Kullback and Richard A Leibler. On information and sufficiency. *The annals of mathematical statistics*, 22(1):79–86, 1951.

[58] Rajnish Kumar, Sidhartha S Padhi, and Ashutosh Sarkar. Optimal number of suppliers to mitigate supply disruption: a case of indian locomotive manufacturer. *International Journal of Logistics Systems and Management*, 31(1):132–149, 2018.

[59] Averill M Law. *Simulation Modeling and Analysis*. McGraw-Hill Education, 5 edition, 2015.

[60] Lei Li and Zelda B Zabinsky. Incorporating uncertainty into a supplier selection problem. *International Journal of Production Economics*, 134(2):344–356, 2011.

[61] Lin Li and Jun Ni. Reliability estimation based on operational data of manufacturing systems. *Quality and Reliability Engineering International*, 24(7):843–854, 2008.

[62] Mingyang Li, Hongdao Meng, and Qingpeng Zhang. A nonparametric bayesian modeling approach for heterogeneous lifetime data with covariates. *Reliability Engineering & System Safety*, 167:95–104, 2017.

[63] Xiaoyang Li, Wenbin Chen, Fuqiang Sun, Haitao Liao, Rui Kang, and Renqing Li. Bayesian accelerated acceptance sampling plans for a lognormal lifetime distribution under type-i censoring. *Reliability Engineering & System Safety*, 171:78–86, 2018.

[64] Zhaotong Lian, Liming Liu, and Stuart X Zhu. Rolling-horizon replenishment: Policies and performance analysis. *Naval Research Logistics (NRL)*, 57(6):489–502, 2010.

[65] Hung-Mo Lin, John M Williamson, and Hae-Young Kim. Firth adjustment for weibull current-status survival analysis. *Communications in Statistics-Theory and Methods*, pages 1–16, 2019.

[66] Jianhua Lin. Divergence measures based on the shannon entropy. *IEEE Transactions on Information theory*, 37(1):145–151, 1991.

[67] Bi Liu, Yunlong Teng, and Qi Huang. A novel imprecise reliability prediction method for incomplete lifetime data based on two-parameter weibull distribution. *Proceedings of the Institution of Mechanical Engineers, Part O: Journal of Risk and Reliability*, page 1748006X18799014, 2018.

[68] Florian Lücker, Ralf W Seifert, and Işık Biçer. Roles of inventory and reserve capacity in mitigating supply chain disruption risk. *International Journal of Production Research*, 57(4):1238–1249, 2019.

[69] Xiaozhou Meng, Benny Thörnberg, and Leif Olsson. Strategic proactive obsolescence management model. *IEEE Transactions on Components, Packaging and Manufacturing Technology*, 4(6):1099–1108, 2014.

[70] Nuno Moniz, Paula Branco, and Luís Torgo. Resampling strategies for imbalanced time series. In *2016 IEEE International Conference on Data Science and Advanced Analytics (DSAA)*, pages 282–291. IEEE, 2016.

[71] Douglas C Montgomery. *Design And Analysis of Experiments*. John Wiley & Sons, Hoboken, NJ, 8 edition, 2013.

[72] Barry L Nelson, Julie Swann, David Goldsman, and Wheyming Song. Simple procedures for selecting the best simulated system when the number of alternatives is large. *Operations Research*, 49(6):950–963, 2001.

[73] Raymond S Nelson III and Peter Sandborn. Strategic management of component obsolescence using constraint-driven design refresh planning. *International Journal of Product Lifecycle Management*, 6(2):99–120, 2013.

[74] Eric C Ni, Shane G Henderson, and Susan R Hunter. A comparison of two parallel ranking and selection procedures. In *Proceedings of the 2014 Winter Simulation Conference*, pages 3761–3772. IEEE, 2014.

[75] Eric C Ni, Susan R Hunter, and Shane G Henderson. Ranking and selection in a high performance computing environment. In *Proceedings of the 2013 Winter Simulations Conference*, pages 833–845. IEEE, 2013.

[76] Eric Cao Ni. Eric cao ni personal website. `https://people.orie.cornell.edu/cn254/`, 2013. Last accessed 4 April 2019.

[77] Frank Nielsen. A family of statistical symmetric divergences based on jensen's inequality. *arXiv preprint arXiv:1009.4004*, 2010.

[78] Michael G Pecht and Diganta Das. Electronic part life cycle. *IEEE Transactions on Components and Packaging Technologies*, 23(1):190–192, 2000.

[79] Nadia Pérot and Nicolas Bousquet. Functional weibull-based models of steel fracture toughness for structural risk analysis: estimation and selection. *Reliability Engineering & System Safety*, 165:355–367, 2017.

[80] Alessandro Persona, Andrea Grassi, and M. Catena. Consignment stock of inventories in the presence of obsolescence. *International Journal of Production Research*, 43(23):4969–4988, 2005.

[81] John E Pinder III, James G Wiener, and Michael H Smith. The weibull distribution: a new method of summarizing survivorship data. *Ecology*, 59(1):175–179, 1978.

[82] Pratik Pingle. *Selection of Obsolescence Resolution Strategy Based on a Multi-Criteria Decision Model*. PhD thesis, Iowa State University, 2015.

[83] G Zell Porter. An economic method for evaluating electronic component obsolescence solutions. Technical report, Boeing Information Space & Defense Systems, 1998.

[84] Varun Jonathan Prabhakar. *Electronic Part Total Cost of Ownership and Sourcing Decisions for Long Life Cycle Products*. PhD thesis, University of Maryland, College Park, 2011.

[85] Sophie L Rasmussen, Thomas B Berg, Torben Dabelsteen, and Owen R Jones. The ecology of suburban juvenile european hedgehogs (erinaceus europaeus) in denmark. *Ecology and Evolution*, 9(23):13174–13187, 2019.

[86] R. Dan Reid and Nada R. Sanders. *Operations Management*. John Wiley and Sons, Hoboken, NJ, 2007.

[87] David R Rink and John E Swan. Product life cycle research: A literature review. *Journal of Business Research*, 7(3):219–242, 1979.

[88] Yosef Rinott. On two-stage selection procedures and related probability-inequalities. *Communications in Statistics-Theory and Methods*, 7(8):799–811, 1978.

[89] Francisco Javier Romero Rojo, Rajkumar Roy, and S Kelly. Obsolescence risk assessment process best practice. In *Journal of Physics: Conference Series*, volume 364, page 012095. IOP Publishing, 2012.

[90] Francisco Javier Romero Rojo, Rajkumar Roy, and Essam Shehab. Obsolescence management for long-life contracts: state of the art and future trends. *The International Journal of Advanced Manufacturing Technology*, 49(9-12):1235–1250, 2010.

[91] R Ross. Formulas to describe the bias and standard deviation of the ml-estimated weibull shape parameter. *IEEE Transactions on Dielectrics and Electrical Insulation*, 1(2):247–253, 1994.

[92] Sheldon M Ross. *Stochastic Processes*. Wiley New York, 2 edition, 1996.

[93] Mark S Roulston. Performance targets and the brier score. *Meteorological Applications: A Journal of Forecasting, Practical Applications, Training Techniques and Modelling*, 14(2):185–194, 2007.

[94] Peter Sandborn. Strategic management of DMSMS in systems. *DSP Journal*, pages 24–30, 2008.

[95] Peter Sandborn. Design for obsolescence risk management. *Procedia CIRP*, 11:15–22, 2013.

[96] Peter Sandborn. *Cost Analysis of Electronic Systems*, volume 4. World Scientific, 2016.

[97] Peter Sandborn. Forecasting technology and part obsolescence. *Proceedings of the Institution of Mechanical Engineers, Part B: Journal of Engineering Manufacture*, 231(13):2251–2260, 2017.

[98] Peter Sandborn and Jessica Myers. Designing engineering systems for sustainability. In *Handbook of Performability Engineering*, pages 81–103. Springer, 2008.

[99] Peter Sandborn, V Prabhakar, and O Ahmad. Forecasting electronic part procurement lifetimes to enable the management of DMSMS obsolescence. *Microelectronics Reliability*, 51(2):392–399, 2011.

[100] Peter Sandborn and Pameet Singh. Electronic part obsolescence driven product redesign optimization. In *Proc. FAA/DoD/NASA Aging Aircraft Conference*, 2002.

[101] Peter A Sandborn, Frank Mauro, and Ron Knox. A data mining based approach to electronic part obsolescence forecasting. *IEEE Transactions on Components and Packaging Technologies*, 30(3):397–401, 2007.

[102] Fabio Sgarbossa, Ilenia Zennaro, Eleonora Florian, and Martina Calzavara. Age replacement policy in the case of no data: the effect of weibull parameter estimation. *International Journal of Production Research*, pages 1–19, 2019.

[103] Yan Shen and Zhenlin Yang. Bias-correction for weibull common shape estimation. *Journal of Statistical Computation and simulation*, 85(15):3017–3046, 2015.

[104] Pameet Singh and Peter Sandborn. Obsolescence driven design refresh planning for sustainment-dominated systems. *The Engineering Economist*, 51(2):115–139, 2006.

[105] Pameet Singh, Peter Sandborn, Todd Geiser, and David Lorenson. Electronic part obsolescence driven product redesign planning. *International Journal of Advanced Manufacturing Systems*, 7(2), 2004.

[106] Rajeev Solomon, Peter A Sandborn, and Michael G Pecht. Electronic part life cycle concepts and obsolescence forecasting. *IEEE Transactions on Components and Packaging Technologies*, 23(4):707–717, 2000.

[107] James K Starling, Youngjun Choe, and Christina Mastrangelo. Optimal technology refresh strategies for strategic dmsms management using ranking and selection. In *2019 Winter Simulation Conference (WSC)*, pages 2524–2535. IEEE, 2019.

[108] James K Starling, Youngjun Choe, and Christina Mastrangelo. Identifying dmsms availability risk at the system level. *International Journal of Production Research*, pages 1–21, 2020.

[109] Dusan Stefanovic, Nenad Stefanovic, and B Radenkovic. Supply network modelling and simulation methodology. *Simulation Modelling Practice and Theory*, 17(4):743–766, 2009.

[110] C. L. Suzman and Samuel Eilon. Stock depletion problems of commodities having decaying field life functions. *International Journal of Production Research*, 2(1):23–40, 1963.

[111] János Sztrik. *Basic queueing theory: Foundations of system performance modeling*. GlobeEdit, 2016.

[112] Mahdi Teimouri, Seyed M. Hoseini, and Saralees Nadarajah. Comparison of estimation methods for the weibull distribution. *Statistics*, 47(1):93–109, 2013.

[113] Ruud H Teunter and Leonard Fortuin. End-of-life service. *International Journal of Production Economics*, 59(1-3):487–497, 1999.

[114] WJ Tomczykowski. A study on component obsolescence mitigation strategies and their impact on R&M. In *Reliability and Maintainability Symposium, 2003. Annual*, pages 332–338. IEEE, 2003.

[115] Luís Torgo, Paula Branco, Rita P Ribeiro, and Bernhard Pfahringer. Resampling strategies for regression. *Expert Systems*, 32(3):465–476, 2015.

[116] John W. Tukey. Comparing individual means in the analysis of variance. *Biometrics*, 5(2):99–114, 1949.

[117] Kenneth D Underwood, Jeffrey A Ogden, and Matthew T McConville. Comparing lifecycle sustainment strategies in an electronic component obsolescence environment. *Journal of Cost Analysis and Parametrics*, 7(2):101–119, 2014.

[118] Kung-Jeng Wang, Phuc Hong Nguyen, Shaw-Yi Wu, and Jin Xue. Technology portfolio adoption considering capacity planning under demand and technology uncertainty. *Journal of Manufacturing Systems*, 47:1–11, 2018.

[119] Ping Wang, Yan Li, and Chandan K Reddy. Machine learning for survival analysis: A survey. *arXiv preprint arXiv:1708.04649*, 2017.

[120] Daniel S Wilks. Sampling distributions of the brier score and brier skill score under serial dependence. *Quarterly Journal of the Royal Meteorological Society*, 136(653):2109–2118, 2010.

[121] Teresa Wu, Jennifer Blackhurst, and Vellayappan Chidambaram. A model for inbound supply risk analysis. *Computers in industry*, 57(4):350–365, 2006.

[122] Zhenlin Yang. A general method for third-order bias and variance corrections on a nonlinear estimator. *Journal of Econometrics*, 186(1):178–200, 2015.

[123] Zhenlin Yang and Dennis KJ Lin. Improved maximum-likelihood estimation for the common shape parameter of several weibull populations. *Applied Stochastic Models in Business and Industry*, 23(5):373–383, 2007.

[124] Zhenlin Yang and Min Xie. Efficient estimation of the weibull shape parameter based on a modified profile likelihood. *Journal of Statistical Computation and Simulation*, 73(2):115–123, 2003.

[125] LF Zhang, Min Xie, and Loon Ching Tang. Bias correction for the least squares estimator of weibull shape parameter with complete and censored data. *Reliability Engineering & System Safety*, 91(8):930–939, 2006.

[126] LF Zhang, Min Xie, and Loon Ching Tang. A study of two estimation approaches for parameters of weibull distribution based on wpp. *Reliability Engineering & System Safety*, 92(3):360–368, 2007.

[127] Liyu Zheng, Raymond Nelson, Janis Terpenny, and Peter Sandborn. Ontology-based knowledge representation for obsolescence forecasting. *Journal of Computing and Information Science in Engineering*, 13(1):014501, 2013.

[128] Liyu Zheng, Janis Terpenny, and Peter Sandborn. Design refresh planning models for managing obsolescence. *IIE Transactions*, 47(12):1407–1423, 2015.

[129] Marc Zolghadri, Sid-Ali Addouche, Kevin Boissie, and Daniel Richard. Obsolescence prediction: a Bayesian model. *Procedia CIRP*, 70:392–397, 2018.